UNIVERSITA' DEGLI STUDI DI PADOVA

SEDE AMMINISTRATIVA: Università degli Studi di Padova

DIPARTIMENTO DI ISTOLOGIA; MICROBIOLOGIA

E BIOTECNOLOGIE MEDICHE

SCUOLA DI DOTTORATO DI RICERCA IN BIOMEDICINA

CICLO XXIII

SELECTIVE TARGETING OF NUCLEIC ACIDS BY SMALL MOLECULES: A DNA STRUCTURE RECOGNITION APPROACH

Direttore della scuola: **Ch.mo Prof. Giorgio Palu'**

Supervisore: **Ch.mo Prof. Giorgio Palu'**

Correlatore: **Prof. Claudia Sissi**

Dottoranda: **Caterina Musetti**

...dedicated to my wonderful mom and dad

"Science may set limits to knowledge,

but should not set limits to imagination."

Bertrand Russell

TABLE OF CONTENTS

LIST OF ABBREVIATIONS

CD	Circular Dichroism
DMSO	Dimethyl sulphoxide
ctDNA	calf tymus Deoxyribonucleic Acid
DNA	Deoxyribonucleic Acid
dsDNA	double strand Deoxyribonucleic Acid
ssDNA	single strand Deoxyribonucleic Acid
dNTP's	Mixture of the four deoxyribonucleotides (dATP, dGTP, dTTP, dCTP)
EDTA	Ethylenediaminetetraacetic Acid
EGTA	Ethylene Glycol Tetraacetic Acid
EMSA	Electrophoretic Mobility Shift Assay
ESI-MS	Electrospray ionization-Mass spectrometry
FAM	6-Carboxyfluorescein
HPLC	High Performance Liquid Chromatography
HTel	Human Telomeric DNA
MALDI-TOF	Matrix-Assisted Laser Desorption Ionization-Time of Flight
mdeg	millidegrees
MMPP	Monoperoxyphthalic Acid
MTT	3-(4,5-Dimethylthiazol-2-yl)-2,5-diphenyltetrazolium bromide
nm	nanometers
NMR	Nuclear Magnetic Resonance
ODN	Oligodeoxynucleotide
PCR	Polymerase Chain Reaction

Phen	Phenanthroline
PMSF	phenylmethylsulfonyl fluoride
Rrna	ribosomal Ribonucleic Acid
RNA	Ribonucleic Acid
RU	Response Units
SDS	Sodium Dodecyl Sulphate
SPR	Surface Plasmon Resonance
TAE	Tris-acetate EDTA
Taq	*Thermus Aquaticus* Polymerase
TBE	Tris-borate EDTA
Tm	Melting temperature
TO	Thiazole Orange
TPA	Trans-platinum Planar Amines
TRAP	Telomeric Repeat Amplification Protocol
TRIS	Tetrahydroxymethylaminoethane
TS	Telomerase substrate
UV	Ultraviolet

SUMMARY

The discovery of new anticancer targets is the key factor for the development of more efficacious therapies. Sequence selective binding of double stranded DNA in the classical B form has been extensively employed to target small molecules to defined polynucleotide portions. More recently, ligand recognition of non canonical DNA foldings has been additionally considered a useful approach to selectively target distinct genomic regions. In this connection, G-quadruplexes represent an interesting system since they are believed to be physiologically significant arrangements. These non-canonical DNA structures are found at the ends of the human chromosomes (telomeres) as well as at promoter regions of several oncogenes where there is a cluster of guanine-rich sequences and they are likely to play important roles in the regulation of biological events. The induction and stabilization of the G-quadruplex arrangement by small molecules can lead to the inhibition of the telomerase activity by interfering with the interaction of the enzyme and its single stranded template. A similar molecular mechanism is likely involved in the transcriptional control that leads to the suppression of the oncogene transcription and, ultimately, in the regulation of the gene expression. As a result, the quadruplex topic is very attractive for the development of a specific anticancer strategy defined by a dramatic reduction of side effects, typical of chemotherapy.

The purpose of this work is to investigate the interactions between novel classes of small molecules and different quadruplex DNA sequences and conformations. These new molecules were properly designed providing systematic

atom-wise substitutions based on rational evaluations of previous studied compounds in order to increase their selectivity for G-quadruplex structures and to reduce toxic effects. Biophysical and biological properties of all new derivatives are herein evaluated at molecular and cellular level.

The thesis work is divided into three main sections based on the structural features of the compounds object of study. The first part focuses on heterocyclic dications: upon changing their molecular binding shape, a correlation with G-quadruplex binding have been drawn. In particular it was possible to rationalize a shift in the binding modes, in particular between end stacking and groove recognition. Nevertheless a correlation between biophysical (G-quadruplex affinity) and biological (telomerase inhibition and cytotoxicity) results was not always clear. This feature may suggest the involvement of cellular targets different from the telomere and that are now under investigation.

In Chapter 3, the DNA binding properties of some phenantroline derivatives in presence and in absence of Ni(II) and Cu(II) are investigated. We confirmed that different complex geometries involving one, two or three ligands per metal ion can affect the pattern of DNA recognition by driving nucleic acid conformational changes.

Finally, in Chapter 4 some transplatin derivatives are evaluated. We focused our attention on defining the compounds capability to form adducts, with the nucleic acids, the nature of adducts and the kinetics of adduct formation not only on double strand DNA but also using single strand as well as G-quadruplex as targets. The results showed how different structural modifications can cooperate to greatly affect the potential interaction of the compounds. Interestingly it turned out their preference to react on single stranded DNA portions than to double stranded ones.

This is probably due to an unfavourable orientation of the reactive groups when the molecule interacts with the DNA substrate. As a result, they appear to crosslink unpaired strands. By extending these results at cellular level they can reflect distinct distribution of platination site along the genome in comparison to cisplatin and even transplatin.

The results obtained increment the available knowledge of DNA-small molecules interaction. In particular it emerged that a conserved interaction mode is consistent with biological effects. On the other hand, a shift in the binding mode can drive to different cytotoxic effects. This can provide a rationale for subsequent drug structure optimization leading to the development of new efficient and selective anticancer agents.

RIASSUNTO

La scoperta di nuovi target anticancro è il fattore chiave per lo sviluppo di terapie sempre più efficaci. Lo studio del legame selettivo a sequenze di DNA a doppia elica nella classica forma B è stato largamente impiegato al fine di direzionare piccole molecole verso porzioni polinucleotidiche definite. Più recentemente, il riconoscimento (da parte di ligandi) di porzioni non canoniche di DNA si può tradurre in un metodo vantaggioso per indirizzare questi composti verso regioni distinte del genoma. A tale proposito, le strutture G-quadruplex rappresentano un sistema interessante poiché sono ritenute fisiologicamente significative.

Queste strutture "non-canoniche" di DNA si trovano alle estremità del cromosoma (telomeri) così come in varie regioni promotrici di oncogeni in cui vi è un'abbondante presenza di residui guaninici e sembrano coinvolte nella regolazione di importanti eventi biologici. Pare infatti che l'induzione e la stabilizzazione di strutture G-quadruplex dalle parte di piccole molecole porti all'inibizione dell'attività della telomerasi interferendo con l'interazione tra l'enzima e il suo substrato a singola catena. Un simile meccanismo molecolare è probabilmente coinvolto anche nel controllo della regolazione dell'espressione genica e può portare alla soppressione della trascrizione di un oncogene. Di conseguenza, "l'approccio G-quadruplex" si rivela molto interessante per lo sviluppo di una strategia anticancro specifica caratterizzata anche da una riduzione drammatica degli effetti collaterali, tipici della chemioterapia.

Lo scopo di questo lavoro è lo studio delle interazioni tra nuove famiglie di piccole molecole e diverse conformazioni di DNA G-quadruplex. Queste nuove molecole sono state opportunamente progettate apportando sostituzioni di atomi o gruppi funzionali basate sulla valutazione di composti precedentemente studiati al fine di aumentare la loro selettività per strutture G-quadruplex e di ridurre gli effetti tossici. Le proprietà biofisiche e biologiche di tutti i nuovi derivati sono state valutate al livello molecolare e cellulare.

Il lavoro di tesi si divide in tre parti in base alle caratteristiche strutturali dei composti. La prima parte è dedicata alla studio di dicationi eterociclici: si è cercato correlare modifiche nella conformazione molecolare con l'affinita' verso strutture G-quadruplex. In particolare è stato possibile razionalizzare cambiamenti della modalità di legame in base alla struttura dei composti esaminati. Tuttavia una correlazione fra i risultati biofisici (affinità G-quadruplex) e biologici (inibizione della telomerasi e citotossicità) non è risultata sempre definita. Ciò può suggerire il coinvolgimento di bersagli cellulari diversi dal telomero umano.

Nel capitolo 3, sono state studiate le proprietà di legame al DNA di alcuni derivati fenantrolinici in presenza ed in assenza di Ni (II) e Cu (II). Abbiamo confermato che complessi caratterizzati da diverse geometrie che coinvolgono una, due o tre molecole per ione possono compromettere o meno il riconoscimento del DNA o determinare cambiamenti conformazionali dell'acido nucleico. Per concludere, il capitolo 4 è dedicato allo studio di derivati del transplatino. In particolare ci siamo focalizzati nel definire la capacità dei composti di formare addotti, la natura dei complessi e la cinetica di formazione del complesso non solo con DNA a doppio filamento ma utilizzando anche substrati a singola catena come il G-quadruplex. I

risultati hanno dimostrato come diverse modifiche strutturali possano avere un ruolo importante nell'interazione dei composti con gli acidi nucleici. E' risultata interessante la loro preferenzialità a reagire con porzioni di DNA a singolo filamento rispetto a sequenze a doppia elica. Ciò è probabilmente dovuto ad uno sfavorevole orientamento dei gruppi reattivi quando la molecola interagisce con il substrato di DNA. Di conseguenza, i composti sembrano formare un cross-link tra due filamenti non appaiati. A livello cellulare, questi risultati riflettono una distinta distribuzione del sito di platinazione all'interno del genoma rispetto al cisplatino e perfino rispetto al transplatino.

I risultati ottenuti incrementano la conoscenza disponibile sull'interazione tra DNA e piccole molecole. In particolare è emerso che la conservazione della modalità di interazione si correla con effetti biologici definiti. Al contrario, una variazione della modalità di legame può portare a effetti citotossici differenti. Ciò può fornire una spiegazione razionale per una successiva ottimizzazione della struttura dei composti finalizzata allo sviluppo di nuovi agenti antitumorali efficaci e selettivi.

Chapter 1

OVERVIEW

1. 1. TELOMERES AND TELOMERASE

1. 1. 1. DNA REPLICATION AND THE "END REPLICATION PROBLEM"

The deoxyribonucleic acid (DNA) is a macromolecule that is usually composed by two polymeric strands coupled together to form a double helix. The backbone of a DNA strand is made by alternating phosphate groups and pentose sugars (2-deoxyribose) connected by phosphodiester bonds[1]. The bases, adenine, guanine, thymine and cytosine, are then linked to the sugars by a β-glycosidic bond to form units called nucleotides[2] (Figure 1.1). The two strands of DNA are connected to each other by hydrogen bonds between the bases. These pairings, also known as Watson and Crick bonds, stabilize the double helix and involve a purin and a pyrimidine base. More specifically, an adenine is coupled with a thymine and a cytosine is coupled with a guanine[3]. The strands are also oriented in antiparallel directions: one is directed from the 5' end to the 3' end and the other from the 3' end to the 5' end.

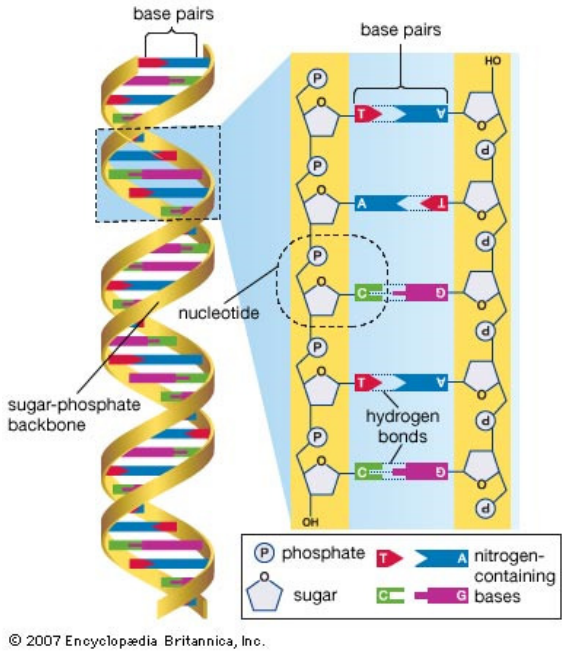

Figure 1.1 DNA double helix and DNA base pairs (www.sciencewithmrmilstid.com/media/basePairs.jpg)

The DNA contains all the genetics information and instructions for development, functioning, surviving and reproducing of all known living organisms and some viruses[4]. For this reason it must be accurately duplicated before each cellular division.

The cell division cycle is the basic tool for the DNA reproduction. It takes place in the nucleus and it is traditionally divided into two periods: the *interphase*, that comprises the G1 (gap1), S (synthesis) and G2 (gap2)[5] phases in which the cell grows in a continuous way, and the *mitosis* (M) phase, during which the nucleus divides itself and produces two genetically identical cells (cytokinesis)[6,7]. During the S phase, DNA replication is driven by the enzyme DNA polymerase. Because this enzyme works only in the 5'—3' direction, the synthesis of the two strands happens with two distinct mechanisms. A strand, called "leading strand", is synthesized continuously while its complement, the "lagging strand", is made by short DNA sequences (between 100 to 200 nucleotides long in eukaryotes) called Okazaky fragments[8]. These sections are then processed to produce a continuous strand of DNA and hence a complete daughter DNA helix[9].

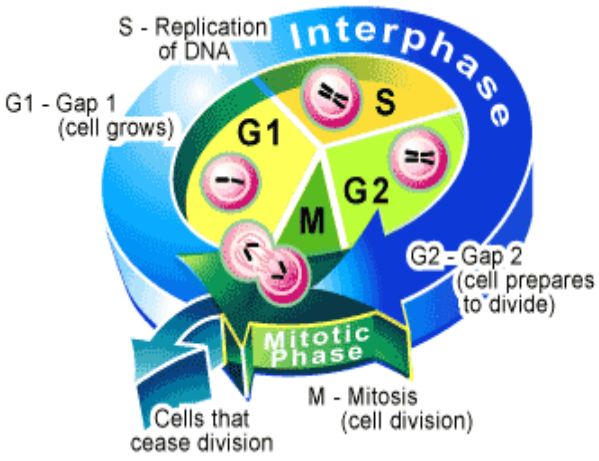

Figure 1.2 Overview of the cell cycle[10]

Since the DNA polymerase is not able to synthesize a chain *ex novo*, it needs an RNA primer with a free 3'-OH group that binds the first nucleotide of the chain that is synthesized. This RNA primer is created by the enzyme primase, and extended by the DNA polymerase III. On the "leading strand" there is only one primer at the beginning of the replication while on the "lagging strand" there are a number of short RNA primers for each fragment. The primer is later removed by endonucleolytic enzymes and the interruptions are refilled by the DNA polymerase and linked together by the DNA ligase, using phosphodiester bonds, to create a continuous strand of DNA. However, the initial primer at the 5' end of the lagging strand cannot be substituted by a complementary DNA sequence because the polymerase enzyme (that synthesizes only in 5'—3' direction) misses the 3'-OH free group to hook the filling sequence. The consequence of this is the unidirectional growth of the new DNA chain and the synthesis of a DNA strand with an incomplete 5' end and a double strand with the 3' extremity that protrudes the 5'. This means that at each replication cycle there is a lack of genetic material (from 50 to 200 bases) due to the "end replication problem"[11]

Unicellular organisms and viral genomes have evolved special mechanisms to overcome the "end replication problem" by simply eliminating the ends (circular chromosome of *Escherichia coli* and simian virus 40), or priming initiation with repeat sequences at the ends of the chromosome (bacteriophage T7) or linking a terminal protein to a nucleotide primer (adenovirus)[12]. Eukaryotic cells, in contrast, have specialized structures that allow completion of the replication of the end of the linear chromosomal DNA molecule.[13] [14] These structures are known as telomeres.

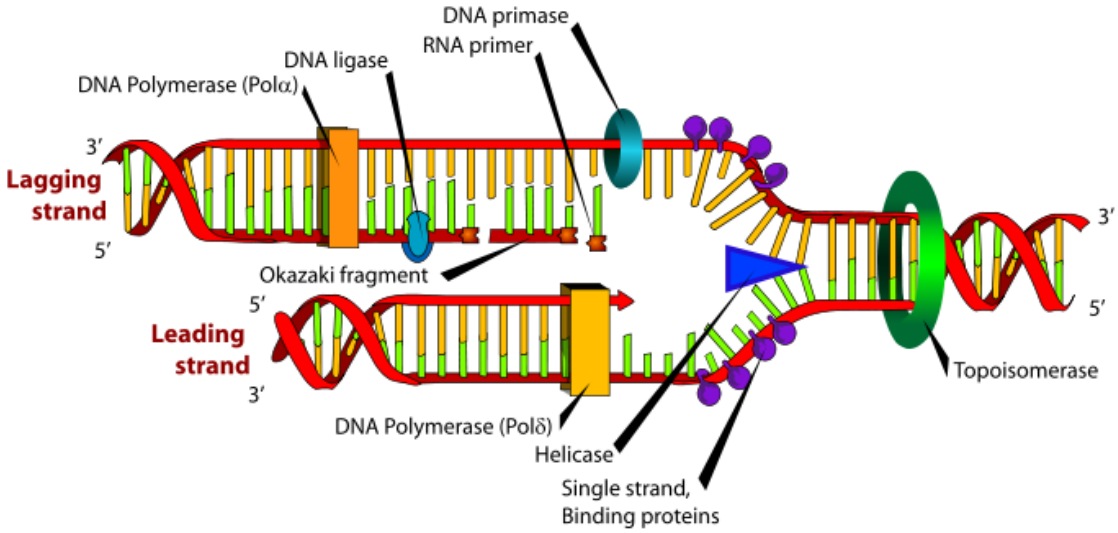

Figure 1.3 Schematic representation of the replication fork

1. 1. 2. TELOMERES

Telomeres (Figure 1.4) are nucleoproteic complexes located at the end of the chromosomes of eukaryotic cells. They were first described by Hermann Muller in 1938[15]. He coined the term "telomere" which comes from the Greek *telos*, meaning end, and *meros*, meaning part[16]. The telomeric sequence varies depending on the organism. In humans, the DNA content of the telomeres consists of tandem repeat of a G-rich sequence (TTAGGG[17,18]) oriented 5' to 3' towards the end of the chromosome.[19]. They are partially double stranded but end with the 3' portion that overhangs the 5' for about 50 to 400 nucleotides[16].

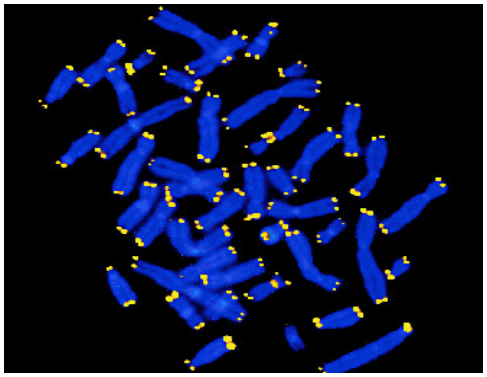

Figure 1.4 Telomeres of human chromosomes (yellow) are shown by *in situ* hybridization with a telomeric probe (cmb.duke.edu/images/rotating/counterpic2.jpg)

It is known from electron microscopy studies that this overhang can loop back and integrate into the duplex repeat track to form a "t-loop"[20] (Figure 1.5), a structure that seems to play a role in preserving the chromosome stability. In fact, it has been recently reported that the destabilization of the t-loop, resulting in the exposure of the 3' end, is recognized by the cell as a DNA damage signal and can start the senescence process that leads to the cell death[21]. For this reason the telomere structure includes some proteins that stabilize the t-loop structure.

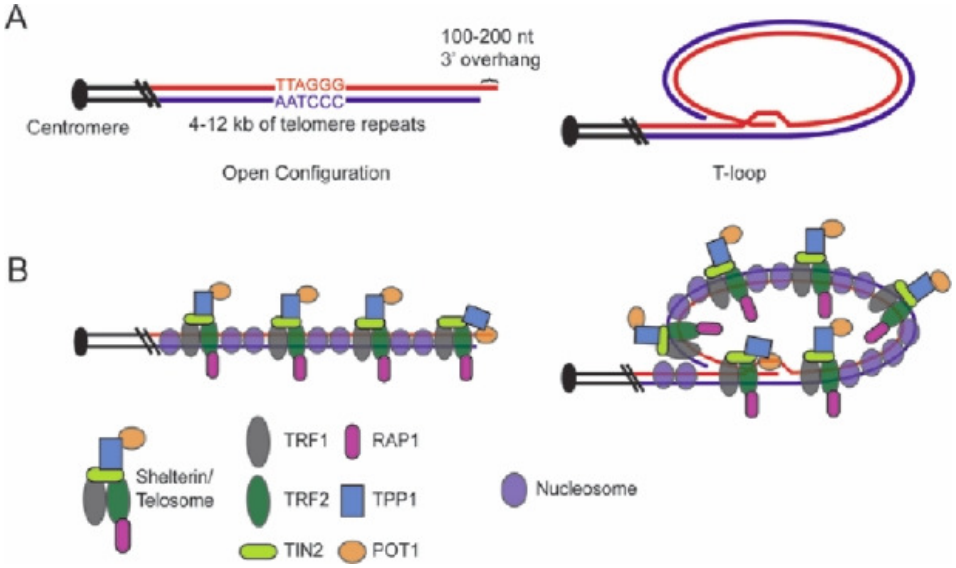

Figure 1.5 Schematic representation of the human telomere[22]

Both the telomeric DNA and the protein complexes associated act as an "end capping" and protect the chromosome from degradation by exonucleases and from end fusions by ligases. Moreover, they help to avoid recombination phenomena that can lead to the formation of dicentric chromosomes. They also play a role in the spatial and functional organization of the chromosome inside the nucleus to promote its separation during the cell division resulting in a key function for the number of

divisions that the cell can stand. Some examples of these proteins include TRF1[23,24], TRF2[25,26] and POT1 that bind directly to the telomeric repeat, the POT1 (Protection of Telomeres 1) that specifically recognizes the single strand DNA; hRAP1 and TIN2 that bind non directly to the telomeric DNA and others like DNAPKcs than can repair DNA damages. These proteins are involved in the modulation of the telomere length and can interact with each other or work synergistically.

1. 1. 2. 1. Cell proliferation potential and telomere length

As previously mentioned, cell replication leads to a telomere shortening of about 30-200 bases at each round of cell division due to the end replication problem. After a number of cycles, the telomeres reach a critical length named Hayflick limit (or phase M1)[27,28] and are no longer able to form secondary structures. However, at this limit, several bases (100) are still protecting the chromosome ends. At this time the cell stops the reproduction cycle and enters in a non-diving state called senescence by activating p53 or by inducing the pRb pathway. If the genes that codify for proteins involved in the cell proliferation control (p53 or pRb) are mutated or if their actions are compromised, the cell can overcome this phase and keep dividing and the telomeres will keep shortening until they reach the second crisis phase (M2). In this case, the chromosome ends are no more protected and the cell is destabilized and dies by apoptosis. If this mechanism is inactivated and the cell can prevail the crisis phase, it can acquire the ability to infinitely replicate itself and become immortal. The main event that can lead to the overcoming of phase M2 is the activation of the telomerase, an enzyme that is not expressed in the somatic cells and is in charge of the maintenance of length of the telomere.

1. 1. 3. TELOMERASE

Telomerase is an enzyme first identified by Carol Greider and Elisabeth Blackburn in 1985 in the ciliate protozoa, *Tetrahymena*[29]. Together with Jack Szostack, Greider and Blackburn recently awarded the 2009 Nobel Prize in Physiology and Medicine[30] for their studies about this enzyme and its role in cancer disease.

1. 1. 3. 1. Structure and mechanism of action of telomerase

Telomerase is an RNA-dependent DNA polymerase known to be almost universally conserved in eukaryotes. It is a ribonucleoprotein enzyme composed of a minimal catalytic core which includes two subunits: the TERT protein and an RNA component (TERC or TR)[31,32].

The human proteic subunit (hTERT) is a heterodimer composed by the proteins p123 and p43 that binds the RNA (TR) with a ratio of 1:1:1. It is the catalytic subunit[33] of the enzyme and acts as a reverse transcriptase in the C-terminal domain[34]. Its active site is characterized by aspartic acid triplets and the sequence in general is very similar to those of viral reverse transcriptases[35].

The human ribonucleic subunit (hTERC) is a large RNA composed by 451 nucleotides in humans and between 148 and 209 in the ciliates[36]. It contains a small portion of 11 nucleotides (CUAACCCUAAC in human), located at the 5' end, that encodes the cognate telomere repeat and functions as a template for the additions of nucleotides at the end of the chromosome[31].

The processive nature of the enzyme in the *Tetrahymena,* for example, is a 60 minute in vitro reaction that produces more than 2000 nucleotides[31]. The elongation

of the telomere happens in several steps[11] : 1) the 11 nucleotides fragment from hTERC is hybridized with its complementary sequence at the 3'end of the telomeric DNA; 2) addition of TTAGGG segments to the 3' end (nucleotide addition progressivity); 3) upon reaching the 5' end template boundary, translocation and repositioning of the 3' end of the DNA and recognition of the 3' template boundary and 4) subsequent rounds of elongation.

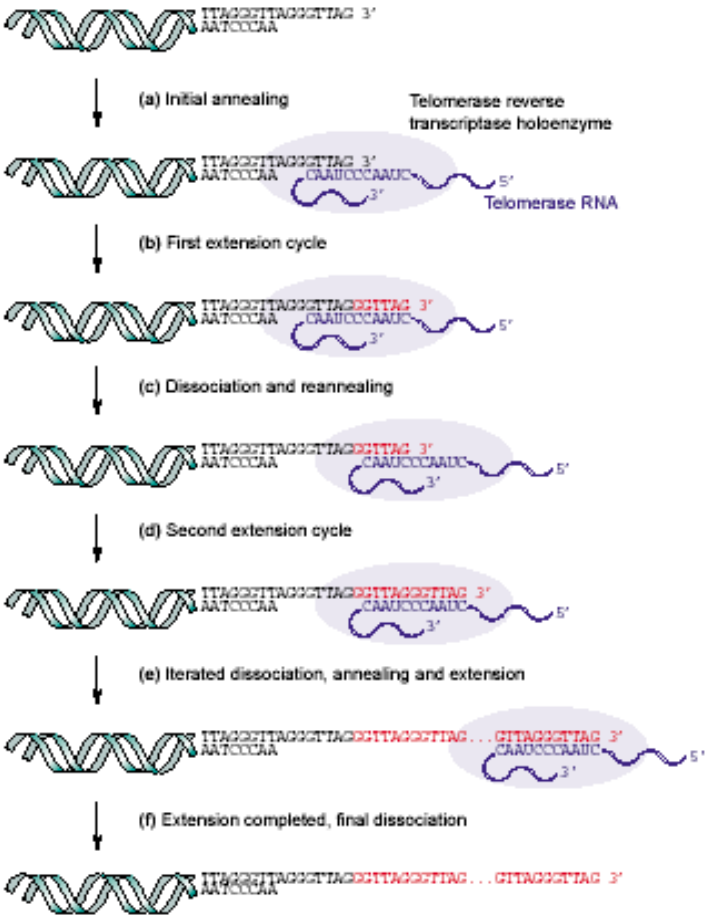

Figure 1.6 Mechanism of action of the telomerase enzyme[37]

Telomere processivity can also be influenced by factors like temperature, substrate concentrations, primer sequence and G-quadruplex interacting agents[38,39]. Transcriptional regulation can also be modulated by proteins that interact with the

enzyme or with the telomeric DNA, by some oncogenes (*c-myc*), by phosphorilation of the hTERT subunits (that activate the enzyme)[34] or by the assembly of the telomerase subunits.

With this mechanism, telomerase helps to stabilize the telomere length in human stem cells, reproductive cells[40] and, most dangerous, in cancer cells[41,42]. The enzyme is also known to be expressed in eukaryotic parasites such as *Plasmodium*, *Trypanosoma* and *Leishmania*[43,44], however, it is inactive in most normal somatic cells. This means that the inhibition of the telomerase enzyme can provide a potential specific target for the treatment of cancer and parasitic diseases and can help to avoid the typical side effects of current chemotherapy.

1. 1. 3. 2. Telomerase and cancer

It is important to highlight that the chromosome ends of the tumor cells are morphologically different than the telomeres of normal somatic cells. As previously mentioned, the somatic telomeres are continuously affected by the end replication problem due to incapability of the DNA polymerase to completely replicate the "lagging" strand. The tumor cells, in contrast, have shorter telomeres (4-6 kilobases) but with approximately constant length. Furthermore, telomerase expression in somatic cells is limited to those characterized by high replication frequency, like germinal and hematopoietic, while the enzyme is active in 80-85% of cancer cells. For this reason the telomerase represents an ideal target for the anticancer strategy.

The inhibition of the telomerase leads to a block in the maintenance of telomeres stability. They undergo a progressive shortening until they reach a critical point that means the end of the cellular proliferation[45,46]. Because there is a loss of

50-200 nucleotides at each replication round, the telomere critical length will be reached after a certain number of cycles and a relative long time period (120 days)[47]. Therefore this approach can be used as support therapy after surgical cancer removal or as prophylaxis or prevention at the first stages of the disease. Another point to consider is the existence of non cancer cells telomerase-positive but, due to the different length of the telomeres and to the different rate of replication between tumor and somatic cells, there is a therapeutic window in which "antitelomerase" agents are effective without alterations of the somatic cells.

Table 1.1 Telomerase and cancer. Percentage of telomerase positive cells in different cancer types

Cancer type	% positivity
Breast	85
Prostate	80
Lung	73
Colon	96
Ovary	93
Kidney	74
Stomach	85
Bladder	97
Neuroblastoma	70
Glioma	75
Head and neck	87

1. 2. G-QUADRUPLEX STRUCTURES

The human telomere single strand DNA is characterized by a tandem repeat of the TTAGGG sequence. Interestingly, it is known by *in vitro* studies that G-rich sequences can easily form G-quartet complexes[48]. These are planar arrays in which four guanines are coupled together by a network of Hoogsten bonds (hydrogen bonds

that differ from Watson and Crick's for the involvement of the nitrogen in 7 position of the guanine). These tetrads are stabilized by the presence of a monocationic atom such as Na^+ or K^+ that coordinates the electronegative carbonylic oxygens provided by the guanines[49] (Figure 1.7).

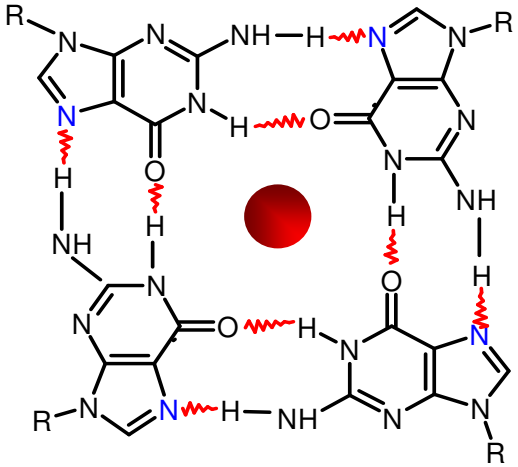

Figure 1.7 Representation of a guanine tetrad stabilized by a monovalent cation (red)

The overlapping of G-quartet tetrads leads to the formation of more complex structures called G-quadruplexes. These high ordered structures cannot be recognized by the enzyme telomerase as it acts only on the single strand template. For this reason, the hybridization of the RNA template onto the primer is prevented and the telomerase activity is then inhibited[48]. The development of small molecules that can drive the formation of the G-quadruplex structure and selectively stabilize this conformation (Figure 1.8) is therefore an interesting approach for an indirect inhibition of the telomerase enzyme, resulting in a potential anticancer strategy. Moreover, the same tandem TTAGGG sequence of the human telomere has been found in some eukaryotic parasites in which the enzyme is expressed[43,44] .

Telomerase inhibition through the induction of G-quadruplex structures can then be an interesting target for the development of antiparasitic agents against

malaria and African sleeping sickness. G-rich strands are also present in different regions of the human genome like promoter sequences of oncogenes such as *c-myc*, *bcl-2*, *c-myb*, *c-Fos*, *c-ABL,* the insulin gene[50], the introne region of the gene hTERT, and others[51]. Their ability to form G-quadruplexes can play a role in the regulation of the gene expression[52]. At this level the G-quadruplex structure seems to be involved in the transcriptional control that leads to the suppression of the oncogene transcription when it is conformational folded[53]. To this end, direct evidences of the G-quadruplex involvement in the transcriptional control are provided by *c myc* and by the insulin gene. In addition to this, the formation of G-quadruplexes has been recently found in the ribosomal DNA and seems to have a potential role in the rRNA biogenesis[54]. Nucleolin, an abundant nucleolar protein[55], is associated with rDNA *in vivo* and it is required for rRNA synthesis. It shows a nanomolar affinity for G-quadruplex structures and thus may bind and stabilize them to increase the rate of polymerase I transcription[56]. For this reason, the nucleolin-quadruplex rDNA complex can be also considered an interesting target for the inhibition of polymerase I transcription and a novel approach for selective interference with cancer cell proliferation[57].

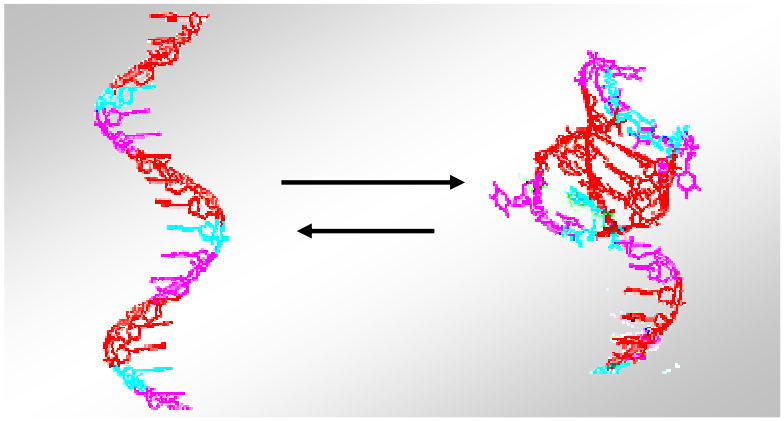

Figure 1.8 Telomeric DNA in equilibrium between linear and folded structure: guanines are represented in red, thymines in pink and adenines in turquoise

1. 2. 1. Classification of G-quadruplex structures

Structural information of the human telomeric G-quadruplex formed under physiologically relevant conditions is necessary for structure-based rational drug design. These structures are characterized by a high polymorphism and it has been reported that there are 26 possible topologies of G-quadruplexes, but only a few[58] have been observed *in vitro*[59]. They can be classified in subclasses according to different structural parameters.

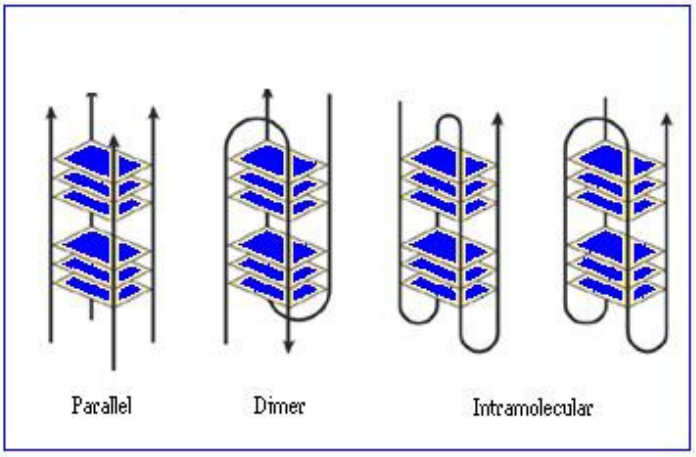

Figure 1.9 Possible G-quadruplex structures inter and intramolecular. Parallel (on the left) is a tetrameric structure made by the association of four strands with parallel orientation; Dimer structure made by two hairpin strands; Monomeric intramolecular structure made by a folded single strand

1. 2. 1. 1. Monovalent cation

Although the structure appears to be stabilized by a hydrogen-bonding network involving N7:N2H and O6:N1H, the central core of the tetrads produces a specific arrangement of lone pairs of electrons from the four GO6, which can coordinate a monovalent ion of the correct size, such as Na^+ or K^+[60]. The smaller Na^+ ion can sit in the plane formed by these atoms, whereas the larger K^+ requires a nonplanar component, which may in fact lie between two such G-quartets (for

example, a metal ion.). The type of monovalent cation contributes also to the geometry of the conformation.

1. 2. 1. 2. Orientation of the chains

The G-quadruplex structure can be formed by one unique G-rich strand (intramolecular) or by the assembly of more chains (intermolecular)[61]. In both cases, they can be oriented in four ways:

1. the chains can be all parallel
2. three chains can be parallel and one antiparallel
3. two adjacent chains are parallel and the other two adjacent are antiparallel
4. two alternating parallel and antiparallel chains

Usually, G-quadruplexes made of four different chains are parallel while in the other cases the orientation depends on the loops.

1. 2. 1. 3. Stoichiometry of the chains

A general single strand sequence that can fold in an intramolecular G-quadruplex is this: $G_mX_nG_mX_0G_mX_pG$, where m is the number of guanines involved in the tetrad formation and X consists in any other base, usually thymine or adenine, which contribute to the connection loops.

Dimeric structures are usually formed by two identical sequences while tetrameric structures can form more complex sequences, intra or bimolecular, according to the experimental conditions.

1. 2. 1. 4. Loops geometry

Connection loops are usually divided in four types:

1. “Edgewise loops”, that connect two adjacent strands
2. “Diagonal loops”, that connect two opposite antiparallel strands
3. “Double chain reversal loops”, that connect two adjacent parallel strands
4. “V-shaped” loops, that connect the angles of two overlapped guanine tetrads with a connection missing

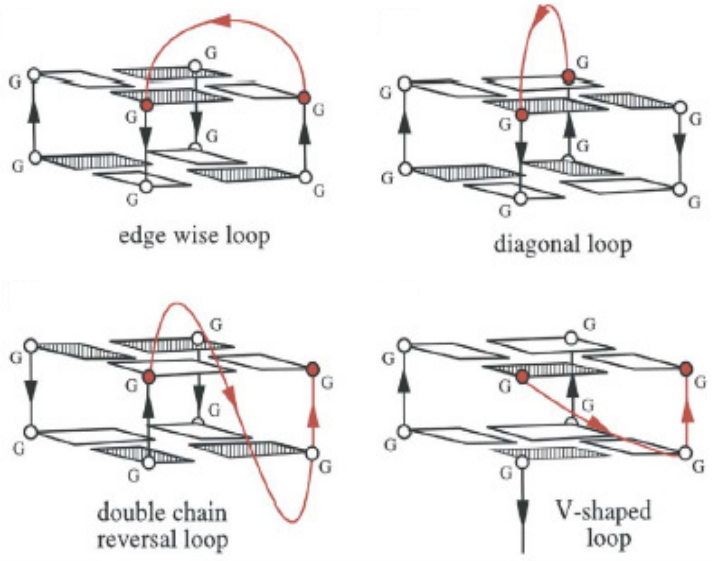

Figure 1.10 Possible connection loops in the G-quadruplex structure[49]

1. 2. 1. 5. Glycosidic conformation

The guanosines involved in the formation of the G-quadruplex structure present a glycosidic conformation that differs from one in the B-form DNA because the sugar orientation can be *syn* or *anti.* Generally in the intermolecular structures (parallel), the guanines are in *anti* conformation while in the intramolecular antiparallel quadruplexes *syn* and *anti* are alternated.

Due to the glycosidic bond conformation in the B-form DNA, the presence of a major and a minor groove is clearly defined, while in the G-quadruplex the

overlapping of the tetrads generates grooves that are not always different[61]. More specifically, if all the chains that forms the quadruplex are parallel (*anti* conformation) the four grooves will be medium width and symmetrical but if the chains are antiparallel the grooves can show different sizes. For example, if there are two parallel and two antiparallel chains adjacent one to each other, the guanines from adjacent parallel chains will have the same glycosidic torsional angle and will generate medium size grooves, while the guanines from antiparallel adjacent chains will have opposite torsional angles and will generate grooves that are large and narrow. If there is an alternation of parallel and antiparallel chains two grooves will be wide and two will be narrow.

1. 2. 2. Telomeric G-quadruplex

The human telomeric sequence is highly conserved. In potassium solution it can form two different intramolecular hybrid types in equilibrium to each other.[62] The intramolecular human telomeric G-quadruplex structure in sodium solution was reported by NMR using the 22 nucleotides human telomeric sequence 5′-AGGG(TTAGGG)3[63] (Figure 1.11.a). The wtTel22 is a four G-tract human telomeric sequence with a 5′-flanking-A and no 3′-flanking sequence. Its conformation in sodium solution is a basket-type, mixed antiparallel/parallel stranded intramolecular G-quadruplex, consisting of three G-tetrads connected with one diagonal and two lateral TTA loops. More recently, a crystal structure of the same sequence in potassium solution has been reported showing the parallel orientation of three G-tetrads connected with three symmetrical side double-chain-reversal TTA loops[64] (Figure 1.11.b). However, the wtTel22 sequence in potassium solution does not form a single G-quadruplex structure. NMR data indicate the presence of multiple

conformations, in equilibrium between hybrid-1 and hybrid-2, and this equilibrium appears to be largely determined by the 3′-flanking sequence[65,66] (Figure 11.1.c). Nevertheless, it seems that this hybrid structure coexists with another antiparallel conformation called “chair-type” (hybrid-3) and can switch to this one by a change in the 5’ end orientation[67].

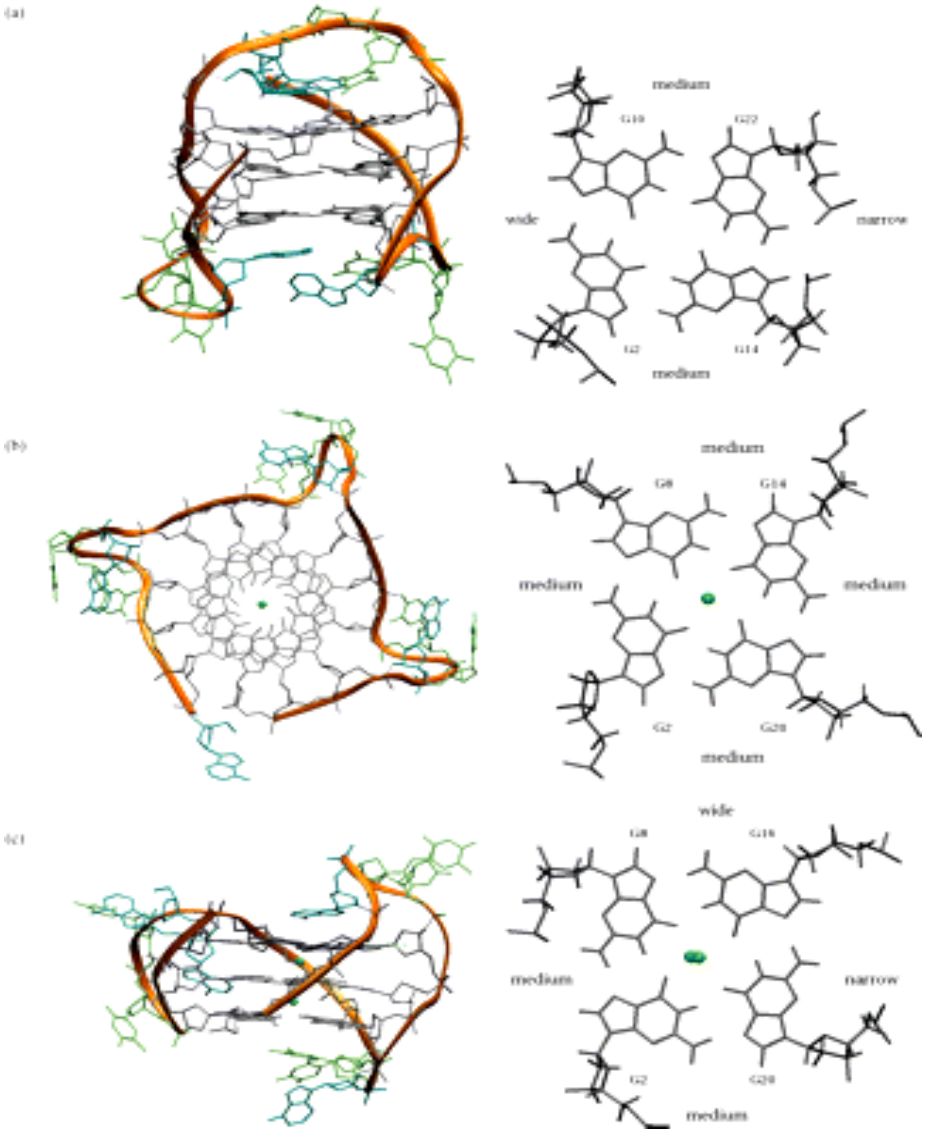

Figure 1.11 Structures of the human telomeric quadruplex formed from the sequence d[AGGG(TTAGGG)$_3$][68]. In each case two views are shown (**a**) one of the deposited structures of the Na^+ form, determined by NMR[63], with a diagonal and two lateral loops. (**b**) K^+ form A, determined by crystallography[64,] with three strand-reversal loops (**c**) K^+ form B, showing the topology determined by NMR[66], with one strand-reversal and two lateral loops

1. 2. 3. G-quadruplex in the promoter region of the *c-myc* oncogene

The oncogenes of the *c-myc* family codify for some phosphoproteins involved in the activation of genes that promote the growth of cancer cells. Moreover, they are known to play a fundamental role in the apoptotic process[69]. In humans, *c-myc* is highly regulated and alterations in its transcription can result in the development of several malignant tumor including cancer of the colon, lungs, breast, cervix, B and T cell lymphomas, osteosarcomas, glioblastomas, and myeloid leukemias[70,71,72].

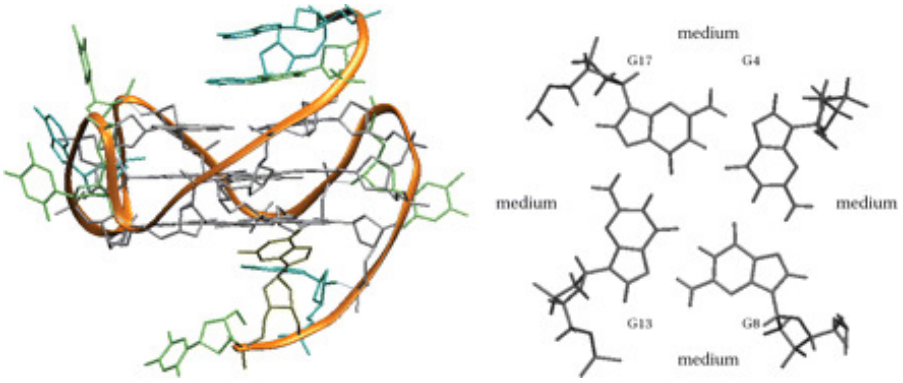

Figure 1.12 NMR-derived topology and one of the deposited structures of the *c-myc* quadruplex[73]

The gene is regulated by four different promoters, however there is an element that has a higher control and it is located on the P1 promoter. This element, known as Nuclease Hypersensivity Element (NHEIII3), consists of a 27 base pairs sequence and it is in charge of the control of more than 90% of the transcriptional activity of the gene. NHEIII3 is a duplex sequence. It has a purine rich strand characterized by guanine tracts, some of them made by 3-4 guanines each. It seems that in the presence of K^+ this double strand sequence can interconvert into an equilibrium between quadruplex and unwound structures. When the sequence is double stranded or unwound, gene transcription results active but when the

equilibrium is shifted towards G-quadruplex conformations (with the aid of the accessory factor NM23-H2), the transcriptional repression occurs and gene expression is silenced[74]. Small molecules that can stabilize the transcriptionally silent DNA forms and avoid their interconversion to the duplex state may play an important role as transcriptional repressors, preventing the expression of the *c-myc* oncogene, and resulting into another selective drug design approach.

1. 3. G-QUADRUPLEX AS A THERAPEUTIC TARGET

The induction and stabilization of G-quadruplex structures can indirectly inhibit the telomerase by interfering with the interaction of the enzyme and the single strand template. Due to a network of reversible bonds, quadruplex DNA can exist as an equilibrium between the single stand and the overlapped structure. If a small agent is able to shift this equilibrium towards the folded conformation, the substrate will not be approachable by the telomerase resulting in a specific approach.

Several ways of interactions have been identified:

- "stacking" with the external tetrads or intercalation between internal tetrads (by π-π interactions of aromatic rings)
- "edge recognition" with atoms that are external to the G-quartet
- interaction with single strand loops
- simultaneously end stacking and loop interaction or simultaneously end stacking and binding into the grooves

G-quadruplex ligands are generally characterized by two common features:

1) An extended planar aromatic cromophore that mimic the planar surface of the G-quartets. This is also the typical core of double helix intercalators. However,

since the plane identified by two bases in the duplex is smaller than a G-quartet tetrad, compounds with a more extended planar array can interact more selectively with the quadruplex DNA.

2) Lateral chains with positive ionizable groups located on different aromatic rings that can bind to phosphate groups of the backbone or to the loop bases or to the grooves, stabilizing the interaction.

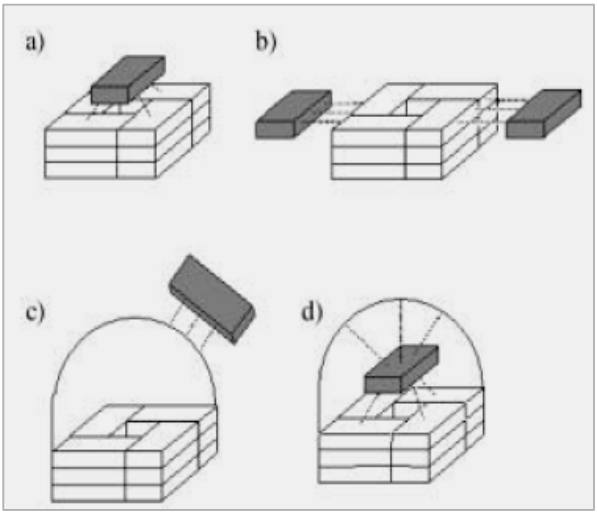

Figure 1.13 Schematic representation of possible ligand-quadruplex binding modes a) "face" recognition, by end stacking or intercalation between internal tetrads b) "edge" recognition; c) interaction with single strand loops d) simultaneously end stacking and loop interaction or simultaneously end stacking and binding into the grooves

1. 3. 1. Compounds that act on the quadruplex DNA

The first molecule known to stabilize the G-quadruplex conformation and inhibit the telomerase activity is the antraquinone BSU1051[75,76]. Besides this ligand, several families of compounds, synthetic and natural, have been evaluated as efficient G-quadruplex binders[77,78,79]. These compounds include acridines such as BRACO 19, anthraquinones, fluorenones, perylenes (PIPER and derivatives), cationic porphyrins like TMPyP4 and TMPyP2, dibenzophenathrolines and macrocycles such as telomestatin, a potent telomerase inhibitor with an IC_{50} of 5nM. A new fluoroquinolone derivative, CX-3543, that interacts with the formation of the complex nucleolin-quadruplex rDNA, is currently in phase II of clinical trials, showing a broad

range of *in vitro* antiproliferative activity (against 80 cell lines) and *in vivo* antitumor ability with no toxic effects at efficacious doses[57].

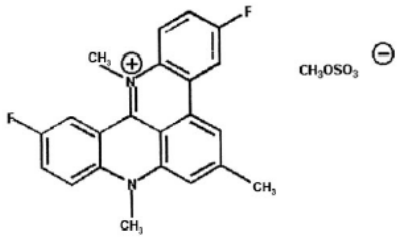

Figure 1.14 Chemical structure of pentacyclic acridine RHPS4

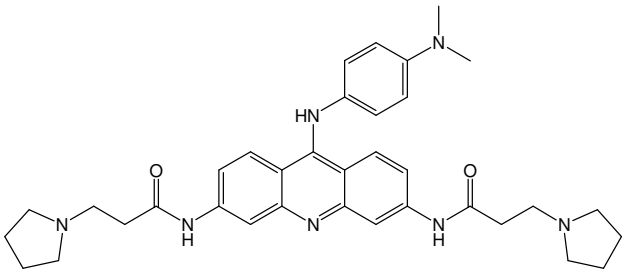

Figure 1.15 Chemical structure of compound BRACO-19, an acridine derivative 3, 6, 9 substituted

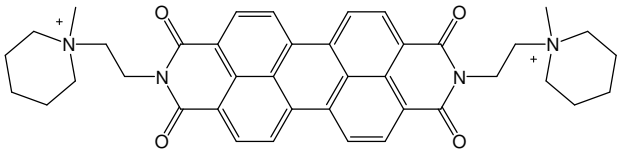

Figure 1.16 Chemical structure of the perilene

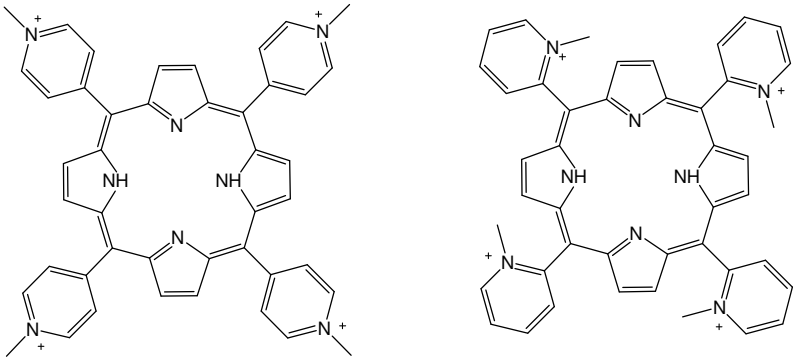

Figure 1.17 Chemical structures of the cationic porphyrins TMPyP4 (left) and TMPyP2 (right)

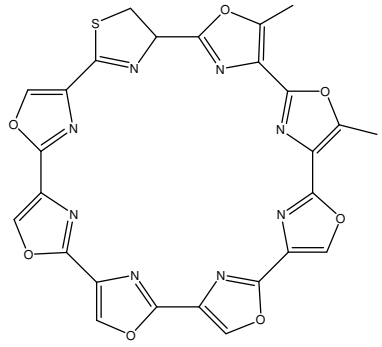

Figure 1.18 Chemical structure of the macrocycle

1. 4. OBJECTIVES OF THIS THESIS

The discovery of new anticancer targets is the key factor for the development of more efficacious therapies. For this reason, G-quadruplex represents an interesting biologically relevant system and an attractive strategy for indirect inhibition of telomerase. The most important goal in the screening is to find a molecule that selectively interacts to this particular structure with little affinity for the double helix. Since the majority of known quadruplex binders have been derived from prototype duplex intercalators, they may exhibit only a little selectivity for quadruplex over duplex structures. This issue leads to a non-specific cytotoxicity that generates the typical side effects of chemotherapy. Moreover since potential quadruplex folding sequences have been found in different regions of the human genome, selectivity for a particular quadruplex conformation is another important concern for the design of new targeted agents.

The purpose of this work is to investigate the interactions between novel classes of small molecules of quite varied structure and different quadruplex DNA sequences and conformations. A particular interest in this screening is to focus on structure-specific binding modes. In Chapter 2 a number of heterocyclic diamidines were investigated. A first screening of the compounds was performed to see how the shape can influence the binding properties and drive the selectivity towards quadruplex versus duplex structures. The second part of the Chapter concerns on the evaluation of a selected compound (DB832) and some derivatives as potential groove binders for human telomeric quadruplex DNA. Indeed, the quadruplex grooves represent attractive targets as they are different from the duplex grooves, and because their dimensions can also vary according to the type of quadruplex sequence.

Chapter 3 focuses on phenatroline-metal complexes as potential quadruplex binders and stabilizers. Peculiar DNA recognition properties are common to phenthroline derivatives. Although phenatroline is a poor G-quadruplex ligand, the fact that it can coordinate metal ions, favoring the formation of extended aromatic systems, has recently turned out in an improved recognition of the quadruplex array. We were interested in evaluate if that DNA-binding can be modulated by different coordinating cations or complex geometries.

Chapter 4 deals about transplatinum derivatives in which the canonical aminic group is replaced with a heterocyclic planar system giving rise to a new group of derivatives called trans-platinum planar amines (TPA). The aim of this chapter is to characterize by biophysical techniques the effects of these modifications on DNA binding and reactivity.

Biophysical and biological properties of all new derivatives have been evaluated at molecular and cellular level. Data were collected by powerful techniques such as thermal melting assay, UV and fluorescence spectroscopy, biosensor surface plasmon resonance, circular dichroism and mass spectrometry. Biological studies such as TRAP assay, inhibition of Taq polymerase enzyme and cytotoxicity with different series of cancer cells were also performed to complement the biophysical data.

The results will be used to select active compounds and suggest rational approaches to work out novel biochemical probes and diagnostic tools in addition to new chemical entities for drug design and development.

Chapter 2

HETEROCYCLIC CATIONS AS POTENTIAL ANTICANCER AGENTS: AN APPROACH THAT TARGETS G-QUADRUPLEX WITH DIFFERENT BINDING MODES

2. 1. INTRODUCTION AND AIM OF THE WORK

Over the past 50 years, the concept that DNA can assume alternative conformations has been demonstrated and the elucidation of their importance in biological functions has been investigated with substantial progress[80]. These structural transitions depend on the local DNA sequence and are brought by changes in ionic strength, salt composition, pH and also interactions with small molecules[81]. An example of a biologically important conformational switch from duplex DNA is provided by G-quadruplex structures. G-quadruplexes are overlapped planar arrays in which four guanines are coupled together by a network of Hoogsten bonds and stabilized by the presence of a monocationic atom such as Na^+ or K^+. These non-canonical DNA structures are found at the ends of human chromosomes (telomeres) as well as at promoter regions of many oncogenes where there is a high population of guanine-rich sequences. The G-quadruplex structures are likely to play important roles in the regulation of biological events[82]. The induction and stabilization of a G-quadruplex arrangement by proteins or small molecules can lead to the inhibition of the telomerase activity by interfering with the interaction of the enzyme and its single stranded telomere template[83]. Quadruplex structures can participate in transcriptional control that leads to the suppression of oncogene transcription and, as a result, in the regulation of the gene expression[84]. G-quadruplexes are also commonly found in DNA aptamers (Thrombin Binding Aptamer) which have been identified by selection process to bind specific targets[85 86]. In addition to this, the formation of G-quadruplexes has been recently found in ribosomal DNA and seems to have a potential role in the rRNA biogenesis[87]. The polymorphic nature of this

system[88] and the significant structural differences with duplex DNA make the quadruplex structures very attractive not only for the development of a specific anticancer strategy but also for a dramatic reduction of side effects, typical of chemotherapy[89].

This second Chapter collects all the results of the work performed at Georgia State University (Atlanta) under the supervision of Prof. David Wilson. It is divided in three sections (subchapters). In the first one we investigate if the molecular binding shape of the heterocyclic diamidines under evaluation can play a role in driving the interaction to the quadruplex over the duplex DNA. The second one is focused on a molecule (DB832) which turned out to be a good quadruplex grooves binder and all the studies that we performed to prove this particular binding mode. The third session is about design and evaluation of some DB832 structural derivatives with the goal of understanding the structural elements of this compound contributing to G-quadruplex recognition through grooves interaction.

2. 2. MATERIALS AND METHODS

2. 2. 1. Instrumentation

Table 2.1 Instrumentation used

CARY 300 Bio UV Visible Spectrophotometer	Varian
CARY Eclipse Fluorescence Spectrophotometer	Varian
Spectropolarimeter J-810-150S	Jasco
Accumet® pH Meter 910	Fisher Scientific
BIACORE® 2000	GE Heathcare Life Sciences
ESI-Q-TOF Mass Spectrometer	Waters Micromass
4800 MALDI TOF-TOF	Applied Biosystem, Inc

2. 2. 2. Synthetic oligonucleotides and compounds

The biotin-free and 5'-biotin labeled lyophilized oligonucleotides were purchased from Integrated DNA Technologies (IDT) with HPLC purification and mass spectrometry characterization. The concentration of oligonucleotides was determined by UV-Vis from absorbance at 260 nm using molar extinction coefficient obtained from nearest-neighbor principle. The G-quadruplex DNA sequences were dissolved in buffer to the desired concentration, heated at 90 °C for 5 minutes and cooled slowly to insure the folding of the sequence prior to each experiment.

F1190 was purchased from Life Chemicals. Thiazole Orange and TMPyP4 were purchased from Mid-Century Chemicals.

The syntheses and purifications of DB compounds were performed by Dr. David W. Boykin's group at Georgia State University, Atlanta, Georgia (USA) and will be reported elsewhere. Appropriate stock solution of each compound was prepared in double deionized water and diluted to required concentrations with appropriate

buffer. Compounds were characterized by UV-Vis to determine their extinction coefficients. Quartz cuvettes with 1 ml of water were used. A blank spectrum was recorded and compounds at known concentrations were titrated into the water. Spectra were registered for the water solutions from a wavelength of 230 to 600 nm. The absorbance at the maximum point was plotted as a function of the compound concentration to determine the extinction coefficient.

Table 2.2 Oligonucleotide sequences used

Tel22 (22mer):	5'-AGG-GTT-AGG-GTT-AGG-GTT-AGG-G-3'
Hybrid 1 (23mer):	5'-TAG-GGT-TAG-GGT-TAG-GGT-TAG-GG -3'
Hybrid 2 (23mer):	5'-AGG-GTT-AGG-GTT-AGG-GTT-AGG-GT-3'
Tel24 (24mer):	5'-TTG-GGT-TAG-GGT-TAG-GGT-TAG-GGA-3'
Tel26 (26mer):	5'-AAA-GGG-TTA-GGG-TTA-GGG-TTA-GGG-AA-3'
TTGGGG (24 mer)	5'-TTG-GGG-TTG-GGG-TTG-GGG-TTG-GGG-3'
***c-myc* (19 mer):**	5'-AGG-GTG-GGG-AGG-GTG-GGG-A-3'
***c-myc* (21 mer):**	5'-TAG-GGT-GGG-GAG-GGT-GGG-GAA-3'
AATT seq with T4 loop:	5'-CGG-AAT-TCG-CTT-TTG-CGA-ATT-CCG -3'
ODN 4	5'-AGG-GTT-AGG-GTT-AG^{Br}G^{Br}-G^{Br}TT-AGG-G-3'
ODN 9:	5'-AG^{Br}G-GTT-AG^{Br}G-GTT-AGG-GTT-AG^{Br}G-G-3'

Table 2.3 Oligonucleotide sequences used for Surface Plasmon Resonance experiments

Biotin labeled HTel G4:	5'-Biotin-AGG-GTT-AGG-GTT-AGG-GTT-AGG-G-3'
Biotin labeled *c-myc*:	5'-Biotin-AGG-GTG-GGG-AGG-GTG-GGG-A-3'
Biotin labeled AATT:	5'-Biotin-CGG-AAT-TCG-CTT-TTG-CGA-ATT-CCG -3'

2. 2. 3. Buffers

The buffers have been prepared using MilliQ water and then filtered:

TK 10/50: 10 mM Tris, 50 mM Potassium Chloride, pH 7.5

SURFACE PLASMON RESONANCE BUFFER (HBS): 10 mM Tris, 50 mM Potassium Chloride, P20 0.015 %, pH 7.0

MASS SPECTROMETRY BUFFER: Ammonium Acetate 50 mM, pH 7.0

2. 2. 4. Thermal Melting Studies

Thermal denaturation studies were conducted on a Cary 300 Bio UV Visible Spectrophotometer in quartz cuvettes of 1 cm pathlength. A cuvette with only buffer was required. The other cuvettes were filled with a 3 μM DNA solution and different ratios of compound-DNA solutions in 10 mM Tris and 50 mM KCl buffer at pH 7.5. The absorbance of the oligonucleotides was detected at 295 nm for quadruplex and at 260 nm for duplex DNA as a function of temperature. Four scans were run for each measurement (melting from 25 °C to 90 °C, annealing from 90 °C to 25 °C and again melting from 25 °C to 90 °C and annealing from 90 °C to 25 °C). A melting curve was obtained for each of them. The melting temperature value (Tm) was recorded from the first derivative of the melting curve values. ΔTm values at 4:1 ratio (compound: DNA) for quadruplex and at 2:1 ratio for duplex DNA were analysed and plotted using Kaleidagraph 4.0 software..

2. 2. 5. Circular Dichroism Studies

CD experiments were performed at 25 °C using a Jasco J-810 Spectropolarimeter with a 1 cm pathlength quartz cuvette.

A 3 μM solution of oligonucleotide in 10 mM Tris buffer (pH 7.5) containing 50 mM KCl was heated at 90 °C for 5 minutes and annealed until room temperature.

Appropriate amounts of the compound were added sequentially to increase the molar ratio. Spectra were recorded from 230 nm to 500 nm at a scanning speed of 50 nm/min and response time of 1 second. Spectra were averaged over four scans. A buffer baseline scan was collected in the same cuvette and subtracted from the average scan for each sample. Data were processed and plotted were performed using Kaleidagraph 4.0 software.

2. 2. 6. Quadruplex-Fluorescence Displacement Assay

All the experiments were performed using a Varian CARY Eclipse Fluorescence Spectrophotometer in a 1 ml cuvette starting from 0.5 μM solution of pre-folded DNA mixed with 1 μM of the fluorophore thiazole orange (an excess is required to be sure that all the binding sites are occupied by the fluorophore) in 10 mM Tris/50 mM KCl buffer at pH 7.5. The addiction of ligand was followed after 3 minutes of equilibration time and after this the fluorescence spectrum was recorded with excitation wavelength at 501 nm (thiazole orange maximum absorbance wavelength) and scanned from 520 nm to 700 nm. The 1/30% fluorofore displacement value was then plotted as a function of the concentration of added ligand.

2. 2. 7. Surface Plasmon Resonance Studies

Biosensor SPR measurements were performed with a four-channel BIACore 2000 biosensor system (BIACore Inc.) and streptavidin-coated (BIACore SA) or neutravidin-coated (BIACore CM5) sensor chips. The chips were prepared for use by conditioning with a series of 1 min injections of 1 M NaCl in 50 mM NaOH followed by extensive washing with buffer. 5'-Biotinylated DNA samples (25-50 nM) in HBS buffer were immobilized on the gold chip surface by non-covalent capture as previously described[90] at flow rate of 1 μl/min until the desired value of DNA response was

obtained (350-400 RU). Three flow cells were used to immobilize the DNA samples, while a fourth cell was left blank as a control. The SPR experiments were performed at 25 °C in filtered, degassed, 10 mM Tris buffer (pH 7.5) containing 50 mM KCl and 0.015% surfactant P20. The compound solutions were prepared by serial dilutions with buffer from stock solution and injected from 7 mm plastic vials with plastic crimp caps (BIAcore Inc.) at a flow rate of 25 µl/min. Known concentration solutions of the compound were injected in the flow cell until a constant steady-state response was reached, then the compound flow was replaced by buffer flow in order to dissociate the complex. To remove remaining bound compound after the dissociation phase, a 2.5 pH 10 mM glycine buffer was used. A set of sensograms, at different concentration of compound for binding to the three different DNA sequences, was obtained. The instrument response (RU) in the steady-state region was determined by linear averaging over a selected time span. The RU for the blank cell was then subtracted for the response in each DNA cell to give a signal that is directly proportional to the amount of bound compound[91]. To obtain the binding constants, the data were evaluated with different interaction models to obtain an optimal fit using BIA evaluation (BIAcore Inc.) and Kaleidagraph software for nonlinear least-squares optimization of the binding parameters:

One site: $r = (K_1C_{free}) / (1 + K_1C_{free})$

Two site: $r = (K_1C_{free} + 2K_1K_2C_{free^2}) / (1 + K_1C_{free} + K_1K_2C_{free^2})$

Three site: $r = (K_1C_{free} + 2K_1K_2C_{free^2} + 3K_1K_2K_3C_{free^3}) / (1 + K_1C_{free} + K_1K_2C_{free^2} + 3K_1K_2K_3C_{free^3})$

where K_1, K2 and K_3 are equilibrium constants for three types of binding sites and C_{free} is the concentration of the compound in equilibrium with the complex and is fixed by the concentration in the flow solution. Errors in fitting results were less than ±10%.

2. 2. 8. Mass Spectrometry Experiments

The mass spectrometry analysis was performed on a Waters Q-TOF micro mass spectrometer equipped with electrospray ionization source (ESI) on a negative mode (Waters Corporate, Milford, MA). The mass range was from 300-3000Da. The sample was introduced into the ion source through direct infusion at 5ul/min flow rate. The DNA concentration was 30 μM. Complexes ligand-DNA at 1:1, 2:1, 3:1, 4:1, 6:1 molar ratios were analyzed. The instrument parameters were as follows: capillary voltage of 3000V, Cone voltage of 30V, desolvation temperature of 150 °C and source temperature of 100 °C. Nitrogen was used as nebulizing and drying gas. Data were analyzed using MassLynx 4.1 software.

MALDI-TOF mass spectra were recorded on a 4800 MALDI-TOF analyzer (Applied Biosystems, Foster City, CA) in a linear-positive mode with delayed extraction. Matrix was prepared by mixing 3-Hydroxypicolinic acid (3-HPA, 1.5mg) in water (30uL) and then mixing with 3 μL of ammonium citrate (50 mg/mL). A mass range of 6000 to 10,000 Da was scanned. Each spectrum was averaged with 400 laser shots. 4000 Series Explore (Applied Biosystems) software was used for the acquisition and data process.

2. 2. 9. *Taq* Polymerase assay

PCR reactions were performed to amplify the 906-1064 sequence of pBR322 (2.5 ng) in the presence/absence of increasing concentrations of tested derivatives. The reaction was carried out in an Eppendorf thermocycler performing 25 cycles of:

30 s at 94 °C, 30 s at 65 °C and 30 s at 72 °C. The reaction products were resolved on a 2% agarose gel in TBE 1X (89 mM Tris base, 89 mM boric acid, 2 mM Na_2EDTA) and stained by ethidium bromide.

2. 2. 10. Telomerase activity assay

An aliquot of $5x10^6$ HeLa cells in exponential phase of growth was pelleted and lysed for 30 min on ice using 100 µl of 0.5% CHAPS, 1 mM EGTA, 25% 2-mercaptoethanol, 1.74% PMSF and 10% w/v glycerol. The lysate was centrifuged at 13000 rpm for 30 min at 4 °C and the supernatant collected, stored at –80 °C, and used as the telomerase source.

Telomerase activity was assayed using a modified telomere repeat amplification protocol (TRAP) assay[32]. Briefly, a proper substrate TS (100 ng) was elongated by telomerase by incubation of the reaction mixture with 1 µg of protein extract at 37 °C for 30' in the presence/absence of increasing drug concentration. Then products amplification was performed by addition of 100 ng of return primer ACX and 2 U *Taq* polymerase. An internal control template (TSNT) with its return primer (NT) was added to the reaction mixture. Then, PCR amplification step was performed (33 cycles of: 30 s at 92 °C, 30 s at 58 °C and 45 s at 72 °C). The reaction products were loaded onto a 10% polyacrylamide gel (19:1) in TBE and visualized after Sybr Green I staining. Telomerase inhibition values are expressed as percent of telomerase inhibition relative to control (no drug) lanes.

2. 2. 11. Cell culture and toxicity assay

HeLa (human epithelial) and 293T (human renal epithelial) cell lines were maintained in DMEM medium supplemented with 10% heat-inactivated fetal calf

serum, 50 U/m of penicillin G and 50 µg/ml of streptomycin, at 37 °C in humidified atmosphere and 5% of CO_2.

MTT assays were performed to evaluate cytotoxic profiles of the tested compounds. Thus, cells were plated in 96 well plates at 10.000 cells/well, and cultured overnight. Afterwards, compounds were added in triplicate and plates were incubated in presence of the drug for 72 hours. At the end of this period, MTT was added to a final concentration of 0.8 mg/ml. After two additional hours of incubation, the medium was removed and 150 µl of DMSO were added per well. Soluble formazan salts were homogenated by manual pipetting and Absorbance at 540 nm was read. Curves consisted in 8 serial dilutions in triplicate in each case, and results were analysed as sigmoidal dose-response curves.

2. 3. SHAPE BASED RECOGNITION AND BINDING TO QUADRUPLEX DNA BY HETEROCYCLIC CATIONS

In this section of the Chapter, a library of new heterocyclic diamidines presenting different substituent groups was selected as a source of candidates. Based on the variety of their shapes they were divided into three series: (1) linear dications, characterized by the presence of a central planar core (Figure 2.1.A), (2) compounds that can assume a highly curved shape and have a variable number of furans, thiophenes and phenyls (Figure 2.1.B) and (3) partially curved compounds with different moieties (Figure 2.1.C). The compounds were tested for selective G-quadruplex DNA recognition based on the idea that linear and highly curved molecules do not have the proper shape to fit into the minor groove of the double helix. This feature can be considered an advantage in terms of selectivity for a potential quadruplex binding approach. In contrast, partially curved compounds can have strong minor groove binding with duplex DNA and are used for comparison with quadruplex DNA interactions. Based on this hypothesis, a screening of the compounds was performed to see how the shape can influence the binding properties and drive the selectivity towards quadruplex versus duplex structures.

Interaction of compounds with DNA was evaluated by using a number of different biophysical techniques with two sequences known to fold into a G-quadruplex conformation: the human telomere Tel22 “wild type” and a 19 base model from the protoncogene promoter *c-myc*. Additionally, a double strand hairpin sequence containing AATT binding sites was used to compare the selectivity of the compounds between quadruplex and duplex DNA.

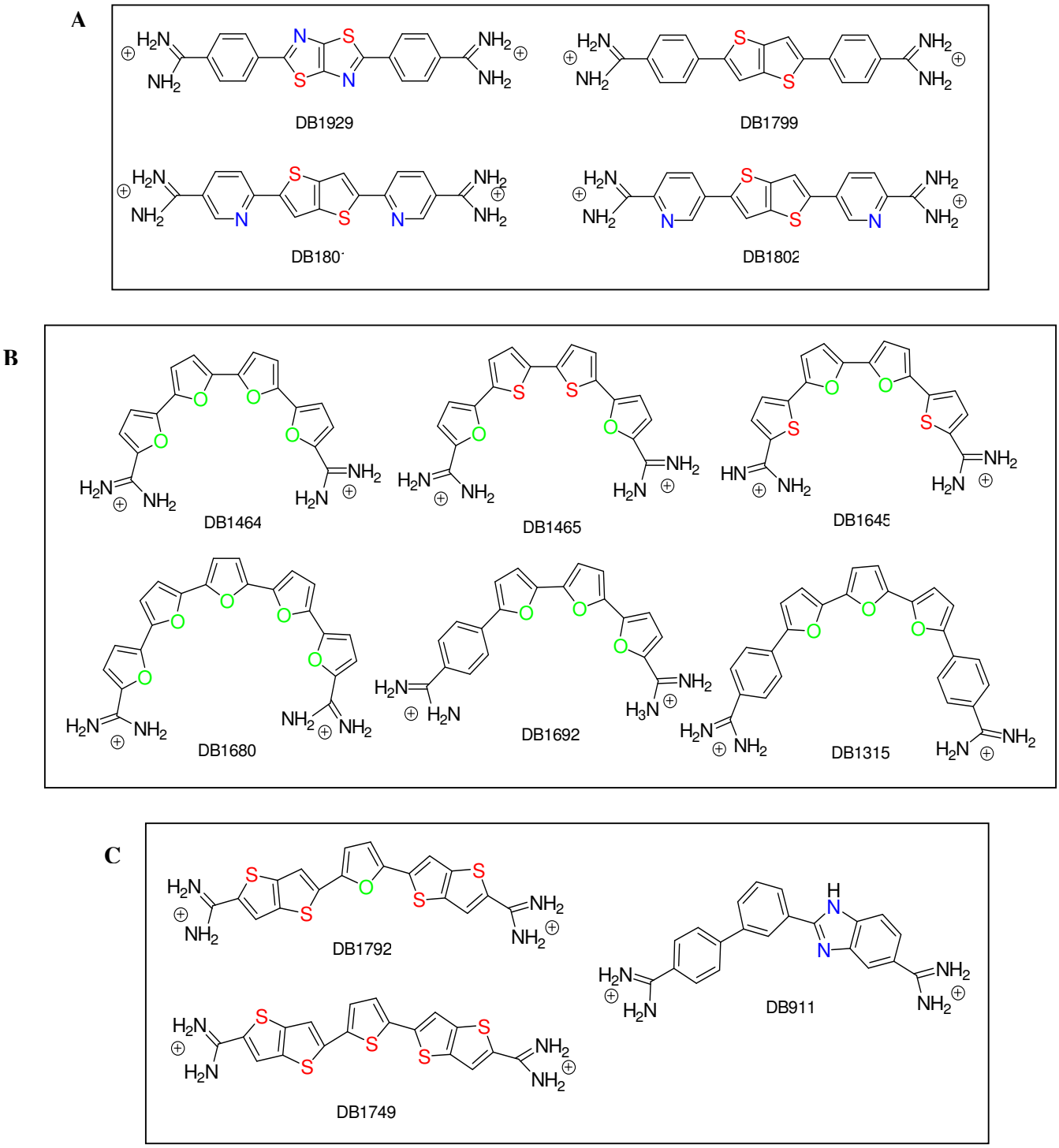

Figure 2.1 Chemical structures of the compounds. Panel A: linear diamidines; panel B: highly curved diamidines; panel C: partially curved diamidines. Compounds with A and B shapes do not generally bind well to duplex DNA while those in C, such as DB911, generally bind well.

Biophysical methods such as UV absorbance spectroscopy and surface plasmon resonance measurements were performed to evaluate the binding properties of the compounds. UV absorbance thermomelting experiments provided indications about stabilization of G-quadruplex sequences. The "Fluorecence Displacement Assay" was also used to test the relative affinity of the compounds with the quadruplex DNA while circular dichroism titrations allowed the evaluation of conformational changes of the oligonucleotide structures induced by the ligands.

Biological studies, based on the TRAP assay and inhibition of Taq polymerase, were performed to complement the biophysical data.

2. 3. 1. RESULTS

2. 3. 1. 1. Thermal Melting profiles

A DNA melting curve is a two-dimensional plot that displays the influence of the temperature on an oligonucleotide solution. The melting temperature of the oligonucleotide is defined as the point at which there is an equal distribution between the folded and the unfolded conformations (50%-50%) and it is represented by the minimum peak of the first derivative of the melting curve. This parameter provides an indication about the stabilization properties of the secondary structure that an oligonucleotide can assume.

In this study, quadruplex denaturation and renaturation has been followed by recording absorbance absorbance at 295 nm for quadruplex and 260 nm for duplex[92], the wavelength that shows the greatest changes[93]. The affinity for the G-quadruplex structure was evaluated by ΔT_m, the difference between the T_m of the complex and the

T_m of the free DNA. The higher the ΔT_m value the higher the ability to stabilize the DNA by the ligand. ΔT_m values for the compounds with Tel22 at molar ratios of 4:1 (compound: DNA), where most compounds had reached a maximum ΔT_m, are plotted on a histogram to compare their stabilization properties (Figure 2). Since a single sequence can fold into several structures according to the size of the monovalent ion that coordinates the system, all the experiments were performed in a 50 mM potassium solution. Potassium folding is, in fact, considered more biologically relevant due to the higher intracellular concentration of this salt[94].

Three different patterns corresponding to the three tested series emerged. In the linear series (black bars in Figure 2.2), compound DB1929 showed a ΔT_m value of 11.5 °C. This is a very high value when compared to the ΔT_m of the other three compounds from the same series (DB1801, DB1802 and DB1799) that have similar structures but two condensed thiophenes instead of thiazoles. Series 3 (white bars), with medium curved compounds, showed the lowest ΔT_m values, indicating that their molecular size and geometry are not favorable for the interaction with quadruplex DNA. In contrast, many of the Series 2 compounds (grey dotted bars) are characterized by high ΔT_m values, shown in Figure 2.2. The data shows the ability of the polyfuran compounds (DB1464, DB1692, DB1680) to efficiently bind and stabilize quadruplex DNA. Lower ΔT_m values are provided by DB1645 and DB1465, which differ from the others by the presence of two thiophene groups, and by DB1315 which is characterized by the presence of two terminal phenyl rings.

The T_m experiment was performed also with a duplex sequence to evaluate the selectivity of the compounds between duplex and quadruplex (Figure 2.3). The (d[5'-CGG-AAT-TCG-CTT-TTG-CGA-ATT-CCG -3']) sequence was chosen because usually

diamidines bind to it with high efficiency[95]. The observed ΔT_m values were very low for all the compounds. The only exception is DB911 that interacts very well with double strand DNA while it shows low affinity for quadruplex.

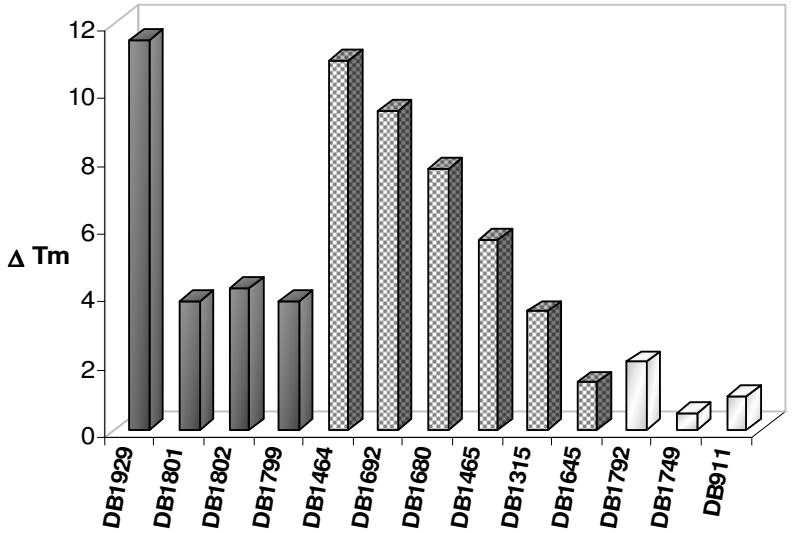

Figure 2.2 Diagrammatic bar array representation of the ΔTm values for the studied ligands with Tel22, d[AG3-(TTAGGG)3], at 3μM in 10 mM Tris buffer with a KCl concentration of 50 mM, pH 7.5. At this salt concentration Tel22 shows a melting temperature of 60 °C.

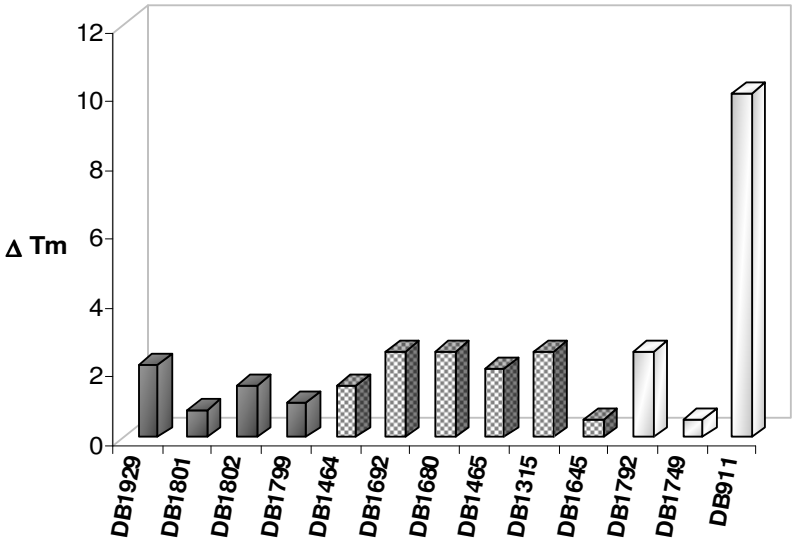

Figure 2.3 Diagrammatic bar array representation of the ΔTm values for the studied ligands with a duplex hairpin, d[5'-CGG-AAT-TCG-CTT-TTG-CGA-ATT-CCG -3'] at 3 μM in 10 mM Tris buffer with a potassium concentration of 50 mM. At this salt concentration the sequence shows a melting temperature of 74 °C.

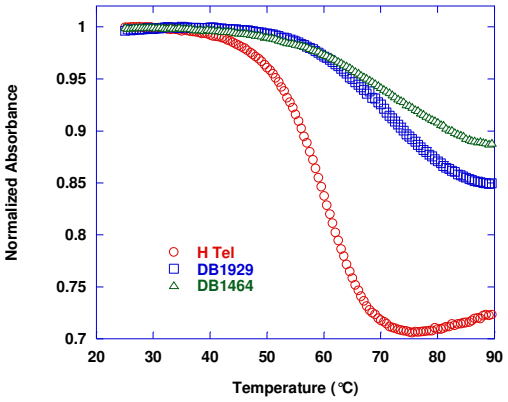

Figure 2.4 A comparison between the melting curves of d[AG3-(TTAGGG)3] sequence in 50 mM KCl at pH 7.5 solution and its 4:1 complexes with two of the best stabilizating ligands

2. 3. 1. 2. Fluorescence Displacement assay

To obtain more information about the affinity of the compounds towards the two quadruplex sequences, the Flourescence Displacement Assay was performed. This assay was based on the displacement by small molecules of a fluorescent probe from DNA. It allows the ranking of a set of putative ligands based on their ability to displace the probe from the specific DNA region where the probe interacts.

The choice of what molecule to use as probe was based on recent studies[96] with Thiazole Orange (TO). This dye was used as a displacement probe because its excitation wavelength (501 nm) is higher than most compounds and therefore does not interfere with the assay. The TO fluorescence quantum yield (Φ_F) is very low in free solution but is enhanced when it is bound to DNA[97]. Therefore it is possible to monitor its displacement by following the decrease of the Φ_F after each addition of compound. Furthermore, TO exhibits little selectivity for one DNA over another and its binding constant is in the order of 10^6 M^{-1} [97].

Each compound was tested with both the human telomere Tel22 (white bars) and *c-myc* (black bars) and the affinity was evaluated by the concentration required to displace 30% of the probe, as represented by the histogram in Figure 4. In

agreement with thermal melting results, the affinity of Series 3 for G-quadruplex DNA turned out to be too low to compete with the TO. In Series 1 the results are different than the ΔT_m order. DB1801 has medium displacement ability but a low ΔT_m. DB1929 also has medium displacement ability but a high ΔT_m. In Series 2 DB1464 and DB1692 also have high ΔT_m values but medium TO displacement effects. With DB1680 both a high ΔT_m and good displacement properties were obtained and DB1315 has a high ΔT_m and even better displacement activity. DB1465 is unusual in that it has a medium ΔT_m value but shows no significant displacement of TO. Compounds that have a high ΔT_m, but poor TO displacement may have a different binding mode. Since the TO binds the quadruplex DNA by end-stacking interactions, the behavior of these compounds suggests a non end-stacking binding mode. To better understand these indications Circular Dichroism (CD) was used.

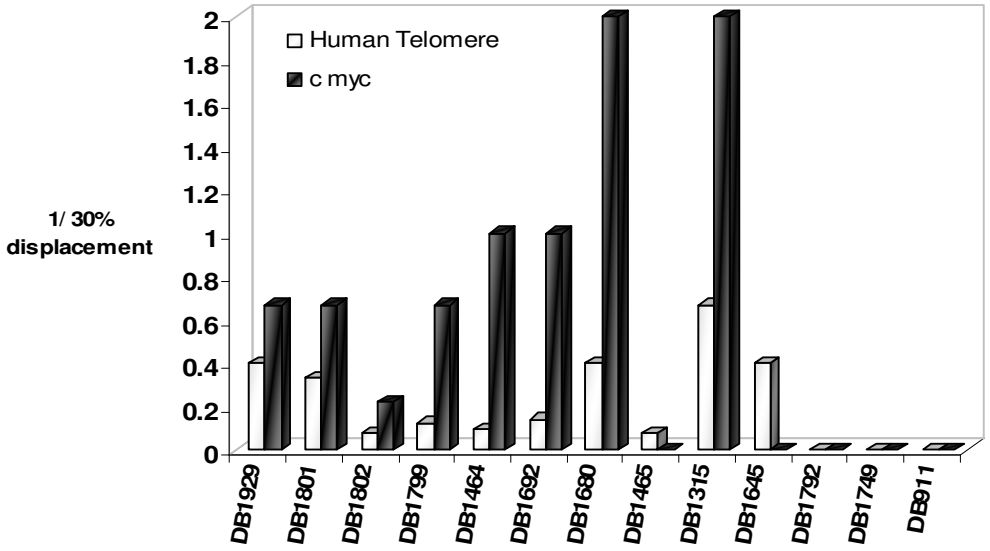

Figure 2.5 Diagrammatic bar representation of the fluorescence displacement assay in 50 mM potassium using thiazole orange as probe and two different quadruplex DNA:Tel22 (white) and *c-myc* (black) . The affinity of the compounds studied with both the G-quadruplex sequences (human telomere and *c-myc*) is evaluated by the inverse of the concentration required to displace the 30% of the probe.

2. 3. 1. 3. Conformational studies by Circular Dichroism

To further evaluate the interaction of the compounds with the G-quadruplex structure, and to understand how they can affect its conformation, circular dichroism studies were performed. The CD signal is a general indicator of DNA folding topologies[98]. For G-quadruplex structures, the conformation of the guanines around the N-glycosylic bond (*syn* or *anti*) affects the CD signals, which are characteristic of a particular G-quadruplex conformation[99]. When the 4 strands are parallel oriented, they have similar glycosydic torsion conformation, while antiparallel strands show mixed glycosydic torsion conformation[100]. This generally results in distinct CD profiles depending on their parallel/antiparallel strand composition[101]. A parallel structure CD spectrum usually shows a maximum around 265 nm and a minimum around 240 nm while antiparallel conformation spectrum presents a maximum at 295 nm and a negative peak around 260 nm[102]. Nevertheless, due to the polymorphism of the G-quadruplex, a mixed-type hybrid structure has been associated to the wild type 22 mer human telomere and it is characterized by a CD profile with peaks at both 265 nm and 295 nm, indicating the coexistence of parallel and antiparallel foldings.

Several sets of CD titrations were performed using the Tel22 sequence. In Series 1, the spectrum obtained by the titration of the human telomere Tel22 with DB1929 (Figure 2.6.A) shows a relatively small induced CD signal in the compound absorption region and an interesting decrease in the DNA region resulting in a negative peak at 260 nm. This indicates a conformational change in the G-quadruplex structure from a mixed parallel-antiparallel to a more antiparallel structure driven by the compound. Interestingly, comparing the spectrum of DB1929 with one of its

structural isomers, DB1801 (Figure 2.6.B), the magnitude of the induced signal in the compound region is similar at the same ratios but the shapes of these signals are different. Moreover, DB1801 does not significantly affect the DNA conformation. DB1802 does not show any significant induced CD while DB1799 is characterized by a small positive-negative-positive induced pattern, completely different from the ones observed for the other compounds of the same series.

Partially curved compounds from Series 3 do not show any significant CD changes in the entire spectrum (Figure 2.7). This result indicates no interaction with the G-quadruplex structure and supports the results provided by the previous experiments.

Compounds from Series 2, such as the five ring molecules, DB1315 and DB1680, present a small CD signal in the compound absorption region and in the DNA region. An impressive induced signal is provided by DB1464 in the compound absorption region (Figure 2.8.A), indicating that the presence of furan substituents leads to a specific arrangement of the molecule that favors the interaction with the human telomere. This arrangement can change in the presence of two thiophenes in the structure, as shown by the CD spectrum of DB1465 (Figure 2.8.B). Increasing amounts of this compound provide a CD pattern with the same characteristics of DB1464 in the DNA region (decreased intensity of the signal) but a completely different induced signal without a positive peak at longer wavelengths (Figure 2.8.B). The DB1692 spectrum also differs from the others, with a large, positive, induced signal (Figure 2.8.C). The different CD patterns of Series 1 and 2 compounds probably arise due to different binding modes (Discussion Section).

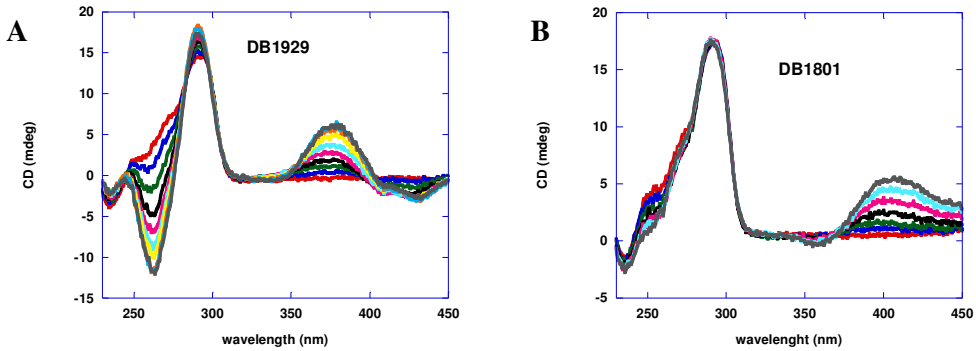

Figure 2.6 CD spectra of linear compounds DB1929 (A) and DB1801 (B) titrated into 3.0 μM of Tel22 in 10 mM Tris containing 50 mM KCl. Compound: DNA ratios ranged from 1:1 to 10:1 for DB1929 and from 1:1 to 6:1 for DB1801

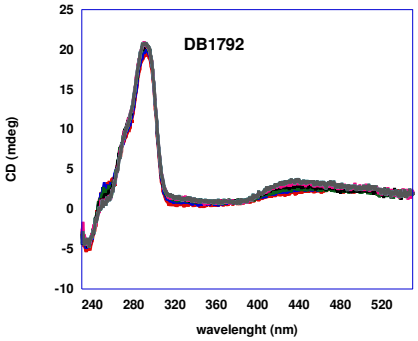

Figure 2.7 CD spectra of DB1792 titrated into 3.0 μM of Tel22 in 10 mM Tris containing 50 mM KCl. Compound:DNA ratios ranged from 1:1 to 6:1

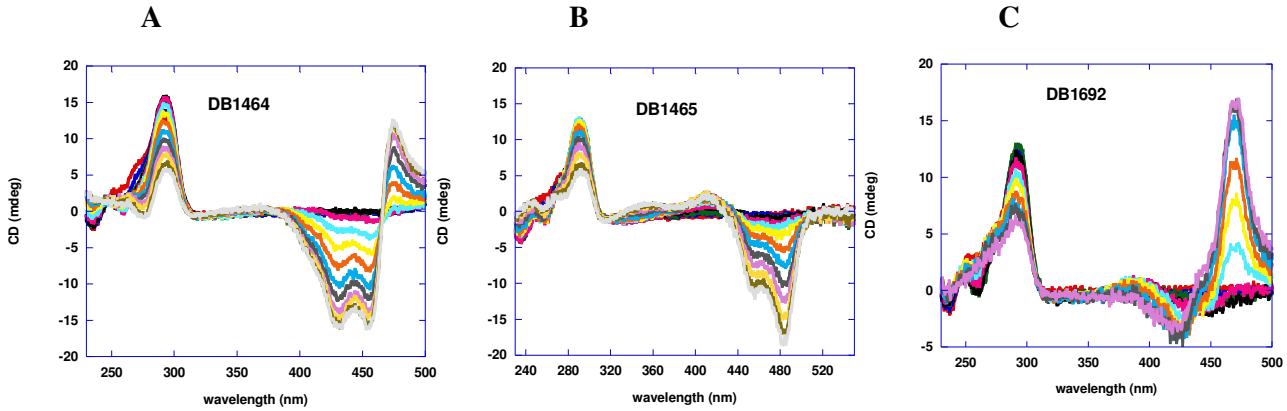

Figure 2.8 CD spectra of Series 2 compounds DB1464 (A), DB1465 (B), DB1692 (C) titrated into 3.0 μM of Tel22 in 10 mM Tris containing 50 mM KCl. Compound: DNA ratios ranged from 1:1 to 13:1 for both DB1464 and DB1465

2. 3. 1. 4. Binding studies by Surface Plasmon Resonance

An evaluation of the binding properties of some of the compounds in Figure 1 to three different DNA sequences was provided by biosensor-SPR methods. According

to this powerful technique, either a small molecule or a nucleic acid sequence can be immobilized on the chip surface to monitor the formation of their complex[103]. In this study a biotin-labeled Tel22 human telomere, a *c-myc* G-quadruplex and a duplex sequence were immobilized on a gold sensor chip and followed by the addition of increasing compound concentrations. A signal indicating the change in bound compound on the sensor surface (RU) is then generated during the formation of the complex between the macromolecule and the ligand. This technique is useful for the analysis of interaction affinity and kinetics[104].

The set of ligands of this investigation were very difficult to test by this technique due to their chemical-physical characteristics such as solubility and surface adsorption. They easily stick on the biosensor surface preventing reliable binding profiles from being obtained in most cases. Series 1, DB1929, and Series 2, DB1464, gave data over a satisfactory concentration range for binding analysis. A comparison of the binding abilities between these two compounds indicates that the curved ligand, DB1464, binds strongly to the quadruplex DNA, with primary binding constants around 10^7 M^{-1} for both the human telomere and *c-myc* while a very weak interaction with duplex DNA is observed under these conditions (Figures 2.9 and 2.10 and Table 2.4). A second binding site is quite weak with *c-myc* but of comparable affinity with Tel22. Linear compound, DB1929, is also able to bind selectively to the quadruplex conformations but with constants about one-half those for DB1464 (Table 2.4). For both the compounds (DB1929 and DB1464) the affinity for *c-myc* is higher and the binding to this sequence occurs with apparently slower rates of association and dissociation. Surface problems prevented a more detailed comparison of binding of these compounds.

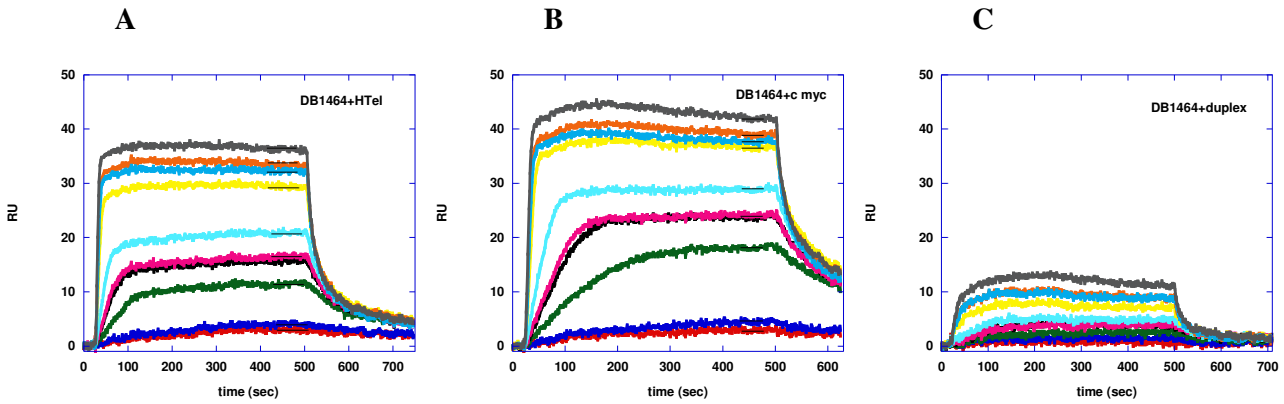

Figure 2.9 Representative SPR sensorgrams for the interaction of DB1464 with the human telomere (A), *c-myc* (B) and an AATT duplex sequence (B) at compound concentrations from 0 to 1 μM.

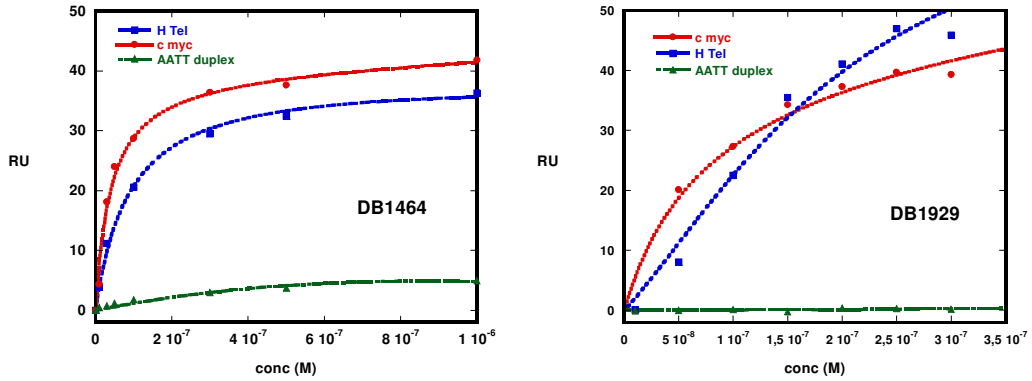

Figure 2.10 Comparison of the SPR binding affinity of DB1464 and DB1929 with quadruplex human telomere (squares), quadruplex *c-myc* (circles) and duplex (triangles) DNA sequences. RU values from the steady–state region of SPR sensorgrams are plotted against the unbound compound concentration (flow solution). The lines are the best fit values using appropriate binding models

Table 2.4 Binding constants (K x 10^{-6} M^{-1}) obtained by fitting the curves using two-sites binding model.

	HTel quadruplex	***c myc* quadruplex**	**AATT duplex**
DB1929	5.0	16	---
	(2 equiv. sites)	0.91	---
DB1464	11	25	0.32
		0.08	

2. 3. 1. 5. Stoichiometry evaluation by ESI-MS analysis

To further evaluate the binding stoichiometries, compounds DB1929 and DB1464 were analyzed also by electrospray ionization mass spectrometry (ESI-MS), a technique that allows the detection of the formation of non covalent complexes at various ligand-quadruplex DNA ratios. Although positive and negative-ion ESI-MS can both be used, negative-ion usually yields a better signal for nucleic acids[105].

The mass spectrum of the free DNA in the negative-ion mode indicates the presence of a five negatively charged ions $[M-5H]^{5-}$ as the most prevalent species (Figure 2.11).

Figure 2.11. Mass spectrum of the human telomereTel22

At 1:1 ratio of DB1929 to human telomeric quadruplex, the primary presence of a 1:1 binding complex (M:Q) is clearly visible (Figure 2.12.A). At increasing ratios both M:Q and 2M:Q complexes are present in increasing amounts (Figure 2.12.B and 2.12.C). At 6:1 ratio (Figure 2.13.D), a very small peak for the $[3M:Q]^{5-}$ complex is observed.

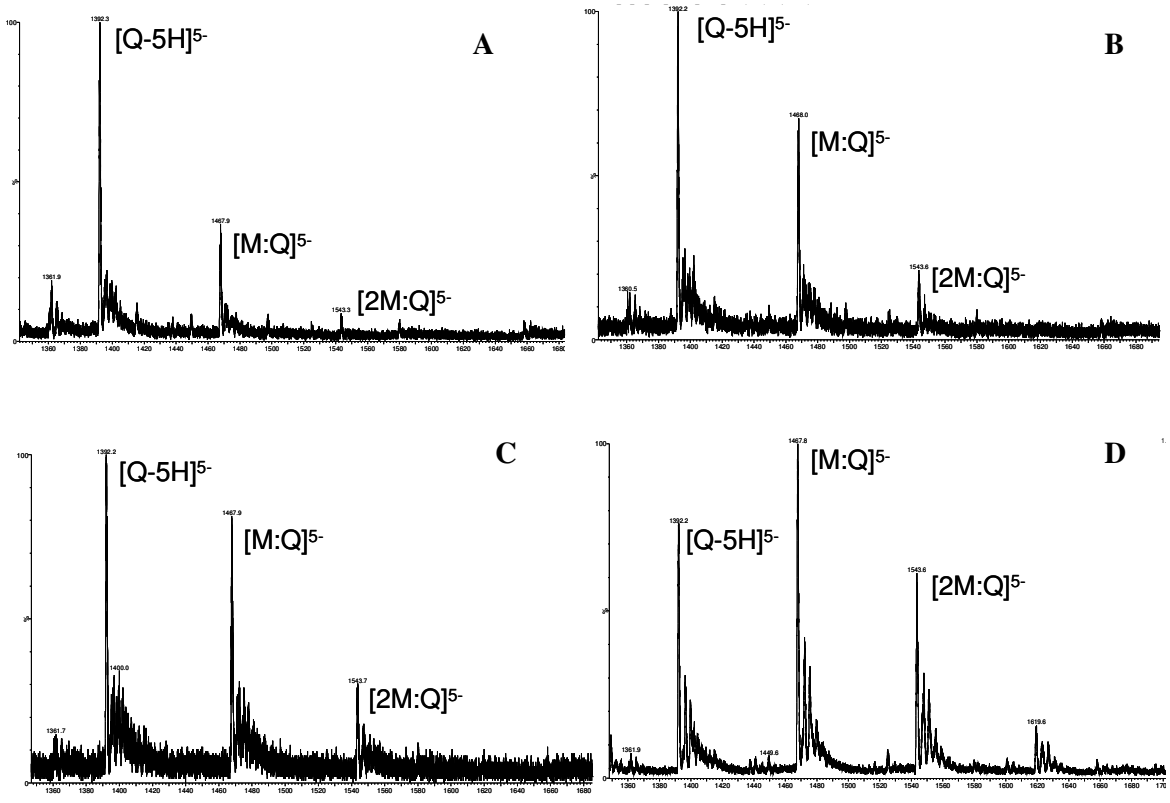

Figure 2.12 Mass spectra at increasing ratios of the compound DB1929 with 30 μM concentration of quadruplex DNA (wt 22 mer). A) 1:1; B) 3:1; C) 4:1; D) 6:1

Mass experiments were also performed with DB1464 and the same quadruplex DNA sequence (Figure 2.13). At 1:1 ratio (compound: DNA) the strong formation of the 1:1 complex is clearly visible (Figure 2.13.B). Mass spectra at higher ratios indicate that the addition of compound decreases the free DNA abundance and leads to the formation of more 1:1 complex as well as 2:1 complex (Figure 2.13.C and D). The 1:1 binding is clearly the most favored for both the compounds. It should be emphasized that the mass spectrometry results are being used to define the possible stoichiometries and not the absolute amount of each species at each ratio since in the gas phase this may not be exactly the same as the solution amount.

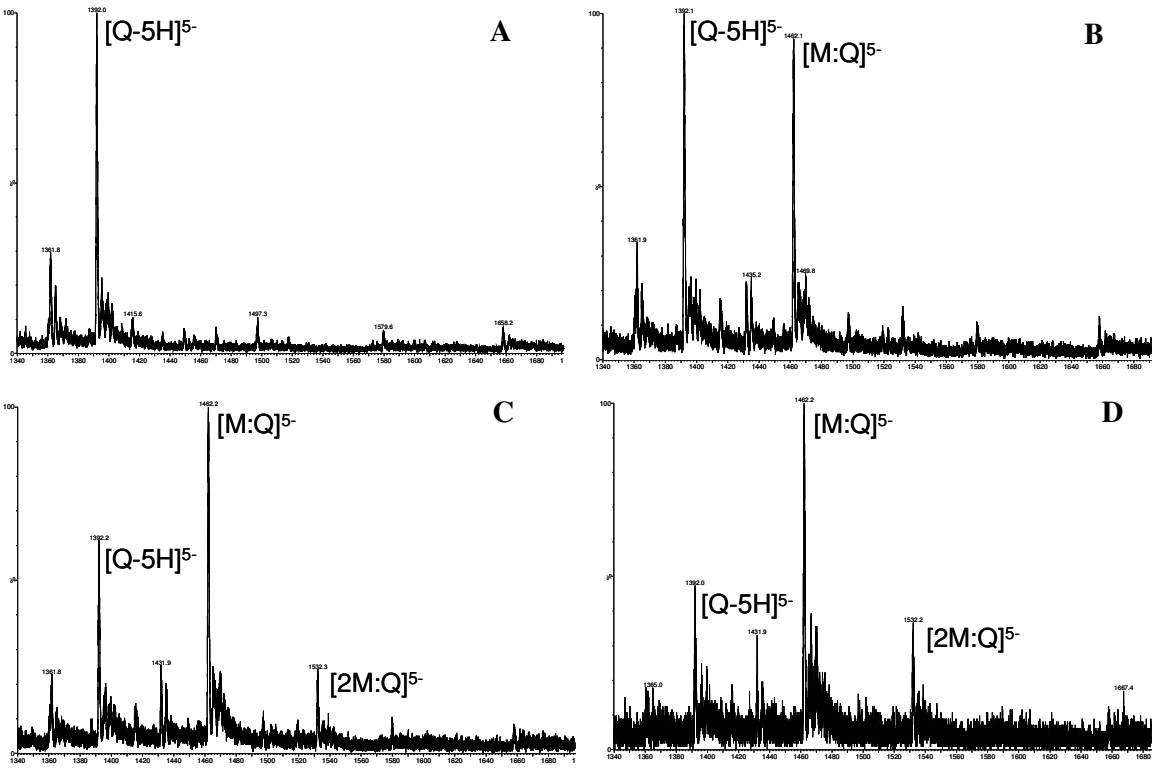

Figure 2.13 Mass spectra at increasing ratios of the compound DB1464 with 30 μM concentration of quadruplex DNA (wt 22mer). A) free DNA; B) 1:1; C) 2:1; D) 3:1

2. 3. 1. 6. Biological results

Selected representatives of each structural series were tested for Taq and telomerase inhibition. In Series 1, DB1801 gives no telomerase inhibition while DB1929 has a 2 μM IC_{50}. These results correlate better with thermal melting experiments than Fluorescent displacement results. As expected, DB1792 from Series 3, which shows poor G-quadruplex binding, did not interfere with telomerase function. All the other tested derivatives from Series 2 inhibit telomerase-mediated DNA elongation in the low micromolar range. The inhibition results for this Series are in reasonable agreement with ΔT_m values with the exception of DB1645 and DB1315. This likely reflects their relevant interference with the amplification process, which occurs at comparable drug concentrations.

The cytotoxic effects of all compounds were also evaluated on this cell line (human epithelial cervical cancer) as well as on 293T (Human Embryonic Kidney), both expressing active telomerase. Reported results were obtained by MTT assay after 72 hours of drug exposure. Again, highly curved derivatives seem to behave distinctly as they turned out to be the most cytotoxic (Table 2.5).

Table 2.5 IC_{50} values (μM) determined for *Taq* polymerase inhibition, TRAP assay and cell cytotoxicity for all tested compounds.

	TAQ	**Telomerase (TRAP)**	**293T**	**HeLa**
DB1929	3	2	34	70
DB1801	0.1	n. o.	-	23
DB1464	0.8	0.4	-	28
DB1680	1.8	0.6	-	6
DB1465	1.3	0.5	4	4.4
DB1315	0.2	0.16	-	3.8
DB1645	4	0.5	5.5	7.6
DB1792	0.6	n. o.	8	34

n. o. : no inhibition observed

2. 3. 2. DISCUSSION

There is now a wealth of information on the interaction of heterocyclic-amidine derivatives and related compounds with DNA duplexes and with the minor groove in particular[106]. With the exception of certain unusual linear compounds[107,108,109] optimum minor groove affinity is obtained with compounds that closely match the shape of the groove. Most linear compounds as well as compounds that are too highly curved to complement the shape of the groove bind poorly to duplexes[110]. Since heterocyclic cations, including both linear and potentially highly-curved compounds, can bind strongly to G-quadruplex structures[111,112] , such compounds in the heterocyclic-amidine series are attractive for the development of

selective G-quadruplex binding agents. To begin this design effort we selected a group of linear (Series 1) and curved (Series 2) compounds that should be poor duplex minor groove binding agents to enhance quadruplex specificity. Both human telomere and *c-myc* oncogene promoter model sequences were used to access quadruplex interactions. As controls, we selected a set of compounds with similar heterocyclic groups and amidine cations that are more similar in shape to typical minor groove binding agents (Series 3). Our initial plan was to use biosensor-SPR methods for quantitative screening of these series but due to unfavorable interactions of several of the compounds with the sensor surfaces we relied more on thermal melting and fluorescence methods to compare relative affinity. CD experiments have been used to provide structural information about the compound interactions with the quadruplexes and effect on DNA conformation.

From the T_m and Fluorescence Displacement results obtained, it is possible to classify the three series based on their affinity for G-quadruplex structures over double helical DNA. Many of the curved compounds in Series 2 interact with G-quadruplexes with high affinity and specificity (Table 2.2). They are followed by a single linear-shaped compound, DB1929, which binds quite well to G-quadruplexes. All these compounds are selective for quadruplex conformations as they did not show significant binding to the duplex sequence evaluated, which has an optimum AATT minor groove binding site. Molecular group substituents can have a strong influence on the affinity of compounds for DNA. For example, comparing compounds in Series 1, the presence of two condensed thiazoles (DB1929) has a role in increasing the binding properties of the linear compounds. On the contrary, a core composed by two condensed thiophenes that characterize the other three linear molecules (DB1801,

DB1802 and DB1799) reduces their stabilization properties of the quadruplex DNA. This may be due to electron-deficiency of the thiazole system that favors the interaction with the tetrad of the G-quadruplex. Clearly linear compounds with different fused ring systems and substituents should be evaluated in detail for quadruplex binding. Relatively small changes in the ring systems that are stacked with the terminal G-tetrads can strongly influence the interaction.

In Series 2, the four furan ring system shows the higher affinity for quadruplex DNA, followed by the five furan ring system. The presence of terminal thiophenes, as well as terminal phenyls, significantly decreases the affinity for the G-quadruplex sequence. Considering the structures of the molecules, the presence of specific groups can play a role in the modification of their binding conformations to the G-quadruplex system. In Series 3 partially curved DB911, known to fit very well the duplex minor groove shape[108] shows very low affinity for the quadruplex DNA (Figure 2.3) while compounds DB1792 and DB1749 poorly interact with all the three DNA sequences tested.

To classify the compound binding modes, two methods were used. Induced CD results for compounds that stack to the ends of the tetrad array are generally small relative to the intrinsic DNA signal[113]. Compounds that are thought to associate in the quadruplex grooves, on the other hand, show much larger induced CDs[114,115]. Displacement assay results can also play an important role in classifying the binding mode. The argument is based on the evidence that the TO molecule used as a probe interacts with the G quadruplex as an “end stacker”[116]. Results with compounds that bind and stabilize very well the human telomere by other assays, but do not exhibit the same potency in this competition study, suggest a non “end stacking” binding

mode, such as interactions with the quadruplex grooves. Based on a small induced CD and competition with TO, all of the compounds of Figure 2.1 that have significant affinity for the *c-myc* sequence are predicted to bind by "end stacking" mode. The parallel *c-myc* structure due to the chain reversal has less accessible grooves relative to antiparallel or mixed structures.

Series 2 compounds, DB1680, DB1315, DB1929, DB1801 and DB1799, are also classified as end-stacking agents with the human telomere based on their small induced CD signals and competition with TO. The tetrafuran compound, DB1464 and DB1465, with the central two furans replaced by thiophenes, on the other hand, give larger and more complex induced CD signals, relative to the DNA peak and to the induced signals of the other compounds. In addition, they show no significant competition with the TO in contrast of their strong binding with the human telomere based on thermal melting and limited SPR studies. This unusual combination of results suggests a groove binding mode for DB1464 and DB1465. The strong negative-positive CD signals of these compounds are also quite different from the weak induced signals of end-stackers and very similar to those for other suggested groove binding agents[114,115].

The shapes of the induced signals appear significantly different comparing the CD spectra provided by some of the Series 2 compounds (DB1464, DB1465 and DB1315) with the ones provided by the linear ligands (DB1929 and DB1801). Because this signal is displayed in the ligand only absorption region, it is directly related to the compound interaction with the macromolecule. Therefore, the induced CD is a useful indication of different binding modes of interaction with the DNA structures.

Mass spectrometry was conducted to help evaluate stoichiometry. We observed a stoichiometry of two compounds per quadruplex for the linear and curved compounds tested in agreement with SPR results. One strong site was observed for both DB1929 and DB1464 and additional binding at higher added ratios of compound to DNA. Because of the decreased binding constant values for the secondary binding modes, these sites cannot be saturated under these conditions. The ionization process is also expected to cause dissociation of the weaker binding modes. Based on the area of free DNA and 1:1 complex at 1:1 ratio, the mass spectroscopy results clearly show stronger binding of DB1464 than DB1929 in agreement with SPR results. SPR with DB1929 suggested a relatively strong secondary site, not in agreement with mass spectroscopy, but the generally weak binding of DB1929 makes fitting SPR results more difficult.

Biological results appear to be in general agreement with biophysical data for Series 1 and 3. However, DB1315 and DB1645 from Series 2 show good telomerase inhibition efficiency, in contrast with biophysical data. It is important to underline that these compounds bind G-quadruplex with altered geometry which can results in poor complex stability in the condition used for enzymatic assay.

Results for the compounds in Figure 1 indicate a high selectivity for G-quadruplex structures over duplex DNA for some curved and linear diamidines. Furthermore, for compounds belonging to both of these series, the number and type of heterocycle rings and the presence of specific subsituents can have major effects on the interaction and binding properties of the ligands, even if they are structural isomers. Partially curved structures interact poorly with quadruplex DNA and can bind from weakly to strong to duplex DNA. CD and fluorescence displacement results

suggest the possibility of an interaction into the grooves of the quadruplex by some of the compounds of Series 2. Other compounds in Series 2 and linear compounds of Series 1 prefer to interact with quadruplex structures by an end-stacking mechanism. The selectivity of these compounds for quadruplexes, the ability of diamidines to be taken up by cells, and the heterocycle and substituent sensitivity of their binding affinities, suggest that linear compounds and compounds that can assume a highly-curved shape are promising for development as quadruplex binding agents.

2. 4. EVALUATION OF THE HETEROCYCLIC DIAMIDINE DB832 AS A POTENTIAL GROOVE BINDER FOR HUMAN TELOMERIC QUADRUPLEX DNA

As previously described in Chapter 1, a new effective approach for the development of antiproliferative agents involves the stabilization of the telomere DNA in secondary structures known as G-quadruplexes. The majority of small molecules reported in the literature as G-quadruplex stabilizing agents are planar aromatic compounds generally derived from duplex intercalators. They usually bind the structure via π-π stacking interactions on one or either both the terminal tetrads. However, other modes of binding have been proposed for G-quadruplex ligands, including intercalation between the tetrads (ethidium bromide, TmPyP4)[117,118], binding into the grooves, electrostatic interactions with the loops and with negatively charged phosphate groups of the backbone.

Essentially, all the known quadruplex end-stackers are designed from duplex intercalators so some of them are not significantly selective for quadruplex DNA over duplex or exhibit only little selectivity among different G4 conformations. That's why the quadruplex grooves are becoming attractive recognition sites of interactions in quadruplex targeting. They are actually different from duplex grooves for shape, width and dimensions. Moreover, due to the high polymorphism of the structure, quadruplex grooves can vary significantly according to the type of sequence, the nature of cation and the *syn/anti* conformation of guanine residues[119,120,121] resulting in an ensemble of possible groove geometries. Selective targeting of the different

grooves will allow the recognition of quadruplex DNA with a high degree of selectivity.

So far there has been little success in developing small molecules that target quadruplex grooves. Some of the ligands reported in literature exhibit only very little selectivity over duplex and moreover they have been characterized only with fairly simple dimeric or tetrameric G4 systems and at substantial ligand concentrations (NMR comcentrations)[122,123]. Anyway, ligands that can interact with the grooves of a biologically relevant structure such as the one formed by the human telomeric sequence have not been reported so far.

Although end stacking interaction is a well-established and well-characterized quadruplex recognition mode, groove binding interaction is difficult to monitor by commonly used screening techniques such as thermal denaturation, surface plasmon resonance (SPR), fluorescence and UV spectroscopy absorbance. However, circular dichroism pattern recognition has been previously used to determine the binding mode with duplex DNA ligands[124]. The induced can be a weak posirive or negative signal, as in the case of duplex intercalators, or can be a large positive signal, as in the case of duplex minor groove binders[125]. Based on this feature, we decided to employ this technique to achieve some indications about the binding mode of our ligands with the quadruplex DNA. A number of topology studies have been performed by employing this technique. It is indeed very attractive because of its potential to discriminate between quadruplex foldings having different parallel and antiparallel strand orientation due to the *anti*/*syn* arrangement of glycosidic angles[126]. It provides also a qualitative indication about the affinity of the compounds to the DNA, if they interact with the same binding mode. Fluorescence displacement assay can be also a

useful tool because it is based on the competition with another ligand for the same binding site. Using a well known fluorescent G-quadruplex end-stacker as probe molecule and monitoring its fluorescence intensity will help to obtain indications about the preferential binding site of the evaluating compound.

This subchapter focuses on DB832, selected from a CD screening of heterocyclic diamidines. DB832 is an achiral molecule characterized by two positive charges on the amidine groups and three aromatic rings, a phenyl and two furans linked together by single bonds (Figure 2.14). Structurally, this compound does not show the typical characteristics of a quadruplex targeting ligand such as large, planar, aromatic surfaces required for extensive π- π stacking with the external tetrads. The structure of this compound suggests that a mixed binding mode involving the quadruplex grooves is possible.

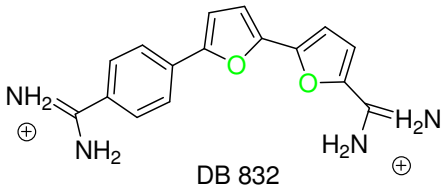

Figure 2.14 Chemical structure of compound DB832

Thermal melting studies indicated the ability of this compound to stabilize several G-quadruplex structures with high selectivity over the duplex DNA. CD studies help to delve into the understanding of the binding mode. To reinforce the evidence of grooves-targeting by this compound, modified oligonucleotides containing 8-bromoguanosines were employed. Based on structural features, it is known the proton in 8 position of the guanines are directly pointed into the grooves of the folded quadruplex, so the replacement of this proton with a bulky substituent such as a

bromine atom turned out to be a good candidate system to test the hypothesis of groove binding. Dr Sugiyama and coworkers have successfully employed this modification and the telomeric DNA sequence and shown that a stable quadruplex architecture could be maintained[127,128]. A comparison between the induced CD signals of several spectra will allow considerations about the binding mode of this molecule.

2. 4. 1. RESULTS

2. 4. 1. 1. Circular dichroism studies with different quadruplex forming sequences

The CD spectrum of DB832 when titrated with the human telomeric DNA in presence of potassium shows an unusual biphasic character: an initial small change followed by an impressive induced signal in the wavelength region corresponding to the ligand absorbance (Figure 2.14.).

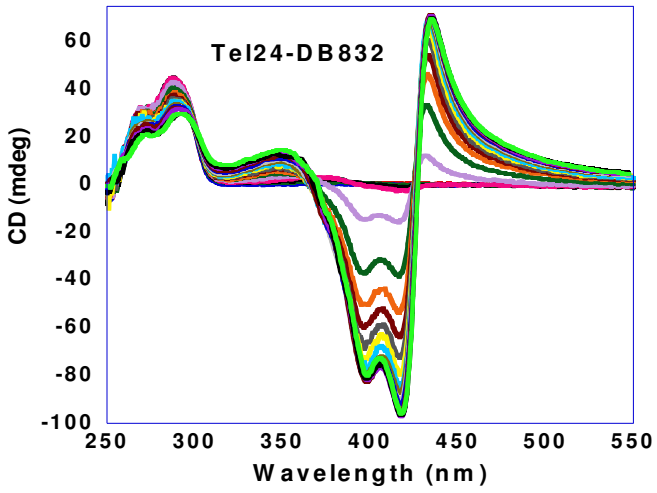

Figure 2.14.A CD spectra of DB832 titrated into 3.0 μM of d[AG3(T2AG3)3] in 10 mM Tris containing 50 mM KCl. Compound:DNA ratios ranged from 1:1 to 25:1

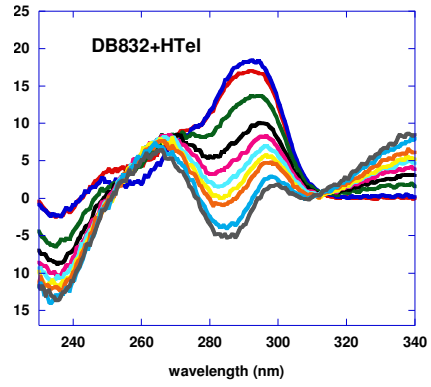

Figure 2.14.B Close-up of the wavelength region of DNA absorbance for the spectra shown in Figure 4.2.A of DB832 titrated into 3.0 μM of d[AG3(T2AG3)3] in 10 mM Tris containing 50 mM KCl, pH 7.5

When the compound is added to the DNA the induced signal is visible after 5:1 ratio (compound: DNA) and it is characterized by a negative band with two inflection points, one at 398 nm and the other at 418 nm. This is followed by a positive band with a maximum at 434 nm. An isoelliptic point is also present at 425 nm, indicating the presence of equilibrium of two different species in solution (Figure 2.14.A). The addition of the DB832 to the human telomeric sequence also affects the CD pattern in the DNA wavelength region, as shown in Figure 2.14.B. The positive band of at 295 nm decreases and becomes negative at saturation level. This data indicate that DB832 induces the formation of a mixed parallel/antiparallel hybrid quadruplex or even that, due to the high polymorphism of this sequence, binds to a mixture of quadruplex conformations. Since the induced signal generated is impressively large it was important to understand if this is due to aggregation phenomena. Some compounds, such as porphyrins, can aggregate onto the surface of quadruplex DNA, resulting in artificially high observed stoichiometries[129]. The compound was then added and the CD signal was monitored until the achievement of saturation point, at 25:1 ratio (Figure 2.14).

Since excitation splitting starts after 5:1 and levels off at 25:1, a high binding stoichiometry for this interaction is suggested. Moreover, this behavior indicates a mixed binding mode suggesting stacking interactions with the external tetrads at first additions and binding into the grooves on the quadruplex at increasing concentrations of compound and probably after some conformational modification of the DNA (see DNA wavelength region). The large magnitude of the signal suggests the formation of stacked complexes in more than one groove.

As a test for groove interactions, two human telomere sequences were synthesized by replacing the hydrogen in position 8 of the guanosines with some bromines. The ODN9 sequence contains 3 bromoguanines on the terminal tetrad at the 5'-end of the quadruplex. These bulky bromines lock all the 3 accessible grooves inhibiting binding from small molecules. Interesting results emerged from the titration data:the spectrum does not exhibit the typical induced signal observed with the unmodified sequence. The weak signal suggests a first binding event of the compounds with the ends but even at very high ratio, the signal does not increase when the grooves are sterically locked. (Figure 2.15). The same experiment was performed with the ODN4 system, where the 3 bromo-guanines are located in only one groove so the other grooves remain accessible. Induced CD signal is still observed after titration of DB832 with this sequence (Figure 2.16), suggesting that the compound is stacking into the accessible grooves. Anyways the magnitude is smaller, confirming that the signal is generated due to formation of stacked species in the remaining grooves and so resulting in decreased intensity.

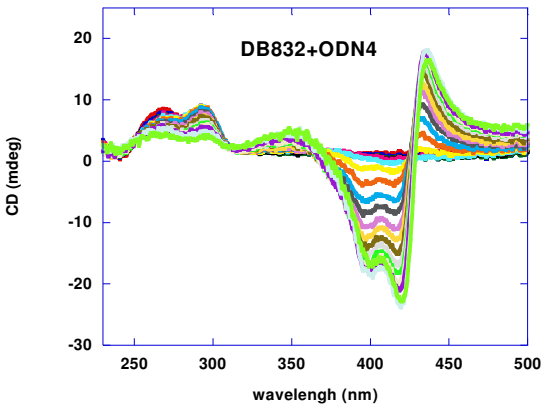

Figure 2.15 CD spectra of DB832 titrated into 3.0 μM of ODN4 d[AGGGTTAGGGTTA^{Br}G^{Br}G^{Br}GTTAGGG] in 10 mM Tris containing 50 mM KCl, pH 7.5. Compound: DNA ratios ranged from 1:1 to 25:1

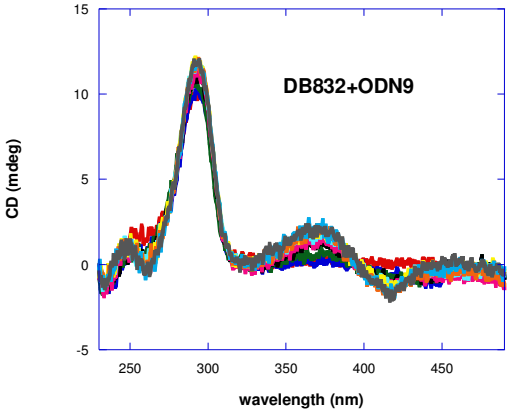

Figure 2.16 CD spectra of DB832 titrated into 3.0 μM of ODN9 d[A^{Br}GGGTTA^{Br}GGGTTAGGGTTA^{Br}GGG] in 10 mM Tris containing 50 mM KCl, pH 7.5. Compound: DNA ratios ranged from 1:1 to 9:1

All the combined CD results with Tel22 (wild type), ODN9, ODN4 suggest groove interactions with the human telomeric quadruplex sequence.

To further investigate whether the binding affinity of DB832 with the G-quadruplex is sequence or conformation specific, other CD experiments were performed using different G- quadruplex forming sequences (Table 2.2). We evaluated the behavior of the compound with an oncogene promoter sequence, *c-myc*, the telomere repeat sequence of Tetrahymena, $(TTGGGG)^{130}$, and two hybrid sequences known by NMR studies to characterize the human telomere. By looking at the spectrum (Figure 2.17) the affinity between the compound and the *c-myc* oncogene promoter sequence is detected by monitoring the progressive decreasing of the signal at 260 nm (DNA absorbance region) but since only a small negative induced signal appears in the compound region, stacking interaction with the ends is the more likely binding mode. The folded structure of *c-myc* in presence of potassium is parallel oriented with the symmetrical grooves completely blocked by reversal loops. This titration reinforces the fact of a preferential affinity to the hybrid conformation and interaction into the grooves at higher ratios. This evidence is also supported by another CD titration performed with a G-rich sequence, $(TTGGGG)_4$, that does not fold into a pure parallel conformation but in a mixed type with a higher parallel component (Figure 2.18).

The changes in the DNA region are quite dramatic and the oligonucleotide conformation is gradually shifted towards the hybrid one typical of the telomeric type. Moreover the induced signal is very small.

It has been recently reported that the hybrid-type intramolecular G-quadrulex appears to be the predominant conformation of the human telomeric in potassium

solution and it is likely to be a dynamic equilibrium between hybrid-1 and hybrid-2 conformations[131 132 133] .

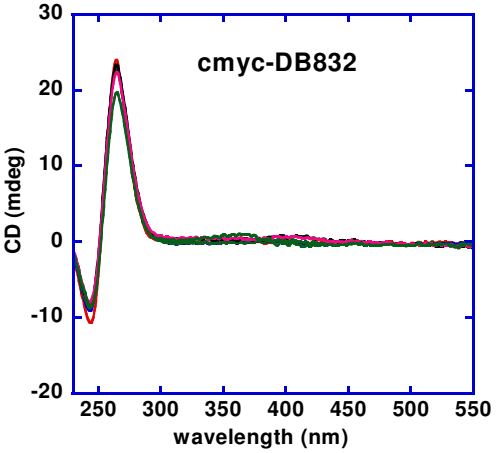

Figure 2.17 CD spectra of DB832 titrated into 3.0 µM of *c-myc* in 10 mM Tris containing 50 mM KCl, pH 7.5. Compound: DNA ratios ranged from 1:1 to 10:1

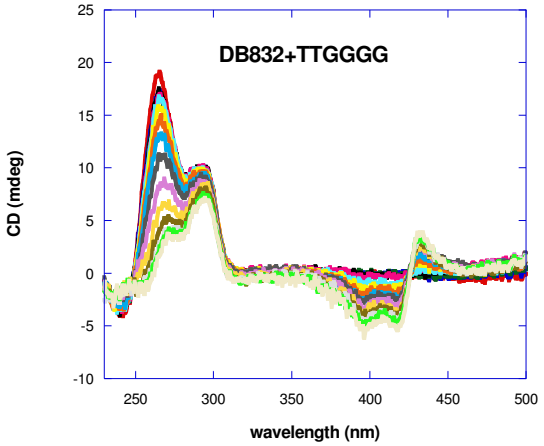

Figure 2.18 CD spectra of DB832 titrated into 3.0 µM of $(TTGGGG)_4$ in 10 mM Tris containing 50 mM KCl, pH 7.5. Compound: DNA ratios ranged from 1:1 to 16:1

Although highly conserved 22mer sequence is known to show intrinsic structure polymorphism, there is not a lot of information about the interconversion of different telomeric G-quadruplex conformations. Since both the conformations seem to coexist in potassium, the energy difference between the two appears to be low[134]. Anyway the kinetics of the interconversion between the two hybrid forms is rather slow and very few exchange peaks were observed on the NMR time scale[133] indicating a high energy barrier of the intermediate state[134]. Yang et all showed that the addition of a thymine residue at the 3'-end stabilizes the major structure and improves the NMR spectral quality. The ^{1}H NMR spectrum of Tel23 is cleaner as the population of minor conformations is clearly reduced as compared Tel22. In the figure below, we report the CD experiments performed with these two hybrid structures that differ from the wild type for the addition of a thymine base at 5' (Hybrid 1) and 3' (Hybrid 2). The compound confirmed the same behavior that showed with the 22 mer

quadruplex sequence. The large induced signal at 433 nm with exactly the same shape and also the same modifications in the DNA region are shown in the spectra above suggesting a high selectivity for this type of conformational folding.

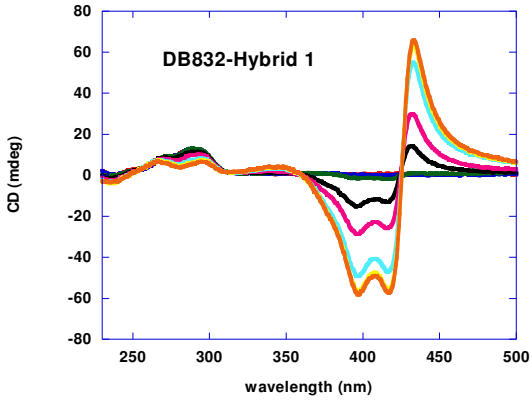

Figure 2.19.A CD spectra of DB832 titrated into 3.0 µM of d[TAG3(T2AG3)3] in 10 mM Tris containing 50 mM KCl, pH 7.5. Compound: DNA ratios ranged from 1:1 to 35:1

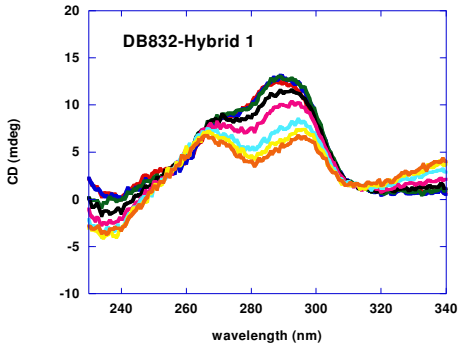

Figure 2.19.B Close-up of the wavelength region of DNA absorbance for the spectra shown in Figure 4.7.A of DB832 titrated into 3.0 µM of d[TAG3(T2AG3)3] in 10 mM Tris containing 50 mM KCl, pH 7.5

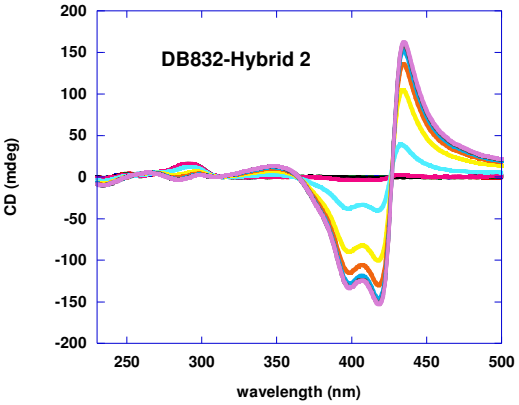

Figure 2.20.A CD spectra of DB832 titrated into 3.0 µM of d[AG3(T2AG3)3T] in 10 mM Tris containing 50 mM KCl, pH 7.5. Compound: DNA ratios ranged from 1:1 to 35:1

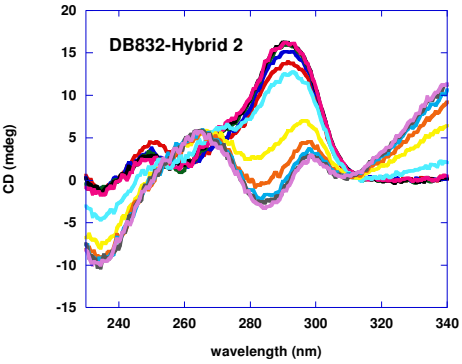

Figure 2.20.B Close-up of the wavelength region of DNA absorbance for the spectra shown in Figure 4.8.A of DB832 titrated into 3.0 µM of d[AG3(T2AG3)3T] in 10 mM Tris containing 50 mM KCl, pH 7.5

To summarize all the data obtained by CD titrations with DB832 and different DNA sequences, a plot with delta CD signal intensities as a function of ratios at 433 nm has been made. The graph highlights the preference for the human telomere wild

type, Hybrid 1 and Hybrid 2 characterized by the presence of a huge induced signal at that particular wavelength. Comparing these sequences to the Bromo substitute ones, the signal looks very low especially with ODN9, which is almost close to zero.

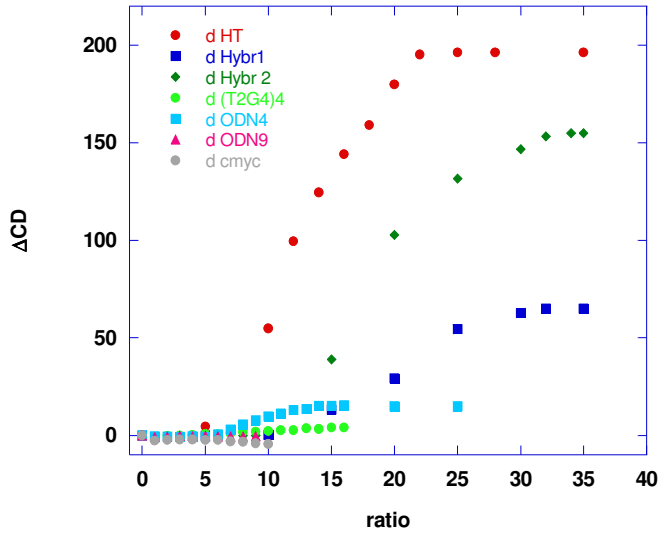

Figure 2.21 Plot comparing DB832 induced signal at 433nm at increasing ratios of compound: DNA with different quadruplex forming sequence in presence of 10 mM Tris containing 50 mM KCl,

2. 4. 1. 2. Biosensor studies

To gain information about the binding affinity in terms of constant, surface plasmon resonance experiments were performed. Unfortunately, due to the high stoichiometry of the system, it was not possible to measure a reliable binding constant. The Biacore instrument can work very well at low concentrations of compound and so the first binding event was easily detectable but if the concentration range is increased to allow the formation of the second one, that is actually weaker, the free compound starts to stick on the chip surface resulting in curves that are not possible to fit. However, sensograms obtained by using the human

telomere sequence and a duplex AATT sequence can be compared to prove binding specificity towards the quadruplex DNA (figure 2.22 and 2.23). The cooperative binding that gives the large induced CD signal cannot be evaluated by this method

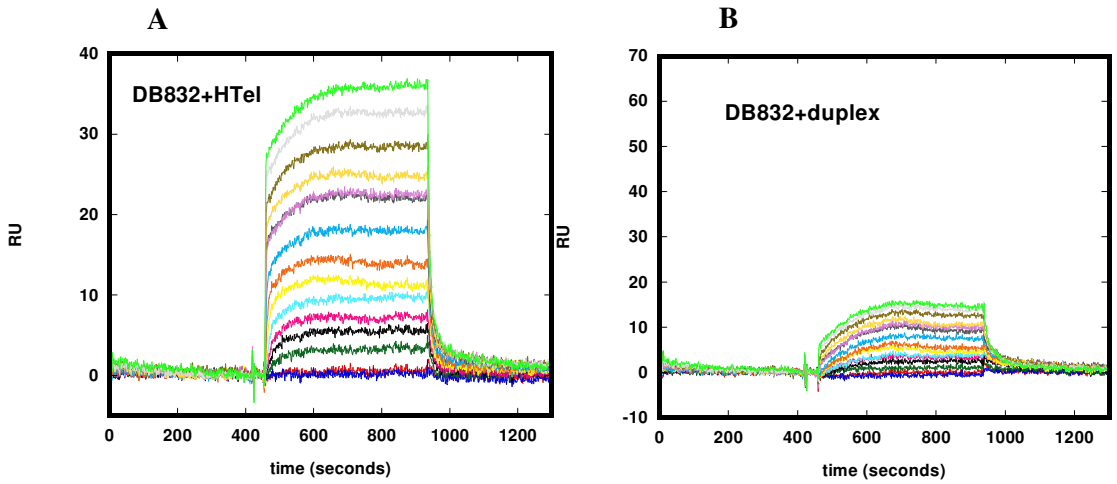

Figure 2.22 Representative SPR sensorgrams for the interaction of DB832 with the human telomere quadruplex sequence (A) and an AATT duplex sequence (B) at compound concentrations from 0 to 2 µM

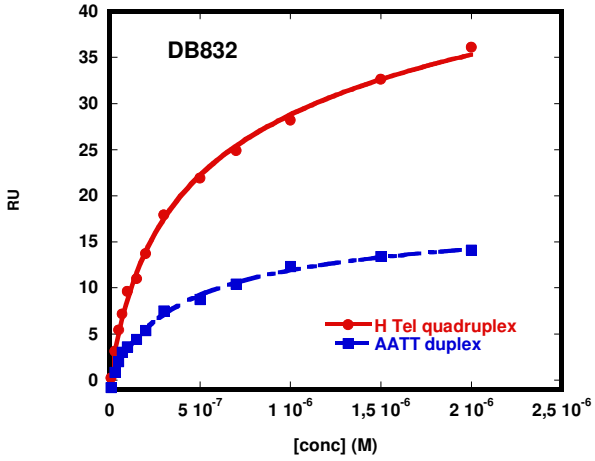

	H Tel G4	AATT duplex
K_1	$2.5*10^6$ M^{-1} ± 10%	$7.1*10^5$ M^{-1} ± 10%
K_2	$2.0*10^4$ M^{-1} ± 10%	-

Figure 2.23 Comparison of the SPR binding affinity of DB832 with quadruplex (circles) and duplex (squares) DNA sequences. RU values from the steady–state region of SPR sensorgrams are plotted against the unbound compound concentration (flow solution). The lines are the best fit values using appropriate binding models

2. 4. 1. 3. Mass Spectrometry experiments with the human telomeric sequence

Mass spectrometry analysis was used to obtain some information about the stoichiometry of DB832 - human telomere complex. Initially, experiments were performed by using electrospray ionization in the negative mode, common for DNA.

The presence of the 1:1 and 2:1 species appeared immediately at 1:1 ratio. Since it is known that the second binding event is shown at higher stoichiometry, 6:1 ratio was injected but the spectrum still indicate the presence of the 1:1 and 2:1 species. Then 8:1 ratio was evaluated but unfortunately it yields a noisy spectrum indicating that at this specific voltage the second complex is dissociated.

The experiment was repeated by MALDI but unfortunately the same behavior was confirmed. It was possible to try higher ratios like 10:1 and 15:1 but only the molecular ion relative to the free DNA, the 1:1 and the 2:1 complexes were observed Figure 2.24).

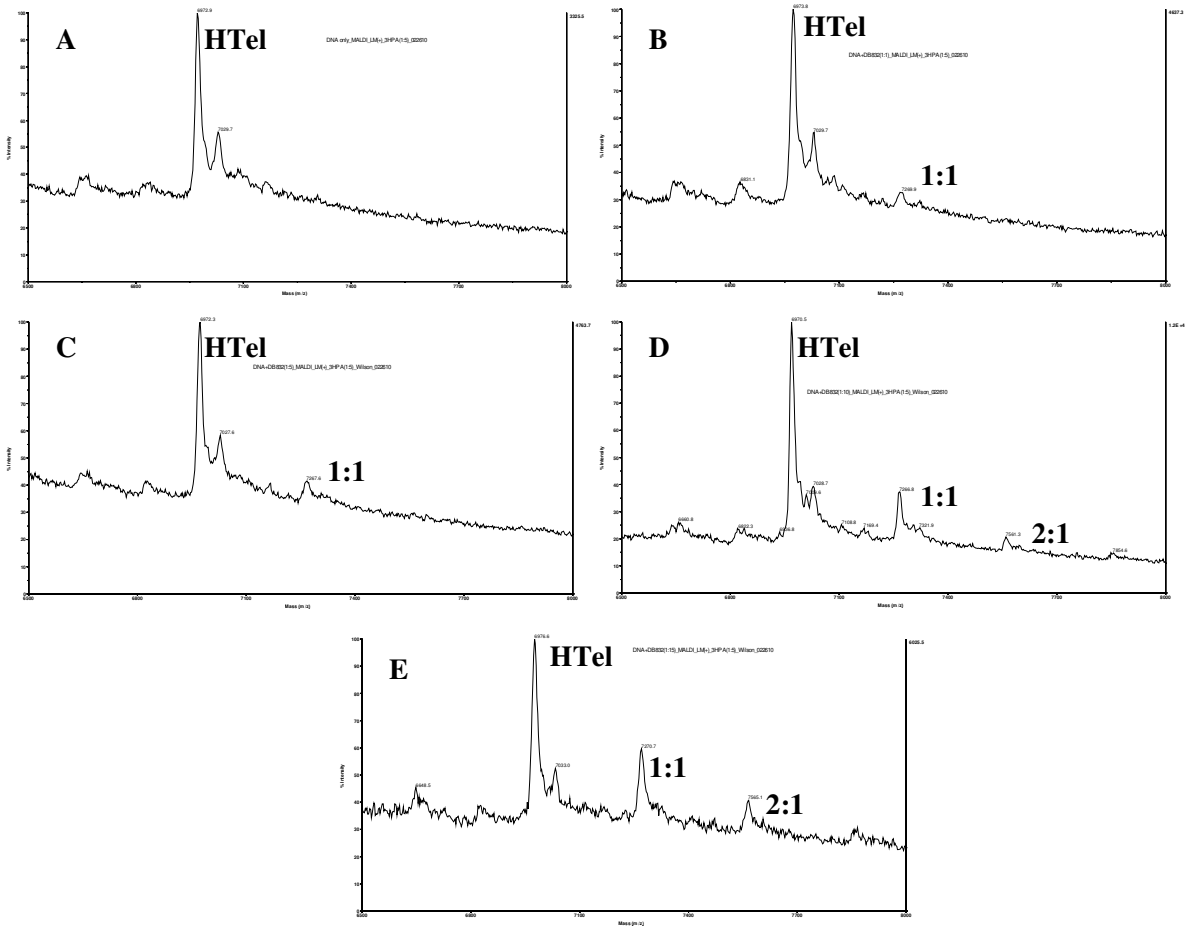

Figure 2.24 Mass spectra of human telomere quadruplex DNA and DB832, detected by MALDI at different rations compound: DNA. A) Human telomere only B) 5:1; C) 8:1; D) 10:1; E) 15:1

2. 4. 1. 4. UV thermal melting experiments

Thermal denaturation studies provide indication about the ability of the compound to interact and stabilize the DNA structure and have been widely used with quadruplex DNA[135]. DB832 was evaluated with four different G-quadruplex folding structures which were also used for CD experiments. Two different duplexes, an AATT rich and a GC rich sequence, were also employed to evaluate specificity of interaction towards quadruplex DNA.

High affinity for Hybrid 1 and Hybrid 2 species emerged, followed by the human telomeric sequence confirming the results obtained by CD experiments. No binding for GC double strand and a small ΔTm value with the hairpin AATT sequence indicate selectivity for quadruplex structures. The ΔTm values showed in the histogram are relative to 4:1 ratios (DB832: DNA) for quadruplexes and 2:1 ratios for duplexes (Figure 2.25).

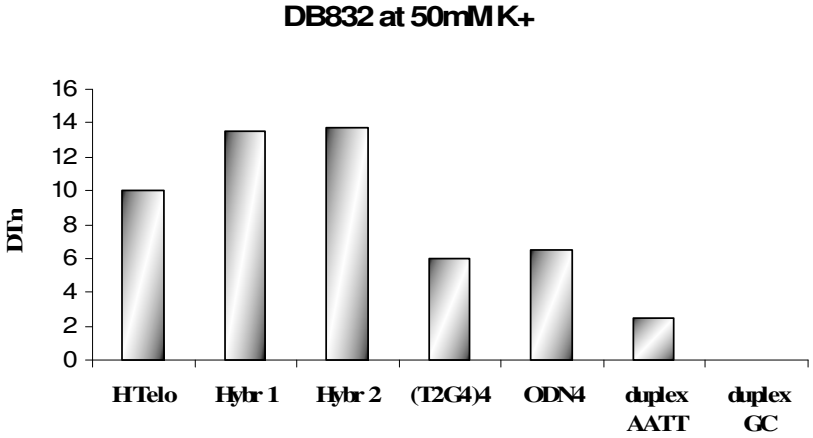

Figure 2.25 Diagrammatic bar array representation of the ΔTm values for compound DB832 with different DNA sequences in 10 mM Tris buffer containing potassium concentration of 50 mM.

2. 4. 1. 5. Fluorescence displacement assay

To further confirm the groove binding mode of DB832, Fluorescence Displacement assay and competition Circular Dichroism experiments were performed.

Fluorescence Displacement assay is based on the displacement of a fluorescent probe, the thiazole orange (TO) in this case, from DNA. It allows to test ligands based on their ability to displace the probe from the DNA region where the probe interacts. TO binds as an end-stacker to the human telomeric G4. From the plot, it is evident that DB832 is not able to displace TO, even at high concentrations. Considering that DB832 and TO have comparable Kb values on human telomeric G4, this could be most likely due to the fact that DB832 preferentially interact with another site of the DNA structures. In fact, when the same assay is performed with *cmyc,* the compound is able to displace 30% of the probe even at at low concentrations (4.5 μM) (Figure 2.26).

This assay reinforces the hypothesis that DB832 interacts with the human telomeric grooves and it is confirmed also by the behaviour of compound TmPyP4, which has a strong affinity for the ends of the human telomeric quadruplex and, as shown in the plot, displaces the TO completely at even modest concentrations.

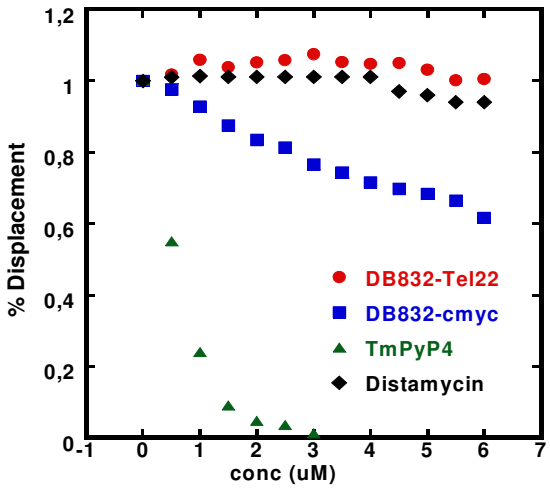

Figure 2.26. Comparison between the results obtained by displacement assay in 10 mM Tris and 50 mM KCl potassium chloride at 7.5 pH. TO was employed as probe molecule. The affinity of the compounds on Tel22 and *c-myc* is expressed as the concentration required to displace 30% of TO from the DNA. TmPYP4 and Distamycin were used as reference compounds for their interactions on the ends and in the grooves respectively

2. 4. 2. DISCUSSION

Searching for compounds that are able to interact with the grooves of the quadruplex DNA is a new attractive and challenging goal in the field. All quadruplex structures have four grooves, defined as the cavities bounded by the phosphodiester backbones and variable by dimensions, according to the overall topology and the nature of the loops[126]. Because of their different geometries than duplex DNA's grooves as well as different patterns of donor-acceptor, hydrogen-bonding sites[136 137], compounds that bind only into the grooves should be able to achieve excellent structure-specific recognition affinity and specificity. Their diversity allows also to obtain selectivity for particular G-quadruplex conformations.

The data provided by techniques such as surface plasmon resonance and mass spectrometry point out the complexity of studying interaction between compound DB832 and quadruplex DNA due to the high binding stoichiometry of the system. Anyway UV termomelting data revealed very good affinity to different quadruplex systems and the ability of the compound to stabilize this particular secondary structure folding (Figure 4.14) with significant specificity.

Interestingly, these results match very well the ones achieved by circular dichroism studies.

As previously mentioned, at the beginning of this chapter, the major difficulty in the identification of a quadruplex groove binder is to provide evidences that are consistent with this particular binding mode. The 8-Bromo guanine containing sequences were indeed an interesting model since they have been well defined by NMR studies and also because their conformations seem to be close to the biologically present ones. Results provided by CD titrations with these sequences indicate a

completely different behavior of DB832. For this reason we believe that this system can be a useful tool to support our proposal that DB832 is characterized by two binding events. The first one is stronger, occurs at lower ligand/DNA ratios and is more likely to be characterized by stacking interactions with the external tetrads of the G-quadruplex. The second one, weaker, happens at very high ratios and involves the grooves. CD results for a cyanine dye, DODC, established that the grooves of telomeric DNA can be targeted by small molecules as stacked species[138]. The large magnitude of the signals suggests also that it may bind into the grooves as a series of stacked species. The compound structure is small and the possibility of more that one species inside of each groove can explain the high stoichiometry. Moreover, by looking at the plot shown in Figure 14.10, the fact that each of the curves distinctly levels off suggests that the high stoichiometry is not due to aggregation phenomena or non-specific interactions.

Another confirmation of our hypothesis is provided by the Fluorescence Displacement Assay. The value of the first binding constant for DB832 with the human telomere in around 10^6 [139] and it is in the same order of the constant detected for the thiazole orange. Since they show the same affinity for the structure, the fact that DB832 cannot displace the thiazole orange, known to interact with the G-quadruplex structure by stacking with the external tetrads[139] can be due to its binding preferentiality for other sites of the structures like the grooves. This is confirmed by the same experiments performed with the parallel oriented *c-myc*, in which DB832 is able to displace the probe because the grooves are inaccessible.

By our knowledge, there is nothing else that we can try to make these evidences stronger. This is due to the fact that there is not any reference or paradigm

that can provide indications for the interactions of a compound into the quadruplex grooves. Anyway, the use of modified DNA models turned out to be a useful source of interesting results. Comparing these with the ones obtained with non modified sequences helps to demonstrate the consistency that DB832 can be considered a quadruplex groove binder.

2. 5. EVALUATION OF DB832 DERIVATIVES AS POTENTIAL GROOVE BINDERS FOR QUADRUPLEX DNA

The results obtained with the compound DB832, described in the previous subchapter, suggested this compound as a starting point for the development of unique ligands with high affinity and selectivity for quadruplex DNA. A mixed binding mode with the human telomere involving stacking with the external tetrads at low ratios and interactions into the quadruplex grooves at higher ratios has been proposed for DB832. Based on this feature, we thought that this molecule could provide a paradigm that can help to understand the optimum compound-DNA interactions that lead to groove recognition.

With the goal of gaining a better understanding of all the structural elements of DB832 contributing to G4 recognition, a series of structurally similar aromatic diamidines were designed, developed and evaluated. Particular emphasis was directed towards compounds that maintained the core structure of DB832: the 5-5-6 rings system. Systematic atom-wise and group-wise modifications were provided on the 5-5-6 scaffold that was hypothesized to be important for the compound binding.

An array of biophysical techniques was employed to characterize these ligands on the telomeric quadruplex DNA to further understand the important structural requirements for groove recognition (Figure 2.27).

Modifications were made in the regions that affect the compound stacking and through changes in shape and substituents. Switching the order of components in DB1093, for example, significantly changes the molecular shape. Converting one or two furans to thiophenes (DB1463, DB1438 and DB1450) makes subtle shape

changes but also can affect stacking. The furan-thiophene change has been shown to have a significant effect in duplex groove binding systems. Ortho or meta nitrogen substitution on the phenyl ring (DB934 and DB1693) or on the central furan ring (DB1999) of DB832 modifies stacking ability and can have potential to participate in hydrogen-bonding interaction in the grooves of G-quadruplex. Insertion of a methyl group to the terminal furan (DB1949) provides changes in stacking ability but also a steric restraint to that region of the molecule. A freely rotatable triple bond addition between the phenyl and the furan (DB1694) is expected to further weaken duplex interactions and potentially enhance quadruplex binding. Finally, the role of the amidine groups can be probed by converting them to imidazolines in DB1972 as well as in DB2037 derivatives. This substitution will provide planarity to the central system and maintain a doubly charged state at physiological pH. To help understand the quadruplex interactions of the new compounds, two central molecules, which have been reported in literature, were used as reference compounds. One, RHPS4 (Figure 2.28) is known to bind to the quadruplex structure via π- π interactions with the terminal guanines tetrads of the human telomeric sequence[140]. The other, Distamycin A (Figure 2.29), was recently assigned as a G-quadruplex groove binder after its NMR evaluation with a parallel four-stranded intermolecular quadruplex[141].

The interactions of the modified compounds with human telomeric quadruplex DNA were probed by an array of powerful methods. Thermal denaturation studies were performed on quadruplex and duplex DNA structures. Furthermore, based on the interesting indications provided by CD studies for DB832, the same experiments were performed with these compounds and the Tel22 wild type quadruplex DNA. An 8-Bromo substituted human telomere sequence, ODN9 was

also employed for CD titrations with selective compounds to compare them and delve into their modes of interactions with the G-quadruplex structure.

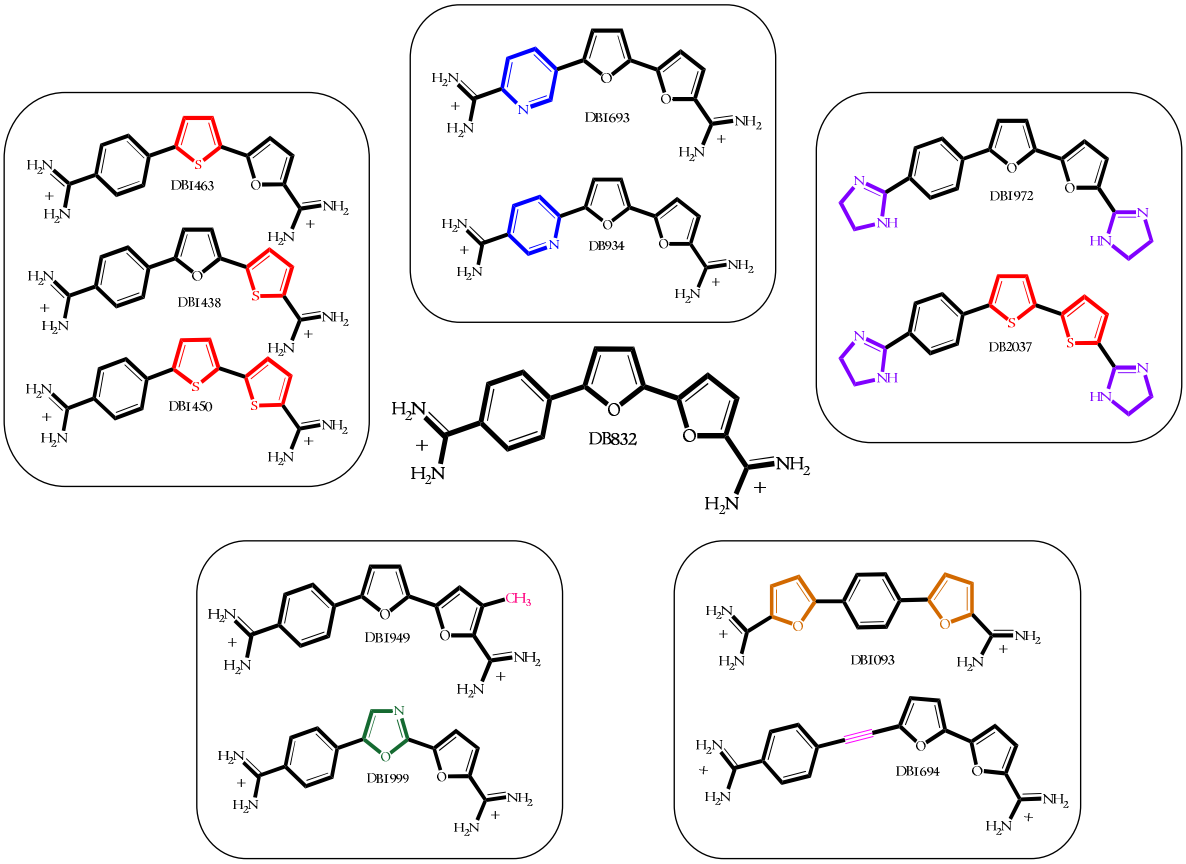

Figure 2.27 Chemical structures of the compounds studied in this Chapter. They all derive from compound DB832, with modifications in different positions

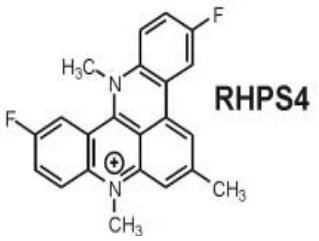

Figure 2.28 Chemical structure of RHPS4

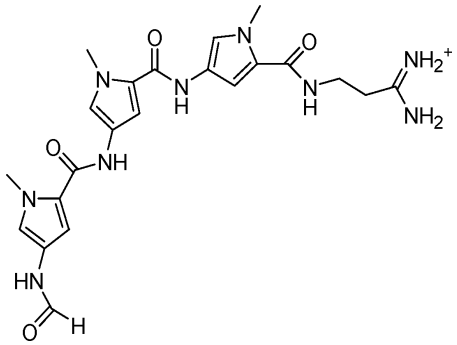

Figure 2.29 Chemical structure of Distamycin A

2. 5. 1. RESULTS

2. 5. 1. 1. Thermal melting experiments to detect affinity and selectivity

UV absorbance thermal melting experiments yield indications about stabilization of the G-quadruplex structure and they were performed to screen all compounds for comparison. Two different DNA sequences were used for this study: the human telomere Tel22 [AGGG(TTAGGG)$_3$] that folds in a G-quadruplex structure and, to evaluate selectivity, a duplex hairpin with an AATT sequence that is very favorable minor groove binding site.

DB832 shows a ΔT_m of 10 °C with the human telomere and around 2 °C with the duplex sequence indicating good selectivity for quadruplex DNA. However, the presence of the phenyl ring between two external furans in the DB832 structural isomer (DB1093) negatively influences the G-quadruplex affinity and the selectivity over duplex. Modifications in 3 position of the external furan such as the addition of a methyl group (DB1949) or the substitution of a carbon atom with a nitrogen (DB1999) does not affect the affinity for the human telomere or the selectivity for this sequence over the double strand. The substitution of the two furan rings with thiophenes (DB1450) results in a higher G-quadruplex ΔT_m that goes from 10 °C to 14 °C but, unfortunately, this modification decreases the specificity with a ΔT_m of more than 12 °C with the duplex hairpin. Affinity for duplex decreases to 5 °C when only the central furan is replaced by a thiophene (DB1463). Interestingly, the same substitution on the other furan, the external one (DB1438), significantly decreases the quadruplex binding properties with a ΔT_m value of 2 °C. The triple bond addition between the phenyl and the furan (DB1694) blunts the duplex interactions while

maintaining good stabilization properties with the quadruplex DNA. The nitrogen substitution on the phenyl ring of DB832 exhibited enhanced stabilization of the quadruplex arrangement when it is placed in the meta position (DB1693) but decreased affinity when it is in ortho (DB934). The convertion of amidine groups to imidazolines (DB1972, DB2037) yields a more planar arrangement while still maintaining a dicationic charge system. This modification might provide an increased stacking surface available for ligand interaction with the tetrads, and thereby, have a higher quadruplex recognition potential.

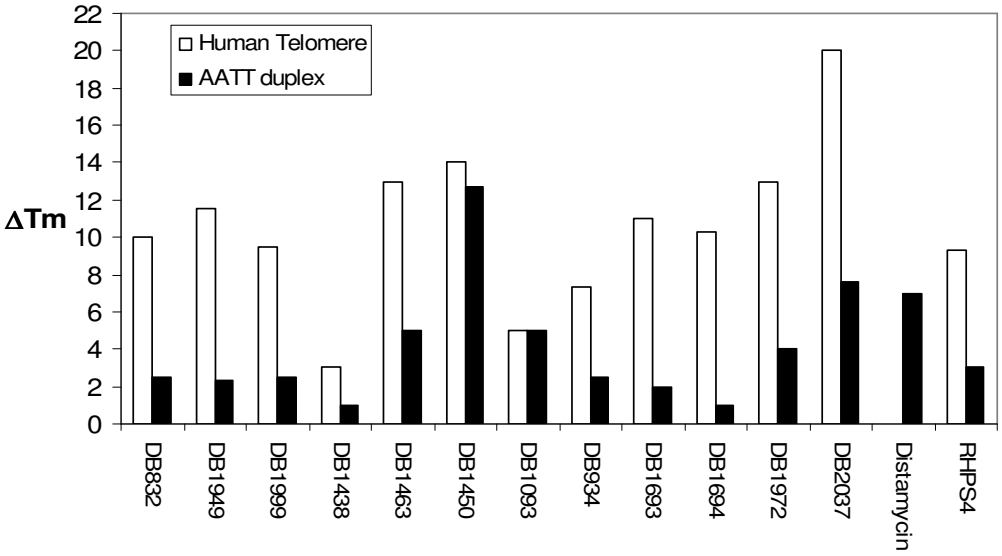

Figure 2.30 Diagrammatic bar array representation of the ΔTm values for the studied ligands. The sequence used were the human telomere quadruplex (white bars) and an AATT hairpin duplex (balck bars), in 10 mM Tris buffer with a potassium concentration of 50 mM, pH 7.5.

The reference compound distamycin, recently proposed as a G-quadruplex groove binder with the 4-stranded TGGGGT[123], did not show any ΔT_m with the human telomere sequence. As it is well known, however, that the polyamide is a strong binder to AT sequences in duplex DNA, Distamycin is the only compound of this group that has reverse selectivity for duplex over quadruplex. Finally, RHPS4, a well-studied quadruplex stabilizing compound that has been reported to bind by π-π

interactions with the external tetrad, shows melting values very similar to DB832 in terms of stabilization properties and selectivity for quadruplex over duplex DNA.

2. 5. 1. 2. Circular Dicroism pattern evaluation

Circular Dichroism studies were performed to evaluate how modifications on the DB832 system influence the DNA conformation and the interaction mode with the human telomere. The CD patterns for the derivatives are compared based on the shape of their induced signals as well as changes in the DNA spectra. From previous work[115] it is known that DB832 CD spectra are characterized by an impressive induced signal with two main peaks, a negative one at 418 nm and a positive at 435 nm (Figure 2.14). A combination of both positive and negative signals, coupled with different induced shapes indicates formation of stacked complexes as was previously shown with the cyanine dye DODC on quadruplex systems[142]. Moreover modifications in the DNA region driven by the compound indicate stabilization of a hybrid quadruplex conformation. Using the induced CD pattern exhibited by DB832 as a model for quadruplex multiple-site recognition, CD studies were conducted for the compounds in Figure 2.27.

The addition of a methyl group on the external furan (DB1949) and the substitution of a furan ring with an oxazole (DB1999) yielded induced CD patterns that resemble the one observed with DB832. These modifications apparently do not affect the interaction mode of the compounds with the human telomeric sequence. The only difference that emerges by comparing the spectra is the magnitude of the signal. However, DB1093, the linear isomer of DB832, exhibits a different pattern with a positive band below 350 nm and a negative indiced above 350 nm with relatively low intensity which is characteristic of ligands intercalating with duplex

DNA or end stacking with quadruplex DNA. Therefore, DB1093 might be an end-stacking molecule with quadruplex systems with relatively low ΔTm (Figure 2.30).

A shape similar to DB832 spectra but with even smaller peaks emerged in the CD spectrum of DB1463 (Figure 2.34), which differs from DB832 by the substitution of the central furan with a thiophene ring. Interestingly, if the same modification occurs on the other furan (the external one) in DB1438, the binding properties radically change. No induced CD is observed and the ΔT_m values, indicating stabilization properties for the human telomere sequence drastically decreases to 2 °C (Figure 2.30).

Compounds DB1972 and DB2037 have a structural characteristic that makes them unique from all the others, the presence of two imidazoline rings instead of the two amidine groups. The presence of these rings affects the equilibrium structure of the compound because the imidazoline reduces the torsional angle with the neighbor ring. This feature provides a more planar shape to the molecule. This kind of shape suggests a more favorable end stacking interaction with the external tetrads of the quadruplex. The induced shape, with a small positive peak followed by a negative, looks different from the CD patterns provided by all the other compounds (Figure 2.36). Interestingly, both the compounds exhibit very similar saturation ratios indicating very similar interaction modes and possibly with a very similar stiochiometry. DB934, with ortho nitrogen substitution on the phenyl ring, exhibited virtually no induced signal, even at high ratios, while DB1693, with meta nitrogen substitution, exhibited a weak exciton-type splitting (Figure 2.35). The fact that the substitution of a single atom makes a large change in compound induced signal shows that recognition of the quadruplex as stacked species is extremely sensitive to the

compound structure. Thermo melthing studies with these two compounds have shown that they have very good quadruplex stabilization potential, suggesting an end-stacking mode of interaction. Most of the compounds in this study had a very little effect on the quadruplex conformation as can be seen from the CD signals corresponding to the DNA region.

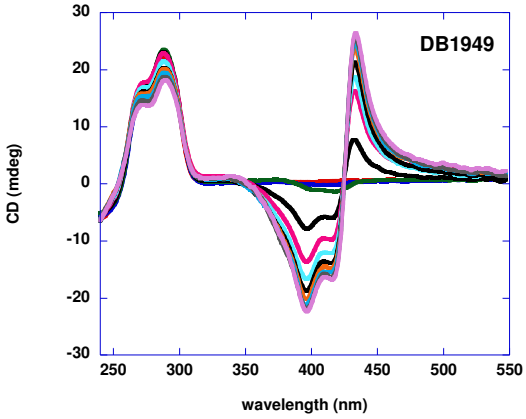

Figure 2.32. CD spectra of DB1949 titrated into 5.0 µM of d[T2G3(T2AG3)3A] in 10 mM Tris containing 50 mM KCl, pH 7.5. Compound: DNA ratios ranged from 1:1 to 10:1

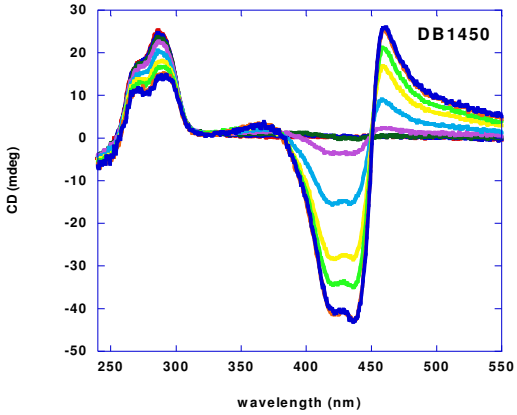

Figure 2.33 CD spectra of DB1450 titrated into 5.0 µM of d[T2G3(T2AG3)3A] in 10 mM Tris containing 50 mM KCl, pH 7.5. Compound: DNA ratios ranged from 1:1 to 8:1

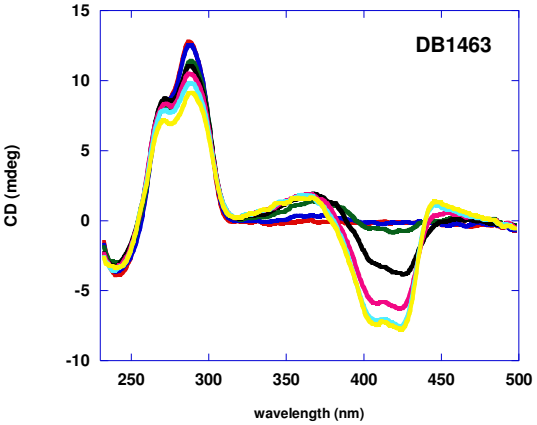

Figure 2.34 CD spectra of DB1693 titrated into 5.0 µM of d[T2G3(T2AG3)3A] in 10 mM Tris containing 50 mM KCl, pH 7.5. Compound: DNA ratios ranged from 1:1 to 11:1

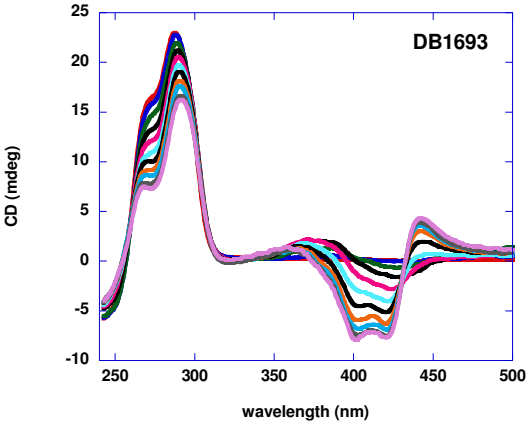

Figure 2.35 CD spectra of DB1693 titrated into 5.0 µM of d[T2G3(T2AG3)3A] in 10 mM Tris containing 50 mM KCl, pH 7.5. Compound: DNA ratios ranged from 1:1 to 8:1

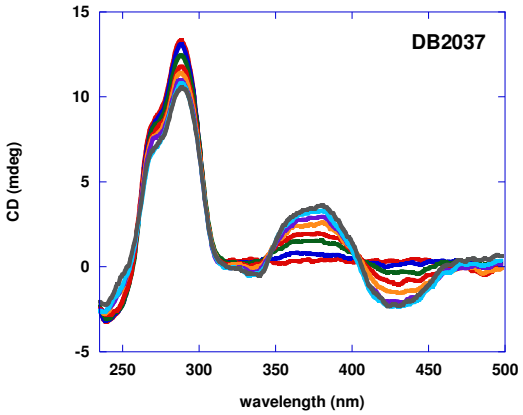

Figure 2.36 CD spectra of DB2037 titrated into 3.0 μM of d[T2G3(T2AG3)3A] in 10 mM Tris containing 50 mM KCl, pH 7.5. Compound: DNA ratios ranged from 1:1 to 7:1

Based on the results obtained from CD spectra, we decided to perform other experiments using the 8-Bromo guanine sequence (ODN 9). This sequence is characterized by the replacement of the hydrogen in 8 position of three guanines with bromine atoms in order to lock them and prevent any compound interaction. Three compounds, that provided a different CD pattern with the human telomere, were tested with this structure to see if the presence of the bromines into the grooves modified the binding interactions of the compounds resulting in a different shape of the induced signal. All the spectra collected for the three compounds are very similar to each other. They present small induced signals in the compound absorbance region characterized by a positive peak followed by a negative peak (Figure 2.37). From previous results, this shape suggests an end stacking interaction that can be reasonable because the grooves are occupied so the compounds can interact only with the external tetrads.

Moreover, DB1972, proposed as an “end stacker” with the human telomere based on its structural characteristics presents exactly the same CD spectrum with the ODN9 sequence. The other two compounds (DB1450 and DB1463) that showed different CD induced shapes when titrated to the human telomere can be proposed as partial groove binders. Likewise DB832, they seem to interact with the human

telomere with a mixed binding mode that starts with the external tetrads at low ratios and saturate into the grooves. Unfortunately, there are no data in the literature that attributes this particular induced shape (small positive peak, followed by a negative) to the "end stacking" interaction mode. However, RHPS4 has been demonstrated to stack on the end of G-quadruplex structures[140].

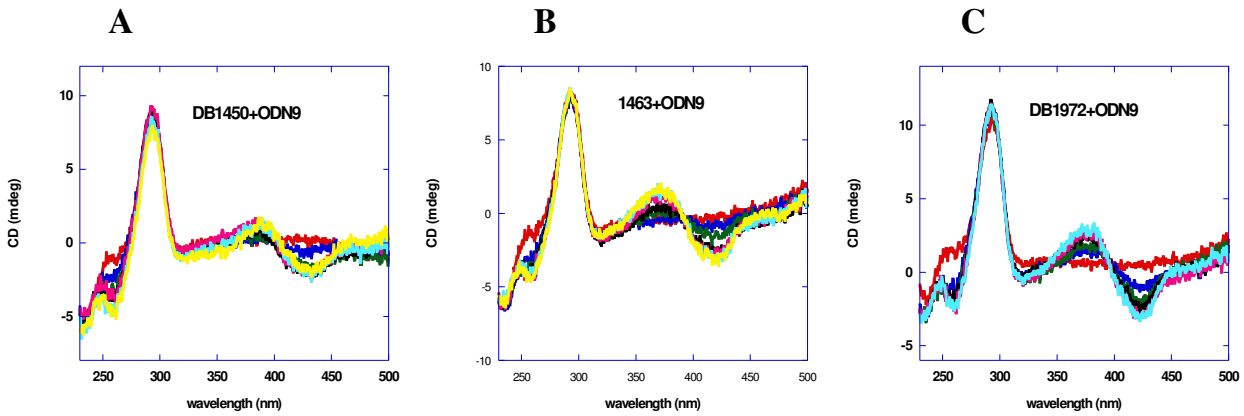

Figure 2.37 CD spectra of DB1450 (A), DB1463 (B) and DB1972 (C) titrated into 3.0 µM of ODN9 in 10 mM Tris containing 50 mM KCl, pH 7.5. Compound:DNA ratios ranged from 1:1 to 6:1 for all the three compounds

In order to understand this hypothesis we decided to employ this paradigm compound in a competition study, titrating it on the ODN9 sequence up to 3:1 (saturation ratio) and then adding DB1972, our candidate "end stacker", to monitor the formation of the induced signal. The spectrum shows a smaller induced signal that starts to appear at 4:1 ratio, later than with the human telomere (Figure 2.38). The presence of the signal can be attributed to the fact that DB1972 has a higher affinity than RHPS4 for the ODN9 sequence and can partially displace it. The same experiment, performed with DB832, resulted in no induced signal formation. In the previous Section we proposed for DB832 a mixed binding mode with the human telomere, characterized first by interaction with the tetrads with a binding affinity around 10^6 M^{-1}. Since the binding constant of RHPS4 with the human telomere is

$1*10^{-7}$, one order of magnitude higher, this explains why there is no signal in the CD spectrum. DB832 is weaker that RHPS4 and cannot readily displace it from the tetrad (Figure 2.39).

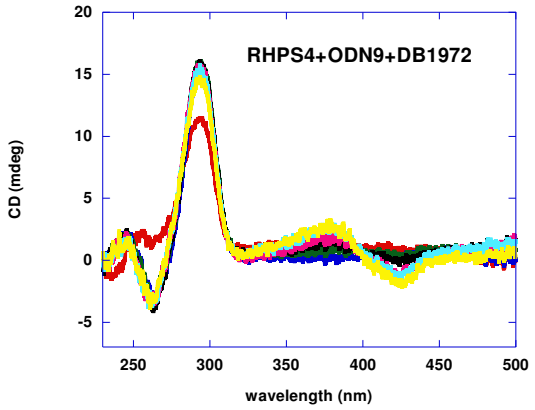

Figure 2.38 CD spectra of RHPS4 titrated into 3.0 μM of ODN9 in 10 mM Tris containing 50 mM KCl, pH 7.5. Compound: DNA ratios ranged from 1:1 to 3:1. The titration is followed by the addition of DB1972, added up to 8:1 ratio

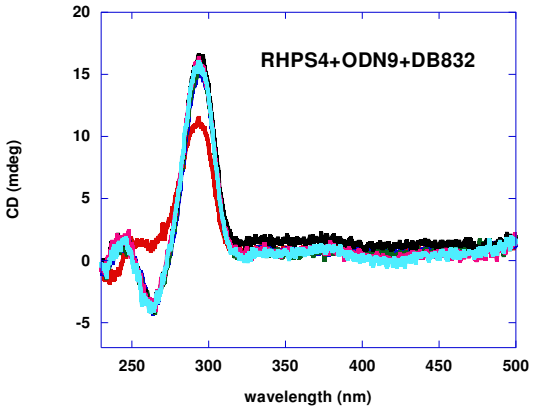

Figure 2.39 CD spectra of RHPS4 titrated into 3.0 μM of ODN9 in 10 mM Tris containing 50 mM KCl, pH 7.5. Compound: DNA ratios ranged from 1:1 to 3:1. The titration is followed by the addition of DB832, added up to 8:1 ratio

Interestingly, closer inspection of the induced CD signals exhibited by most of the compounds reveals a pattern emerging upon complex formation. A very weak induced signal is observed for all the compounds until the ratio 3:1, followed by a dramatic increase above that ratio for DB832, DB1949 and DB1450. Other compounds have weaker induced that are less than the original DNA CD signal. A weak induced signal with duplex DNA is generally observed for intercalation type mechanism[124]. However, with quadruplexes, intercalation is not commonly observed due to the high energetic cost required to replace the coordinating cations along the quadruplex helical axis and also due to the conformational restrains posed by the terminal diamidine units of the DB compounds[143]. Current literature does not provide any CD pattern attributable to specific recognition mode for quadruplex DNA since it has not been established so far. Nevertheless this technique can be used to prove

interaction of small molecules to the quadruplex DNA. It is also possible to compare them to obtain information about their mode of binding and conformational changes on the DNA structure.

The compounds evaluated in this Chapter are DB832 derivatives. Based on their CD spectra some of them yield induced signals that suggest similar behavior to DB832 while some others indicate different type of interaction with the human telomere potassium conformation. The information that we can obtain from these experiments allow us to hypothesize what the binding mode can be. Moreover, the employment of modified DNA models, such as 8-Bromo substituted sequences, that have been developed to stabilize the naturally occurring major structure of the human telomere in solution[144], turned out to be a wonderful tool to support our evidences of binding into the G-quadruplex grooves for DB832 and some of its derivatives. The CD pattern provided by the ODN9 sequence is similar to the one provided by the wild type. However, the induced signal generated at the end of the titration shows a completely different shape. In order to assign to this shape a clue indication about the interaction mode we found the reference compound RHPS4 as another helpful probe. Comparing CD spectra of DB832 titrated into the wild type sequence with the one obtained by the titration with the ODN9 sequence (with the grooves occupied by the bromines), the intensity of the signal impressively decreases strongly supporting an interaction into the grooves. Additionally, when the same sequence is saturated also at external tetrad level by the presence of a planar molecule like RHPS4, the signal is almost completely extinguished

To conclude, through the screening process, DB832 and some derivatives can be identified as quadruplex groove binders based on results obtained. The observed

weak induced signal at low ratios is consistent with the binding on either one or both the end of the quadruplex. On the other hand, a high induced relative to interaction of stacked species can clearly suggest the quadruplex grooves as proper binding sites.

Chapter 3

PHENANTHROLINE DERIVATIVES AND METAL COMPLEXES AS SUITABLE SCAFFOLDS FOR EFFECTIVE G-QUADRUPLEX RECOGNITION

3. 1. AIM OF THIS CHAPTER

Several classes of small molecules have been developed that efficiently target G-quadruplex DNA. Most of the ligands reported to date are based on planar organic aromatic arrays where a π-delocalized system allows the binding to the structure by stacking interactions with the external guanine quartets. The introduction of a positive charge on the molecule can further enhance the binding affinity through interaction with the phosphates of the DNA backbone. Although the majority of these compounds are based on purely organic systems, an interest in the investigation of metal complexes as potential quadruplex binders and stabilizers recently emerged. In these complexes the metal center acts as an anchor that holds in place a scaffold of ligands based on the properties of its own coordination sphere and it organizes it in specific geometries and orientations which can be optimal for stacking with the guanine quartet[145]. Additionally, the coordination of the metal to proper π-delocalised ligands (such as canonical G-quadruplex ligands) can withdraw the electron density yielding an electrondeficient ligand and so increasing its π–π interacting capabilities. Furthermore, the electropositive metal can be positioned at the centre of the guanine quartet thereby favouring the DNA folding by neutralizing the negative charge of the carbonilic groups of the bases[146]. As a result, G-quadruplex stabilization properties cannot be intrinsic of the ligand but governed by the balance between the geometry of the metal center and the nature of the aromatic ligand. The relative ease of synthetic route of many metal complexes allows the possibility of modifications on the ligands or the substitution of the metal center resulting in a broad variety of complex combinations[147].

Recently, a number of metal ion complexes have been evaluated for G-quadruplex binding: they comprise porphirine, salphen, terpyridine, bisquinolinium and phenanthroline analogues coordinated to a variety of metal ions including Zn^{2+} to Ni^{2+}, Cu^{2+}, Mn^{2+}, Ru^{3+}, V^{4+} and Pt^{2+}[148,149,150,151,152,153,154]. They are generally the result of the coordination of one metal ion to one selected ligand. To provide a relevant π-delocalized system these ligands can be penalized by a critic loss of water solubility. In this connection, we thought that the insertion of the metal ion would provide a surface in which two aromatic units are involved in the coordination thus improving the water solubility of the system. Moreover, we decided to investigate if quadruplex DNA recognition can be a result of transition metal ion-driven ligand assembly through coordination.

As leading ligand we selected the phenanthroline scaffold. It is known that this molecule can efficiently bind several metal ions such as Fe^{2+}, Zn^{2+}, Ni^{2+}, Rh^{3+} Ru^{3+} and Cu^{2+} due to its bidentate ligand nature. These coordination properties are of great interest in different fields. Ferroin, for example, composed by three phenanthroline molecules coordinating one Fe^{2+} is currently used as an indicator in analytical chemistry[155]. Additionally, phenanthroline can coordinate metal ions with different stoichiometry endowed of different DNA recognition properties. Several studies showed that phenanthroline-DNA affinity is enhanced when it is complexed with metals. However they indicate that most of Phen-metal ion complexes interact with the double helix not through an intercalation process but through insertion into the minor groove. Indeed, the geometry of the complex cannot properly fit the minor groove shape and allows only a partial stacking of the ligand planar surface within the

DNA base pairs. This feature resulted interesting in the design of new quadruplex interactive compounds with the goal of improving selectivity for the quadruplex system over the double helix.

In this Chapter we examined the DNA binding properties of phenantroline and several derivatives in presence and in absence of metal ions. In particular, we evaluated phenanthroline-based ligands that may form metal ion complexes with different stoichiometries involving one, two or three ligands per metal ion. This property can be indeed modulated by the nature and position(s) of the substituents introduced in the phenantroline ring system[7]. This would allow us to investigate if different complex geometries are likely to affect the pattern of DNA recognition and, consequently, the nucleic acid conformational equilibria.

The linked compounds can be divided into two groups of derivatives: one composed by mono-phenantroline derivatives containing one or two N,N-dimethylamino ethylamino protonable side-chains (Fig 1A). The second one is composed by ligands containing two phenantroline moieties covalently linked trough amine or thioether bond (bis-phenantrolines) (Fig 1B).

For all the tested compounds we characterized the metal ion binding in terms of affinity and stoichiometry. Then binding properties of ligands and the corresponding metal complexes with quadruplex and duplex DNA were tested by a number of techniques including: UV absorbance, fluorescence melting, circular dichroism and gel electrophoresis. Biological studies such as enzymatic assays on polymerase and telomerase and cell cytotoxicity evaluation have been performed to complement the biophysical data. Finally, a particular interest was turn to the

potential capability of these molecules to cleave or covalently bind duplex and quadruplex DNA.

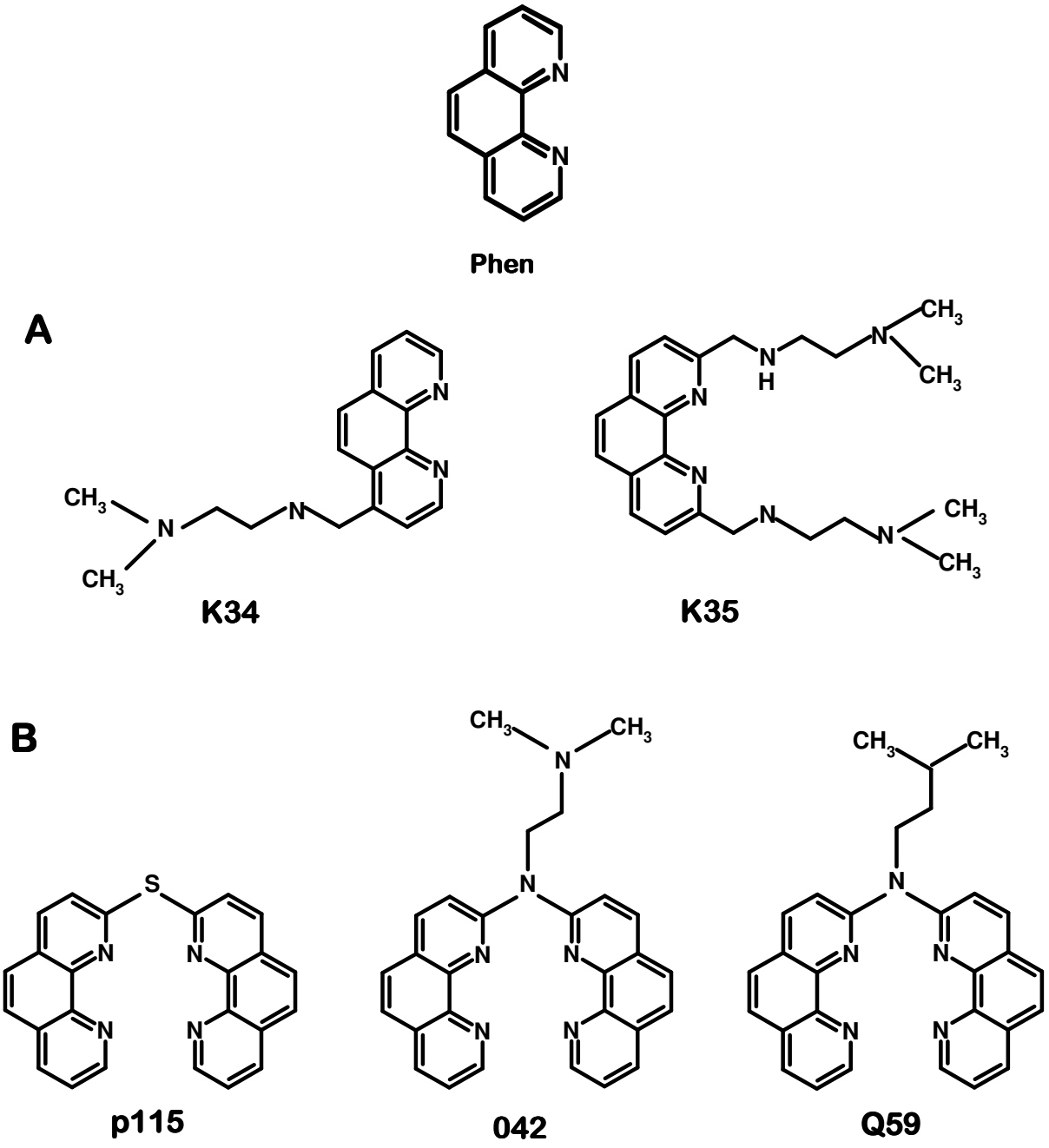

Figure 3.1 Structures of the tested compounds: mono-phenanthroline (A) and bis-phenanthroline (B) derivatives

3. 2. MATERIALS AND METHODS

3. 2. 1. Instrumentation

Table 3.1 Instrumentation used

Autoclave	International PBI
Gel Dryer	Hoefer Scientific Instruments
Developing sheets Hyperfilm MP	Amersham Pharmacia Biotech
Lambda 20 Spectrophotometer	Perkin Elmer
Spectropolarimeter J-810-150S	Jasco
Thermostat RTE-111	Thermo Neslab Instrument
LightCycler	Roche S.p.A
Phosphor Imager STORM 840	Amersham Pharmacia Biotech
Scintillation Counter TRICARB 2800 TR	Perkin Elmer
Speed Vac	UniEquip, Milano
pHmeter 713 Metrohm	Metrohm Italiana s.r.l
Geliance 600 Imagyng System	Perkin Elmer
Centrifuge Allegra X-22R	Beckman Coulter
Incubator HERA cell 150	Heraeus Instruments
Microplate Reader model 680	Biorad
Optical microscope	Carl Zeiss S.p.A.
Auto ITC HT Microcalorimeter	MicroCal, GE Healthcare
ESI-TOF Mass Spectrometer	Mariner
Horizontal Electrophoresis Apparatus	Biorad
Vertical Electrophoresis Apparatus	CBS Scientific

3. 2. 2. Nucleic acids and synthetic oligonucleotides

Plasmid pBR322 purchased by Fermentas International INC (Burlington, Ontario, Canada). It is a double-stranded supercoiled circular DNA, 4361 base pairs in length.

Calf thymus DNA (ctDNA) was purchased from Sigma. It is double stranded DNA containing less than 1% of proteins. Solutions were prepared by resuspending ctDNA in the proper buffer over night at 4°C. The solution was shacked for about one hour and finally filtered with a 5□m diameter Millipore filter. Molar concentration was calculated by Lambert – Beer equation at 260 nm using molar extinction coefficient □ 6600 $M^{-1}cm^{-1}$.

Lyophilized synthetic oligonucleotides were purchased from Eurogentec S.A. (Seraing, Belgium) and Metabion International AG (Martinsried, Germany) and provided with HPLC purification and mass spectrometry characterization. Oligonucleotides concentration was determined by UV-Vis from absorbance at 260 nm using molar extinction coefficient obtained from nearest-neighbor model[189].

Prior to each experiment, G-quadruplex forming sequences were dissolved in buffer to the desired concentration, heated at 90 °C for 5 minutes and cooled slowly to insure the folding of the sequence. Ds-scrambled DNA was prepared by heating the two complementary strands at 90 °C for 5 minutes and slowly cooling to insure the annealing of the sequence.

3. 2. 3. Ligands and metal ions solutions

The syntheses and purifications of phenatroline derivatives were performed by Prof. A. Paul Krapcho's group at University of Vermont. Appropriate stock solutions of each compound were prepared in DMSO or water (K34) and diluted to the required concentrations with appropriate buffer. Copper solphate and Nichel Chloride were dissolved in deionized water; metal ion concentrations were determined by ICP (Optima 3000 DV Perkin Elmer).

Table 3.2 Oligonucleotide sequences used

Tel22 (22mer):	5'-AGG-GTT-AGG-GTT-AGG-GTT-AGG-G-3'
Scramble (22mer):	5'-GGA-TGT-GAG-TGT-GAG-TGT-GAG-G -3'
Coscramble (22mer)	5'-CCT-CAC-ACT-CAC-ACT-CAC-ATC-C-3'
Tel26 H1 (26mer):	5'-AAA-GGG-TTA-GGG-TTA-GGG-TTA-GGG-AA-3'
Tel26 H2 (26mer):	5'-TTA-GGG-TTA-GGG-TTA-GGG-TTA-GGG-TT-3'
2GGG (24mer):	5'-TAC-AGA-TAG-TTA-GGG-TTA-GGG-TTA-3'

Table 3.3 Oligonucleotide sequences used for Fluorescence Melting experiments

HTS (23mer):	Dabcyl-5'-AGG-GTT-AGG-GTT-AGG-GTT-AGG-GT-3'-FAM
1F (18mer):	FAM-5'-GTGAGATACCGACAGAAG- 3'
3F (18mer):	5'-CTTCTGTCGGTATCTCAC-3'-Dabcyl

Table 3.4 Oligonucleotide sequences used for *Taq* polymerase inhibition experiments

Tup	5'-TGAGGATCCGCCTGGACAGCATGG- 3'
Tdown	5'-GTCGAATTCTCGGCGAGAAGCAGG- 3'

Table 3.5 Oligonucleotide sequences used for Telomerase Activity Assay

TS (18mer):	5'–AAT-CCG-TCG-AGC-AGA-GTT-3'
ACX (30 mer):	5'–GCG-CGG-CTT-ACC-CTT-ACC-CTT-ACC-CTA-ACC-3'

3. 2. 4. Buffers

All buffers have been prepared using MilliQ water and then filtered:

TK 10/50: 10 mM Tris, 50 mM potassium chloride, pH 7.5

TBE 1X: 89 mM Tris, 89 mM Boric Acid, 2mM EDTA, pH 8.0.

TAE 1X: 4 mM Tris, 4 mM Acetic Acid, 0.1 mM EDTA

GEL LOADING BUFFER (10X): 50% glycerol, 50% water, 0.05% bromophenol blue, 0.05% xylene cyanol

PCR BUFFER 10X (FERMENTAS): Tris-HCl 100 mM (pH 8.8 a 25°C); potassium chloride 500 mM; 0.8% Nanidet; magnesium chloride 25 mM.

TRAP BUFFER 10X: 200 mM Tris-HCl, pH 8.3;); 630 mM potassium chloride; 15 mM magnesium chloride; 10 mM EDTA; 0.5% TWEEN 20.

LiP: 40 mM lithium hydroxide; potassium chloride or sodium chloride at the reported concentrations, at pH 7.4 with phosphoric acid.

ITC BUFFER: 10 mM Tris, 20 mM potassium chloride, pH 7.5

3. 2. 5. Fluorescence Melting Studies

Melting experiments were performed in a Roche LightCycler fluorimeter, using an excitation source at 488 nm and recording the fluorescence emission at 520 nm. Target DNAs were HTS) and ds-random (Fluorescin 5' labelled 5'-GTGAGATACCGACAGAAG-3' annealed with its complementary strand labeled with Dabcyl at 3' end). Mixtures (20 □L) contained 0.25 □M of target DNA and variable concentrations of tested derivatives in 10 mM lithium hydroxide, 50 mM potassium chloride at pH 7.4 with phosphoric acid.). They were first denatured by heating to 95 °C for 5 min and then cooled to 30 °C at a rate of 0.5 °C min^{-1}. Then temperature was slowly increased (1 °C/min) up to 90 °C and again lowered at the same rate to 30°C. Recordings were taken during both these melting and annealing reactions to check for hysteresis. T_m values were determined from the first derivatives of the melting profiles using the Roche LightCycler software. Each curve was repeated at least three times and errors were ± 0.4°C.

3. 2. 6.UV Titrations

Spectrophotometric titrations were performed in the 240-440 nm range at 25 °C in a 1 ml or 3 ml cuvette in 10 mM TRIS, 20 mM potassium chloride at pH 7.5 with a Perkin-Elmer Lambda 20 apparatus. Complex formation was followed recording ligand spectra upon incremental additions of metal ion solutions.

To determine complex stoichiometry, different amounts of metal ion and ligands solutions were mixed to reach a final constant total concentration (0.3 mM).

3. 2. 7. Job plot

A plot reporting the ligand absorption as a function of the ions molar fraction (χ_i) is obtained. Maximal value corresponds to the molar fraction of the formed metal complexes.

$$\chi i = \frac{[I]}{[I] + [Phe]}$$

3. 2. 8.Circular Dichroism Studies

Circular dichroism spectra from 230 to 350 nm were recorded using 10 mm path-length cells on a Jasco J-810 spectropolarimeter equipped with a NESLAB temperature controller and interfaced to a PC 100 in 10 mM Tris, 50 mM potassium chloride at pH 7.4. Before data acquisition, 4 □M DNA solutions (strand concentration) were heated at 95 °C for 5 min and left to cool at room temperature o.n. The reported spectrum of each sample represents the average of 3 scans recorded with 1-nm step resolution. Observed ellipticities were converted to mean residue ellipticity [□] = deg x cm^2 x $dmol^{-1}$ (Mol. Ellip.).

3. 2. 9.Mass spectrometry

All mass spectra were obtained using a Mariner™ mass spectrometer, Applied Biosystems (Foster City, CA). Analytical solutions were prepared in water/methanol (10/90 %) and contained 1 nM ligand and different stoichiometric amounts of metal ions. A Harvard model 11 syringe pump (Holliston, MA) set at a flow rate of 20 µl/min was used to infuse the sample solutions. The ESI source was operated in positive ion mode with an electrospray voltage of 4.5 kV. Spectra were acquired over the *m/z* range 100-4000 by summing 100 scans.

3. 2. 10. Electrophoretic Mobility Shift Assay (EMSA)

Single stranded oligonucleotide (Tel22 or 2GGG) were 5'-labeled with ^{32}P and T4 polynucleotide Kinase, by incubating the reaction mixture at 37 °C for 30 min. The kinase activity was inactivated by heating the reaction mixture at 85°C for 5 min, followed by two phenol extractions. A mixture of purified labelled and unlabelled oligonucleotides (total final concentration 1 □M) and tested ligands was heated to 95 °C for 10 min in 10 mM Tris-HCl, pH 8.0 and let to cool at room temperature o.n. in the presence/absence of 50 mM potassium chloride. After incubation, the samples were analyzed by native 16% PAGE in 0.5X TBE containing 20 mM potassium chloride in the running buffer. Gels were dried and resolved bands were visualized and quantified on a PhosphorImager (Amersham).

3. 2. 11. DNA modification

DNA cleavage experiments were performed incubating pBR322 (20 □M) or ^{32}P-labelled Tel22, ss-scrambled or ds-scrambled (1-10 □M) at 37 °C for 30 min in the presence/absence of increasing amount of metal complex in 10 mM TRIS, 50 mM potassium chloride, pH 7.5 . Reactive mixtures containing Ni^{2+} and Cu^{2+} complexes

were added of MMPP (5 mM) or Ascorbic Acid (0.1 mM) respectively. pBR322 reaction products were resolved on a 1% agarose gel in TAE buffer containing 1% SDS and visualized by ethidium bromide staining. Shorter DNA sequences were loaded on a sequencing gel and reaction products were identified by autoradiography. The amounts of undigested DNA were quantified and plotted as a function of metal ion complexes.

3. 2. 12. *Taq* Polymerase Assay

Taq polymerase reaction in the presence/absence of ligands and their metal complexes were performed using pBR322 (2.5 ng) as template and appropriate primer sequences Tup and Tdown (0.5 μM) to amplify the 906-1064 sequence of plasmid by PCR. The reaction was carried out in a Perkin Elmer thermocycler performing 25 cycles of: 30 s at 94°C, 30 s at 65 °C and 30 s at 72 °C. The reaction products were resolved on a 2% agarose gel in 1X TBE and stained by ethidium bromide.

3. 2. 13. Telomeric Repeat Amplification Protocol (TRAP Assay)

An aliquot of $5x10^6$ JR8 cells in exponential phase of growth was pelleted and lysed for 30 min on ice using 100 μl of 0.5% CHAPS, 1 mM EGTA, 25% 2-mercaptoethanol, 1.74% PMSF and 10% w/v glycerol. The lysate was centrifuged at 13000 rpm for 30 min at 4 °C and the supernatant collected, stored at –80 °C, and used as telomerase source.

Telomerase activity was assayed using TRAPeze telomerase detection kit (Chemicon International). Each reaction was performed using 1 μg of protein extract and including in the reaction mixture increasing complexes concentration. The

reaction products were loaded onto a 10% polyacrylamide gel (19:1) in TBE 0.5X. Gels were stained with SbrGreen I.

3. 2. 14. Cell cultures and toxicity assays

HeLa (human hepitelial) and 293T (human renal epithelial) cell lines were maintained in DMEM medium supplemented with 10% heat-inactivated foetal calf serum, 50 U/ml of penicillin G and 50 µg/ml of streptomycin, at 37°C in humidified atmosphere and 5% of CO_2.

To evaluate toxic profiles of the potential antitelomerasic compounds, MTT assays were performed: cells were plated in 96 well plates at 10.000 cells/well, and cultured overnight. Afterwards, compounds were added in triplicate and plates were incubated in presence of the drug for 96 hours. At the end of this period, MTT was added to a final concentration of 0.8 mg/ml, and two additional hours of incubation were performed. After medium removal, 150 µl of DMSO were added to each well. Soluble formazan salts were homogenated by manual pipetting and the absorbance at 540 nm were read. Results were analyzed as sigmoidal dose-response curves .

3. 3 RESULTS

3. 3. 1. Phenantroline derivatives form very stable complexes in solution

The complex formation of the tested ligands with several divalent metal ions (Ni^{2+}, Cu^{2+}, Zn^{2+}, Mg^{2+}, Mn^{2+}) was investigated by spectroscopic titrations. Addition of metals to tested derivatives induced remarkable changes in the ligands absorption spectra (Figures 3.2, 3.3 and 3.4). In particular, upon addition of Ni^{2+} or Cu^{2+} ions to Phen or to its derivatives a bathochromic and hyperchormic shift of the absorption spectra was observed whereas different variation can monitored with bifunctional ligands. Interestingly, well defined isosbestic points were observed when all the new ligands were titrated with metal ions. Isosbestic points were generally well defined in our experimental conditions supporting equilibria involving only two species. Unfortunately, these complexes do not show useful d-d or charge transfer transitions for spectroscopic analysis[156]. A linear dependence of ligands absorption upon coordinating ion concentration was generally observed even at micromolar ligand concentration; this is indicative of remarkably high formation constants.

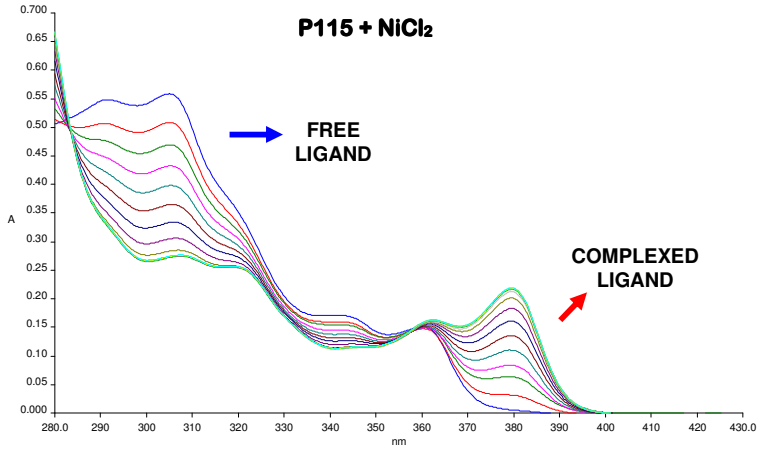

Figure 3.2 titration of P115 0.02 mM monitored in 10 mM Tris, 20 mM KCl at increasing additions of $NiCl_2$ (0-0.1 mM) 1.25 mM.

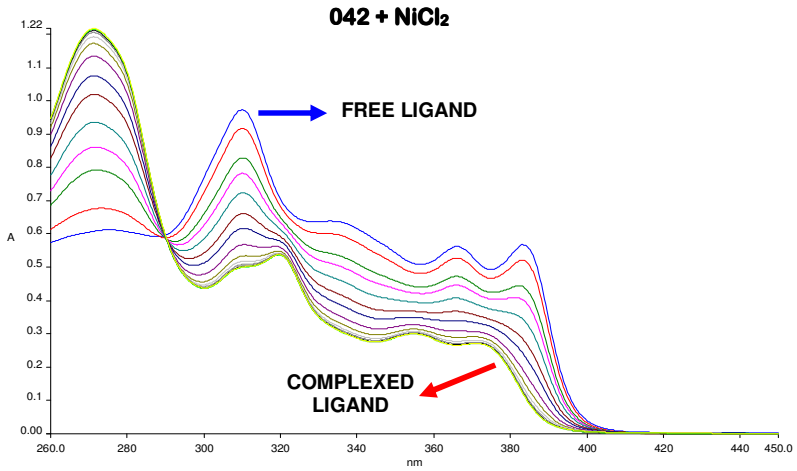

Figure 3.3 titration of 042 0.031 mM in 10 mM Tris, 20 mM KClat increasing additions of $NiCl_2$ (0-0.12mM) 3.33mM.

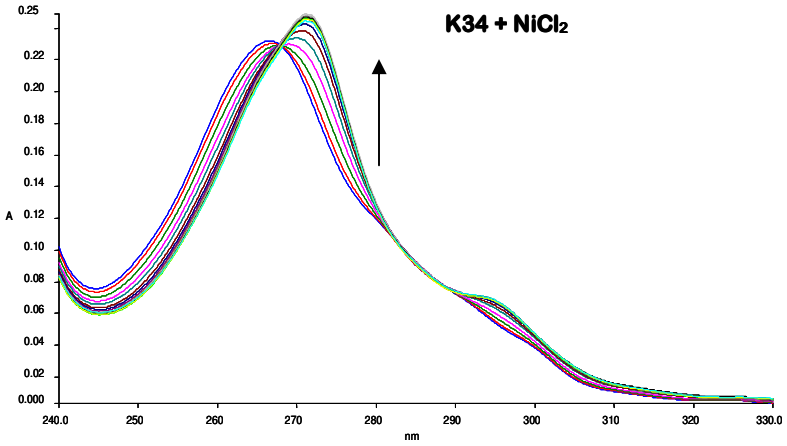

Figure 3.4 Titration of K34 (17 µM) with Ni(II) (0-30mM) monitored in 10 mM Tris, 50 mM KCl, pH 7.5. Arrow indicates the effects of incrementing metal ion concentration

The high metal ions affinity of these ligands prevented accurate evaluation of the binding parameters by UV-Vis titrations. However, we took advantage of the changes in the ligand absorption properties to determine the stoichiometry of the complexes formed in solution. By applying the method of continuous variations (Job plot) we verified a different complexation preference of our ligands. For K34 it depends on the nature of the metal ion: indeed, a 1:1 complex was predominant with Cu^{2+}, while Ni^{2+} favoured a 2:1 stoichiometry. On the opposite, only a 1:1

stoichiometry was always adopted by K35, probably due to the presence of 2,9 substituents containing amino groups that can be involved in metal coordination. Additionally, their steric hindrance can largely impair the stability of complexes containing multiple ligand units. This could also explain why K35 showed a reduced affinity for Ni^{2+}, albeit with K_d in the micromolar range (53 μM).

Job plots confirmed a 1:1 stoichiometry for bis-phenantroline derivatives (Figures 3.5 and 3.6). Noteworthy, for this set of ligands, highly efficient complex formation was confirmed with Zn^{2+}, Ni^{2+} or Cu^{2+} (Figure 3.7). Lower binding affinities were monitored using Mg^{2+} or Mn^{2+} although K_d was still in the μM range (13.8 ± 0.3 μM and 15.8 ± 0.7 μM for P115, respectively).

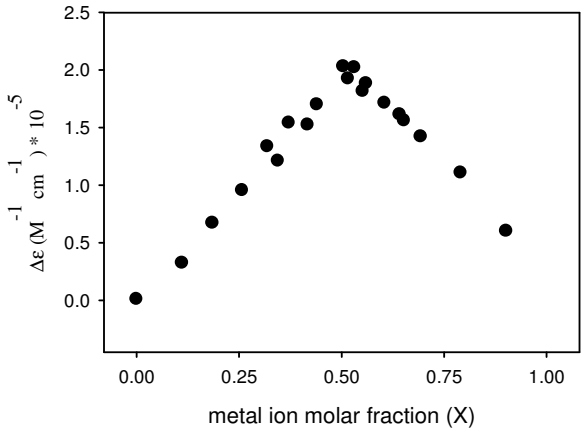

Figure 3.5 Job plot for 042-Ni^{2+} (total concentration 0.3 mM) complex formation monitored in 10 mM TRIS, 50 mM KCl, pH 7.5. Absorbace was measured at 271 nm

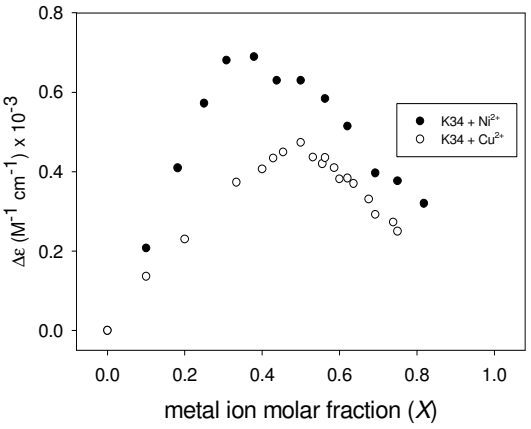

Figure 3.6 Job plot for the ligand-metal ion (total concentration 0.3 mM) complex formation monitored in 10 mM Tris, 50 mM KCl, pH 7.5

The spectroscopic data relative to Ni^{2+} and Cu^{2+} complexes where confirmed by ESI-TOF mass spectrometry (Figures 3.8, 3.9, 3.10) and the results are summarized in Table 3.6. The mass spectrometry data are fully consistent with the spectroscopic ones, the only exception being the K34Ni^{2+} system for which the 1:1 complex was also detected (as well as the 3:1 although at very low peak

intensity). We cannot exclude dissociation of one phenantroline moiety from the complex(es) as a consequence of fragmentation occurring in the mass spectrometer. Additionally it should be noted that the ligand-metal ion mixtures used for MS analysis were prepared in 90% methanol which can justify the subtle changes in complex distribution observed.

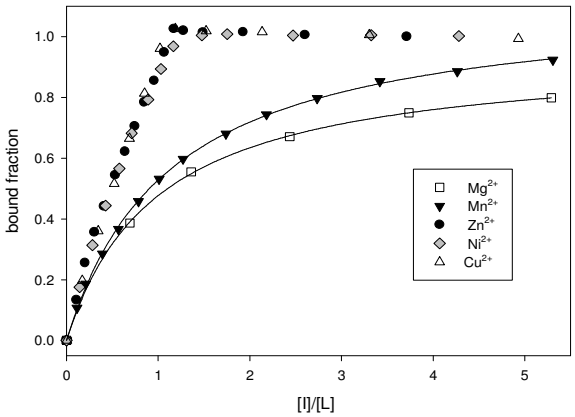

Figure 3.7 variation of the p**115** bound fraction as a function of different metal ion vs ligand ratio.

LIGAND/ION MOLAR RATIO IN RESOLVED PEAKS

	Ligand/ion molar ratio in injected solution	**PheCu^{2+}**	**042Cu^{2+}**	**p115Cu^{2+}**	**K34Cu^{2+}**	**K35Cu^{2+}**
ESI-MS	1:1	0,1:1,2:1	0,1:1	1:1	1:1	1:1
	2:1	0,1:1,2:1	-	-	1:1	1:1
	3:1	0,2:1,3:1,1:1	-	-	1:1	1:1
UV-Vis titration		nd	1:1	1:1	1:1	1:1
	Ligand/ion molar ratio in injected solution	**PheNi^{2+}**	**042Ni^{2+}**	**p115Ni^{2+}**	**K34Ni^{2+}**	**K35Ni^{2+}**
ESI-MS	1:1	1:1,2:1	1:1	1:1	1:1	0,1:1
	2:1	2:1,3:1	-	-	1:1,2:1	0,1:1
	3:1	3:1	-	-	2:1,3:1,1:1	0,1:1
UV-Vis titration		nd	1:1	1:1	2:1	1:1

Table 3.6 Summary of the species detected in solution by ESI-TOF and UV-VIS

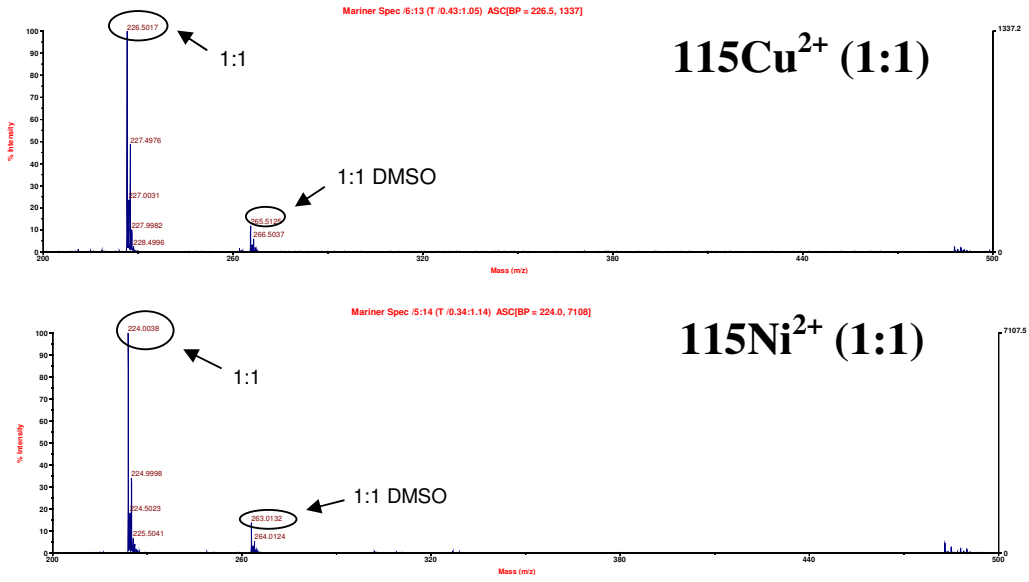

Figure 3.7 Mass spectra of P115 in complex with Cu^{2+} (top) and Ni^{2+} (bottom) at 1:1 molar ratio

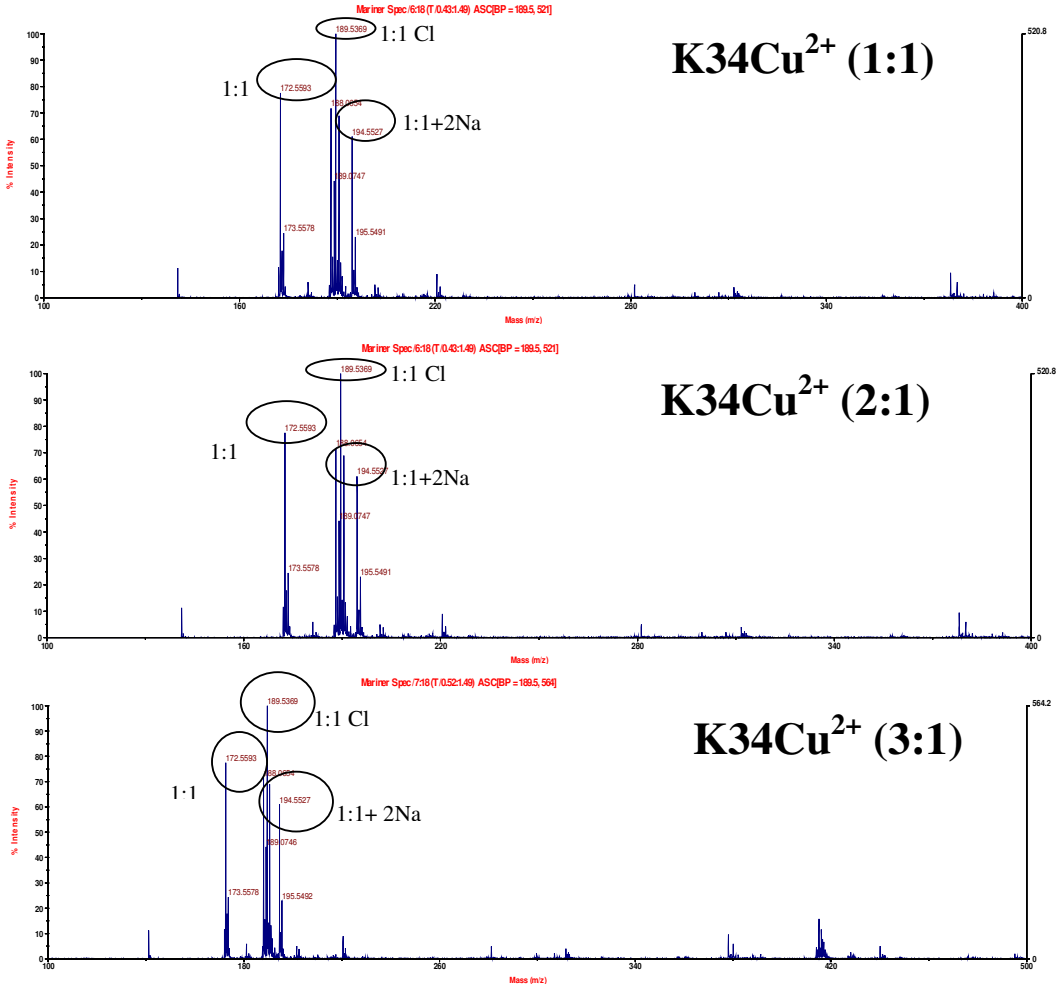

Figure 3.8 Mass spectra of K34 in complex with Cu^{2+} at 1:1, 2:1 and 3:1 molar ratio

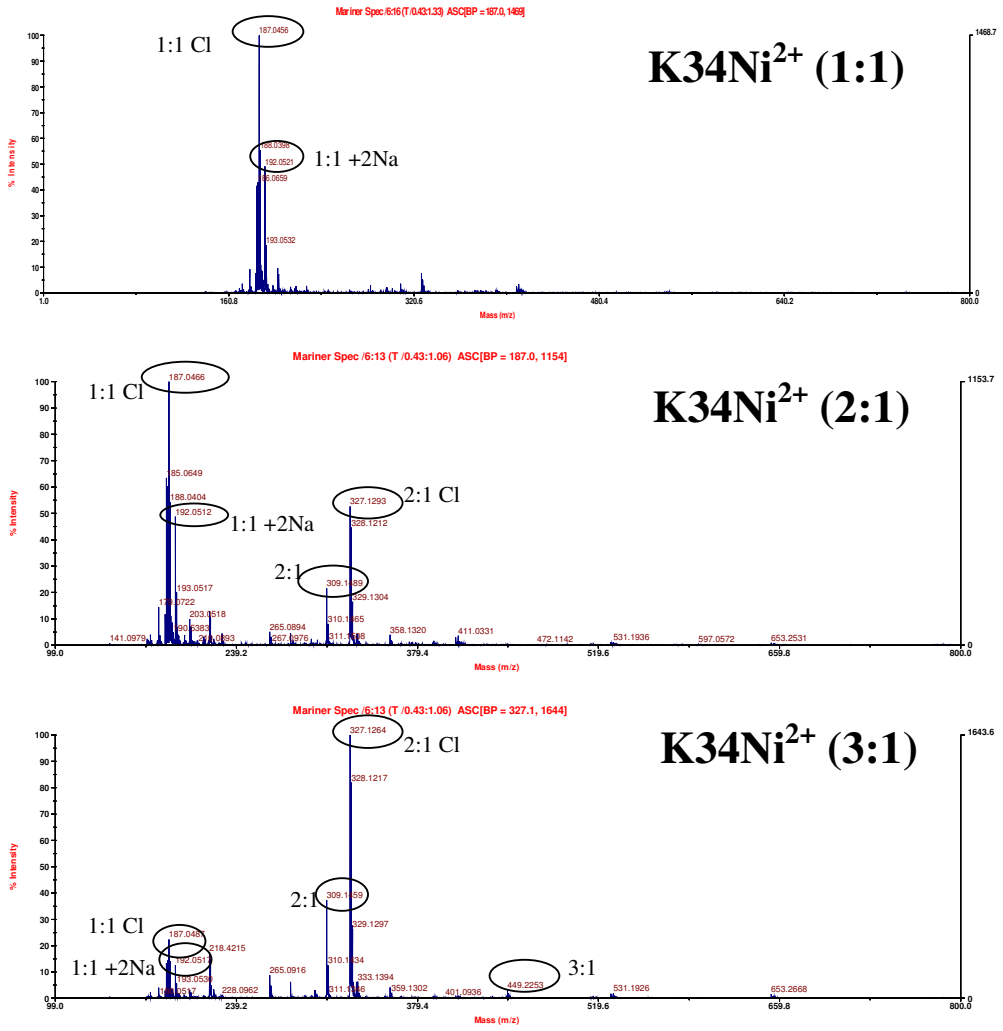

Figure 3.9 Mass spectra of K34 in complex with Ni^{2+} at 1:1, 2:1 and 3:1 molar ratio

3. 3. 2. Phenanthroline complexes effectively and selectively stabilize G-quadruplex conformations

The interaction of our metal complexes with G-quadruplex structures was monitored by fluorescence quenching assay using a synthetic oligonucleotide (HTS) formed by four repeats of the human telomeric sequence labelled with a fluorophore (fluorescein) at the 3'-end and a quencher (Dabcyl) at the 5'-end[157]. When the sequence folds into a G-quadruplex arrangement the fluorophore and the quencher are close to each other and the fluorescence signal vanishes. In turn, unfolded DNA is

characterized by an intense fluorescence signal as the quencher is far apart from the fluorophore. This allows an easy monitoring of G-quadruplex thermal stability; additionally, shift of the DNA melting temperature to higher values provides a reliable indication of ligand affinity.

Concerning monofunctional derivatives in our experimental conditions, neither metal ions nor ligands alone (0-30 μM) were able to promote G-quadruplex stabilization (Figure 3.10).

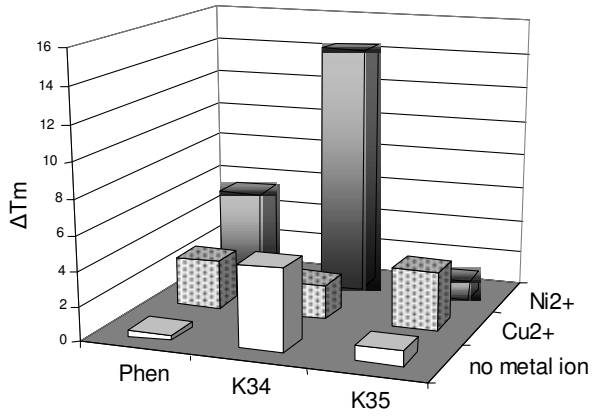

Figure 3.10 Increase in HTS (0.25 μM) thermal stability produced by tested ligands (5 μM) in the presence/absence of 2 equivalents Cu^{2+} or Ni^{2+} (for predominant species see text). Conditions: 50 mM potassium buffer, pH 7.4. Heating rate 0.2°C/min. Error ± 0.4°C.

The addition of stoichiometric amounts of metal ions to the tested ligands leads to complexes that can remarkably enhance HTS melting temperature, which testifies an increased recognition of the G-quadruplex structure. Remarkably, this effect parallels the attitude of the tested ligands to form complexes containing two phenantroline units coordinated to one metal ion. This is strikingly evident in the case of K34. The preferred 1:1 coordination complex with Cu^{2+} produces no G-quadruplex stabilization whereas the 2:1 coordination promoted by Ni^{2+} causes efficient stabilization of (and binding to) the quadruplex form. In line with this,

complexes of K35, always preferring the 1:1 stoichiometry, failed to produce any significant G-quadruplex stabilisation with either ions. Only with the most stable $(K35)Cu^{2+}$ complex, HTS was significantly stabilized although a 10fold increase in complex concentration was necessary to obtain results comparable to $(K34)_2Ni^{2+}$.

The importance of the correct ligand:metal ion ratio in stabilising the G-4 structure was highlighted by analyzing the consequences of varying such a ratio from 1:4 to 8:1. As shown in Figure 3.11, thermal stabilisation of the quadruplex structure is maximal at a 2:1 ratio using either K34 or Phen as ligand. Besides a different affinity for the target DNA, the lower stabilizing effect recorded with the Phen ligand likely reflects the co-existence of different complex species at equilibrium as shown in Table 3.6. This result can help explaining mass spectrometry data recently reported for G-4/Phen/metal ion complexes[158]. In fact, in the presence of Ni^{2+} only the $(Phen)_2Ni^{2+}$ species could be detected bound to the G-quadruplex. This might reflect fragmentation events during the ionization step. However, according to our results, mass-spectrometry data can well be described by preferential binding of $(Phen)_2Ni^{2+}$ to the G-quadruplex folded nucleic acid.

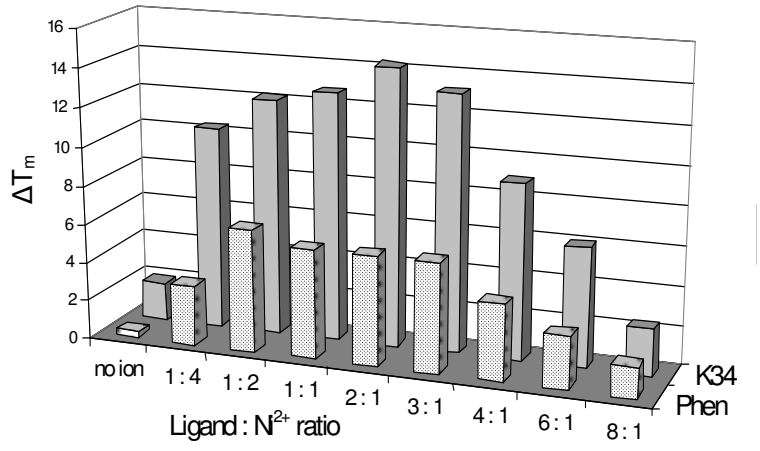

Figure 3.11 Thermal stability increase (ΔT_m) of HTS (0.25 μM) as a function of ligand:Ni^{2+} ratio at 5 μM concentration of tested ligands.

Double stranded DNA binding properties were also monitored. Addition of a stoichiometric amount of the strand complementary to the G-rich sequence did not affect the efficiency of Phen-adduct G-quadruplex recognition. Moreover, the melting profile of a dsDNA unable to form G-4 structures was not affected by any of the tested ligands or by their metal complexes thus supporting effective stacking interactions with G-quadruplex structures only.

Distinctly bis-phenathroline derivatives P115, 042 and Q59 showed to be able to stabilize the G-quadruplex folding in the micromolar range (Fig. 3A) even in the absence of metal ion. According to the above described model, this results can reflect the simultaneous availability of two Phen moieties to interact with the G-quadruplex structure. The larger effect showed by 042 in comparison to Q59 indicates that the protonated nitrogen in the side chain contributes to G-quadruplex binding through electrostatic interactions with the DNA phosphates. Moreover, an effective interaction still occurs when the nitrogen connecting the two phenathroline units is eventually replaced by a sulphur bioisostere as in P115. Metal ion complex formation by these bifunctional ligands dramatically increases ligand-stabilizing effects on G-quadruplex with maximal variation of the DNA melting temperature occurring at concentrations as low as 1 □M (Figure 3.11.B). This effect turned out to be function of metal ion nature, the observed ranking order being $Ni^{2+}>Cu^{2+}>Zn^{2+}>>Mn^{2+}>Mg^{2+}$ (Figure 3.11.C). If the poor G-quadruplex stabilization recorded with Mn^{2+} and Mg^{2+} likely rests in a non quantitative complex formation in solution (Figure 3.11.B), the modulation observed among the other tested ions is connected to the metal ion coordination properties.

Interestingly, in analogy to monofunctional derivatives, fluorescence quenching experiments performed using a labelled dsDNA (unable to fold into a G-quadruplex structure) as a substrate showed that neither ligands of group 2 nor any of the tested metal complexes were able to significantly alter the melting profile of the double-helical structure (Figure 3.11.D). This behaviour suggests a remarkably selective stabilization of the G-quadruplex arrangement and demonstrates that the tested metal complexes are suited to effectively discriminate between duplex and quadruplex folding.

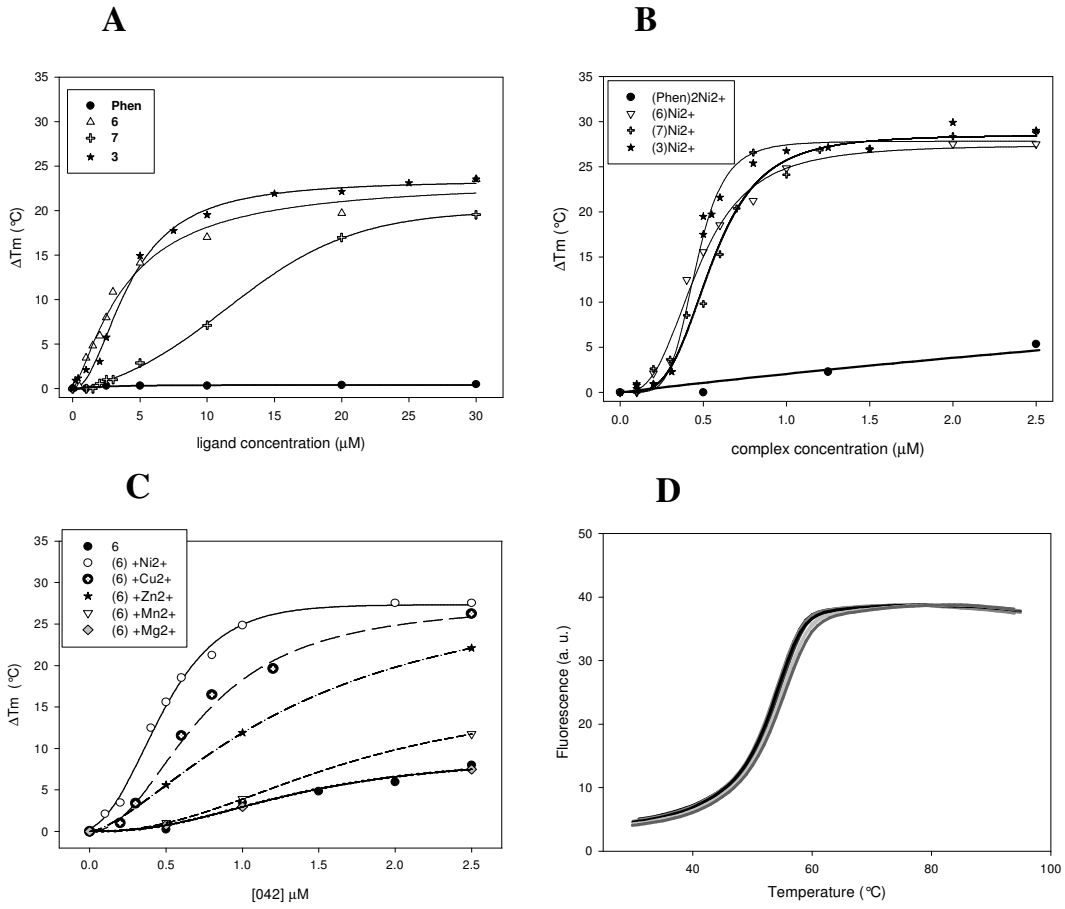

Figure 3.11 Variation of DNA (0.25 μM) melting temperature (ΔTm) at increasing concentrations of tested ligands or their metal complexes recorded in 50 mM potassium buffer, pH 7.4. A: addition of tested ligands to HTS in the absence of divalent metal ions; B: addition of tested Ni^{2+}metal complexes to HTS; C: addition of 042 in the presence of 1 eq. of different divalent metal ions to HTS; D: addition of 042Ni^{2+} (0-5 μM) to a dsDNA

The above data were fully supported by circular dichroism spectroscopy performed using the HTS sequence (not labelled)[159]. In our experimental conditions Tel22 is folded into a hybrid conformation as confirmed by the intense CD band at 295 nm associated to a shoulder at 270 nm. Addition of ligands or metal ion alone produced no changes or only modest changes in the CD spectra (Figures 3.12 and 3.13.A). Distinctly $(K34)_2Ni^{2+}$ complex caused a substantial increase in G-quadruplex band intensity (290 nm), confirming stabilisation of the folded conformation (Figure 3.13.B).

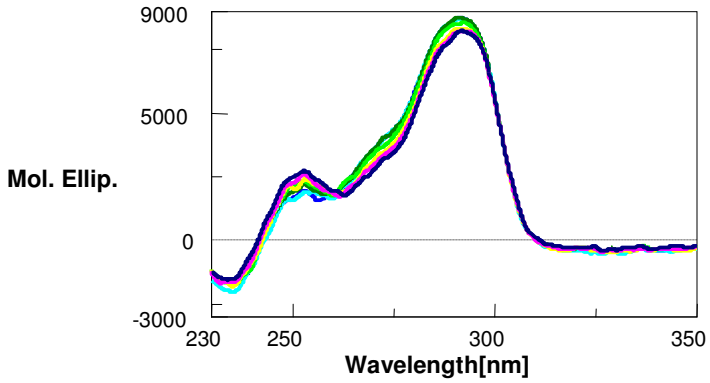

Figure 3.12 CD spectra of the oligonucleotide Tel22 (4μM) titrrated with $NiCl_2$ (from 4 to 35 μM) in 10 mM Tris, 50 mM KCl buffer at pH 7.5

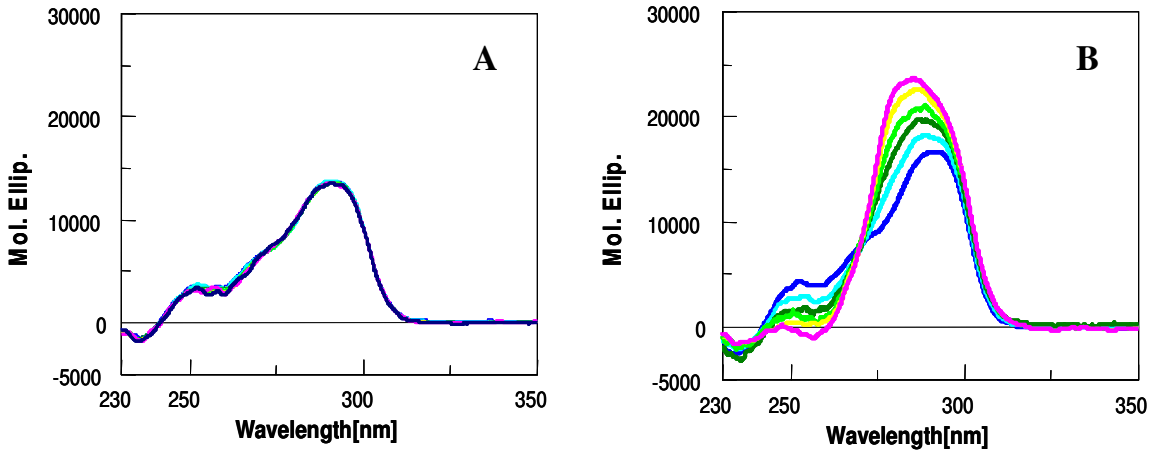

Figure. 3.13 CD spectra of Tel22 (4 μM) in 10 mM Tris, 50 mM KCl, pH 7.5, upon addition of increasing amounts of K34 (A) or $(K34)_2Ni^{2+}$ (B) (maximal ligand concentration 35 μM)

The simultaneous negative band appearing at 260 nm might suggest a preference of the bound G-quadruplex for an antiparallel form. These variations are mainly relevant for the complexes deriving from bifunctional ligands. Additionally, in agreement with the melting data, these ligands can promote similar changes in the DNA dichroic spectrum although with a remarkably reduced efficiency (Figure 3.14.B).

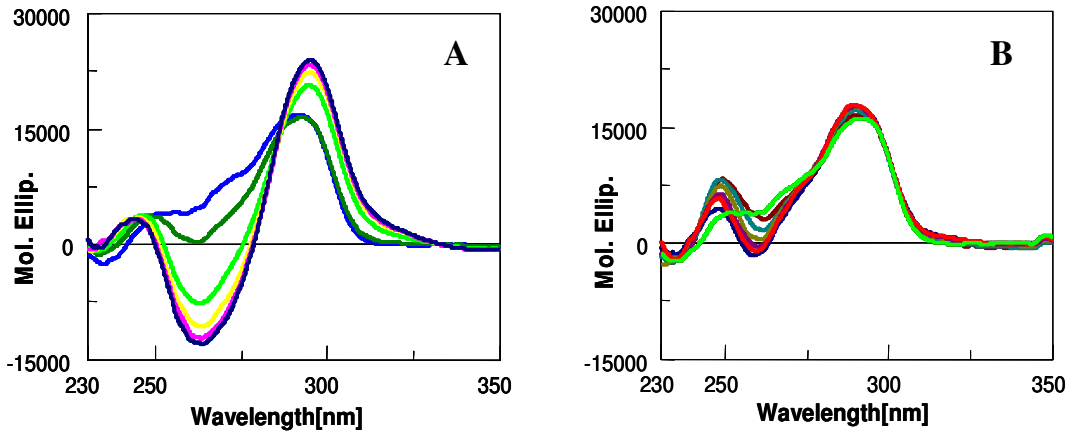

Fig.ure 3.14 CD spectra of Tel22 (4 μM) in 10 mM Tris, 50 mM KCl, pH 7.4, upon addition of 042:Ni^{2+} (0-20 μM) (A) or 042 (0-20 μM) (B)

3. 3. 3. Bis-phenanthroline complexes can induce G-quadruplex folding even in the absence of potassium

The results thus far described were obtained using a G-quadruplex folded DNA as the target. However, in a physiological environment G-rich sequences can be poorly folded into this peculiar structural arrangement[160,161].

To asses whether the test complexes could induce G-4 formation from essentially unfolded species, we performed gel shift assays (EMSA) using a sequence containing two human telomeric repeats (Figure 3.15). Even including K^+ in the reaction mixture to mimic physiological conditions, in the absence of any ligand this sequence is

essentially unfolded. Interestingly, in the presence of bis-phenanthroline complexes, a band corresponding to the dimeric G-quadruplex readily appears.

To evaluate if the presence of physiologically relevant metal ions is required to promote G-quadruplex induction by our complexes, we additionally used the four-repeat telomeric sequence Tel22. In the absence of potassium ions, this sequence migrates as an unfolded sequence and no melting transitions can be observed by increasing the temperature (Figures 3.15.A and B).

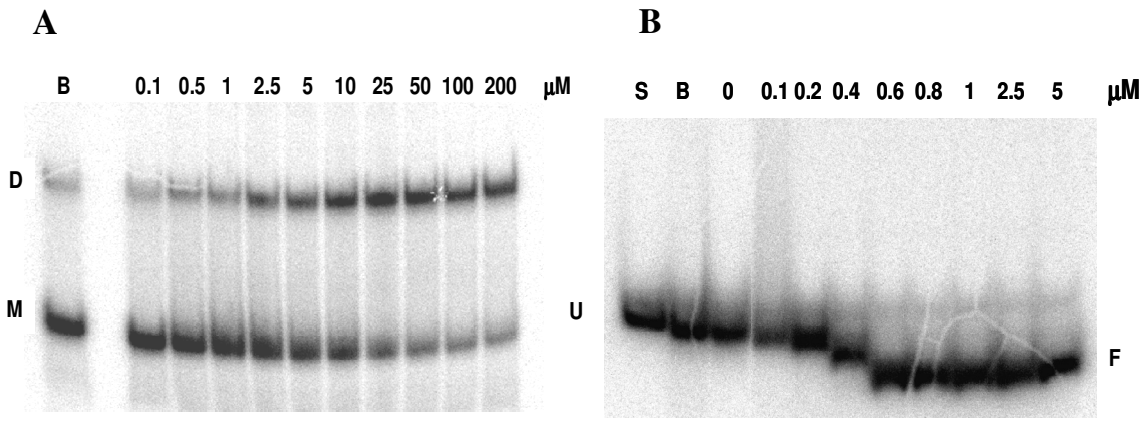

Figure 3.15 Effect of increasing concentrations of p115Ni^{2+} on the assembly of G-quadruplex structures by: (A) a two telomeric repeats sequence (2GGG, 1 µM strand concentration) in 10 mM Tris, 50 mM KCl at pH 7.4. M = monomeric forms; D = dimeric G-quadruplex forms. (B): a four telomeric repeats sequence Tel22, 1 µM) $^{+}$ in 10 mM Tris, at pH 7.4, U refers to the unfolded oligonucleotide, F to the G-quadruplex form

Upon addition of bis-Phen complexes, this oligonucleotide increments its electrophoretic mobility and a melting transition sets on consistently with the induction of DNA folding into a compact G-quadruplex form. In agreement with the above results, the CD spectra recorded under comparable conditions (Figure 3.16) showed the appearance of an intense dichroic signal (a positive and a negative band at 290 nm and 260 nm, respectively) promoted by the presence of the metal complexes. This again points to the induction of G-quadruplex folding. Moreover as

the final CD spectrum matches the one recorded at the same drug-DNA molar ratio in the presence of K^+ (Figure 3.14.B) thus suggesting induction of a common structural motif. Interestingly, ligands *per se* did not promote DNA folding in the absence of K^+ (data not shown), although the G-quadruplex folded form was rapidly induced upon addition of a stoichiometric Ni^{2+} to the Tel22-ligand mixture.

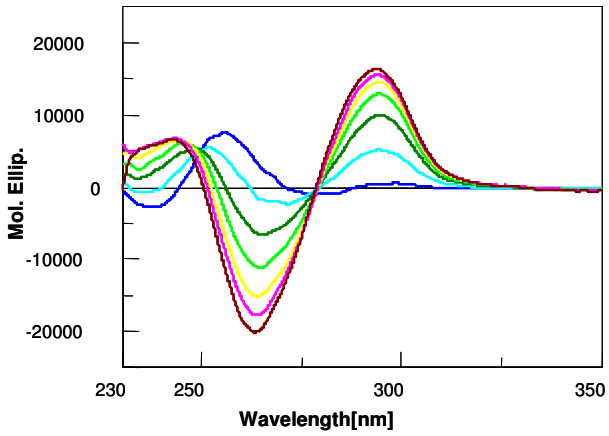

Figure 3.16 CD spectra of Tel22 (4 μM) in 10 mM Tris, pH 7.4, upon addition of increasing amounts of P115:Ni^2

3. 3. 4. Bis-phenanthroline complexes can impair telomerase-mediated DNA processing

As telomeres represent a potential pharmacological target for G-quadruplex binders, potential biological effects of phenanthroline derivatives were monitored by evaluation of their interference with Taq polymerase amplification and telomerase mediated elongation of suitable templates.

None of the tested ligands or their metal complexes showed significant interference with the DNA amplification process. Exceptions are $P115Ni^{2+}$ or $P115Cu^{2+}$, when used at concentrations higher than 20 and 40 μM respectively. In full agreement with the melting experiments, poor G-4 binders like K35-metal complexes were unable to inhibit telomerase in the micromolar range. On the contrary,

$(K34)_2Ni^{2+}$ inactivated the enzyme at 10 μM concentration. In agreement with the prominent G-quadruplex affinity exhibited by bis-phenanthroline metal complexes, telomerase inhibition occurred at sub-micromolar concentration as determined by TRAP assay (Figures 3.17 and 3.18).

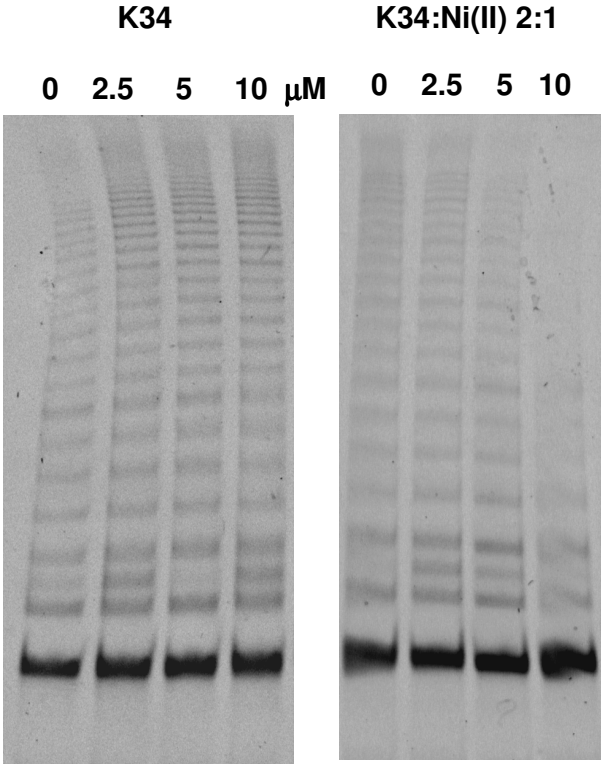

Figure 3.17 Trap assay performed with increasing concentrations of K34 in the presence/absence of 0.5 equivalents of Ni^{2+}. The cell extract used was obtained from JR8 cells

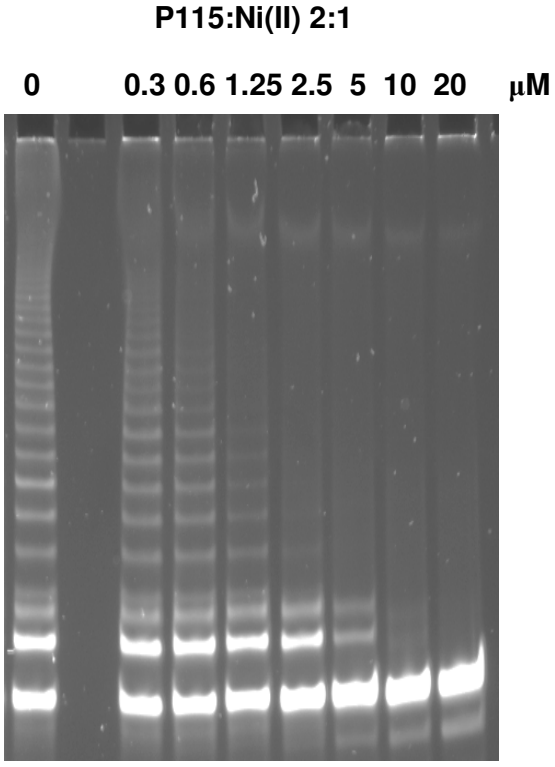

Figure 3.18 Trap assay performed in the presence of increasing concentrations of 042:Ni^{2+}. The cell extract used was obtained from JR8 cells. IC refers to internal control, T to telomerase elongated products

In particular, all Ni^{2+} complexes exhibited IC_{50}s of about 0.7 μM, over one order of magnitude lower than the related $K34Ni^{2+}$ complex. It should be pointed out that the IC_{50} values determined according to this protocol do not simply reflect the efficiency of ligand-DNA binding on the enzyme processivity since interference of the complexes with the amplification of G-quadruplex structures can occur. Nevertheless, they represent a clear indication that metal complexes can efficiently interfere with

telomerase action in a physiological environment where they retain the appropriate stoichiometry/geometry. This result has a double bearing: first it indicates that phenanthroline-based ligands in the presence of 2:1 stoichiometric amounts of metal ion can be used with no need for the usually performed complex isolation/purification steps, second, it confirms stability of the active species at physiological conditions

3. 3. 5. Bis-phenanthroline complexes are poor DNA modifiers

Phenanthroline metal complexes are very effective DNA-modifying agents. Their reactivity can produce DNA-cleavage in the presence of copper or alkali labile adducts in the presence of nickel metal ions[162]. To asses the reactivity of our novel complexes toward DNA, dsDNA, ssDNA and G-quadruplex were used as substrates. In agreement with the known lack of reactivity of $(Phen)_2Ni^{2+}$ [163], none of the tested Ni^{2+} complexes were able to covalently bound DNA both in the presence or absence of an oxidizing agent (MMPP). It is known that adduct formation is promoted by $Phen^{2+}$ complexes whereas $(Phen)_2Ni$ are unreactive. This results further sustain the relevant presence of two phenantroline units coordinated by one Nichel ion in solution.

When the Cu^{2+} complexes were used in the presence of a reducing agent (ascorbic acid) Phen and K34 promoted extensive and comparable DNA cleavage. On the contrary, limited DNA digestion was monitored for P115, whereas 042 and Q59 were almost inactive (Figure 3.20).

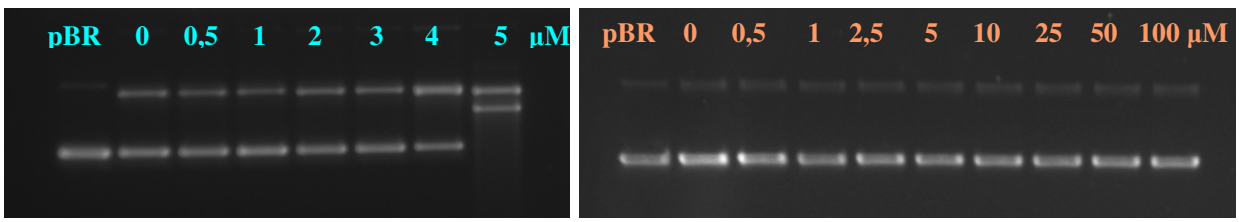

Figure 3.19 1% agarose gel of pBR322 with increasing concentrations of $K34Cu^{2+}$ (left) and K34Ni2 (right) in 10 mM Tris, 50 mM KCl buffer

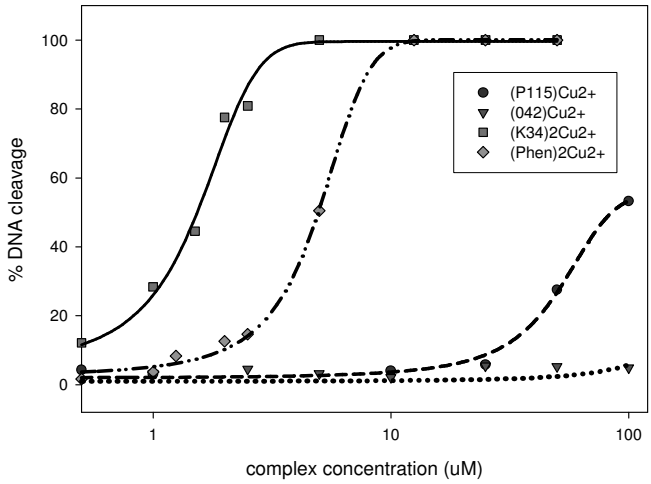

Figure 3.20 Percentage of cleaved pBR322 after incubation for30 min at 37°C of the supercoiled plasmid with increasing concentration of tested Cu^{2+} complexes in the presence of ascorbic acid

A sequence analysis of the cleavage sites induced by metal complexes showed that they are randomly distributed along each target DNA, thus suggesting that the damaging event is likely related to non-specific interactions (Figure 3.21).

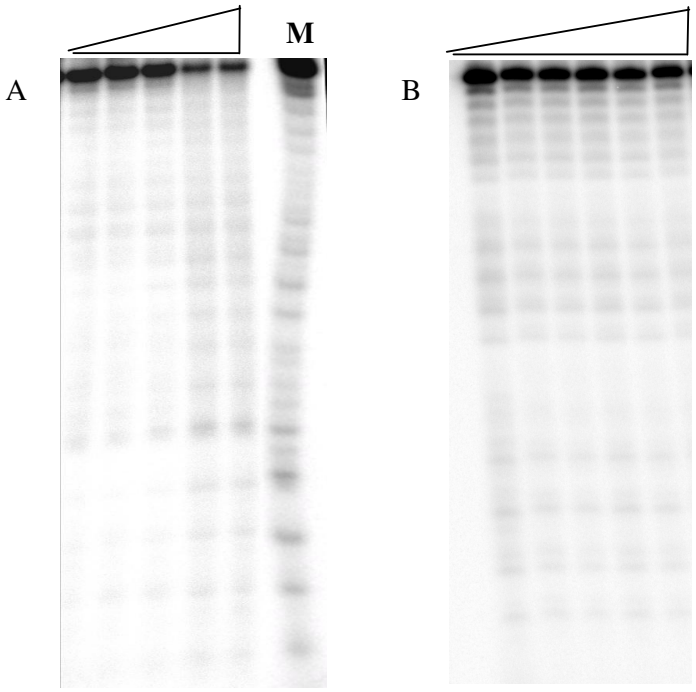

Fig.ure 3.21 Effect of increasing concentrations of 115:Cu^{2+} (A) and 115:Ni^{2+} (B) (0-20 μM) on the cleavage of G-quadruplex folded oligonucleotides (1 μM strand concentration) in 10 mM TRIS, 50 mM KCl at pH 7.5. M refers to Maxam and Gilber purine ladder

3. 3. 6. Phenanthroline:Ni(II) complexes are poorly cytotoxic

Cytotoxic effects of tested complexes were investigated on human cervical cancer (HeLa) and human embryonic kidney (293T) cell lines, both constitutively expressing telomerase[164]. The effective drug concentration able to reduce the 50% of cell population after 96 hours drug exposure (EC_{50}) was determined for each ligand, ion and metal complex by MTT assay. The results, summarized in Table 3.6, indicate that the metal ions alone are poorly toxic for both cell lines in our experimental conditions. In turn, the tested ligands were generally as cytotoxic as their Cu^{2+} complexes, while Ni^{2+} complexes showed generally higher IC_{50} values.

Table 3. 6 Cytotoxic properties of tested ligands and complexes

	IC_{50} (µM)	
	293T	**HeLa**
Cu^{2+}	>100	>100
Ni^{2+}	>100	>100
115	2.60	6.00
115-Cu^{2+}	2.40	5.00
115-Ni^{2+}	12.50	67.00
042	0.80	4.00
042-Cu^{2+}	0.16	28.00
042-Ni^{2+}	0.88	67.00
Phe	4.2	4.00
(Phe)2Cu^{2+}	0.7	3.00
(Phe)2Ni^{2+}	9.0	79.00
K34	9.50	4.00
K34-Cu^{2+}	11.00	3.00
$(K34)_2Ni^{2+}$	>100	>100

Since telomerase inhibition is expecting to promote cellular effects only after long incubation time, the inhibition of the cell growth by some selected compounds can be due to other mechanisms. It will be interesting to evaluate the long term

cytotoxicity by extending the incubation time or if the compounds are able to provide telomeres shortening.

3. 4. DISCUSSION

It has been recently demonstrated that coordination of planar ligands by transition metal ions may improve effective G-quadruplex recognition by increasing the stacking surface of the binder. As G-quadruplex stabilization is generally the result of efficient π interactions between a terminal guanine tetrad and the planar system of a ligand, we expect positively charged complexes having a large planar arrangement, to represent effective G-quadruplex binders. From our data, coordination to the central metal ion likely produces an extension of the aromatic surface available to stacking interactions. Conceivably, this is obtained when two phenanthroline rings are facing one another in an almost planar arrangement. For this reason, the stabilization of the quadruplex folding by K34 turned out to be efficient in the presence of Ni^{2+}, which promotes this coordination mode, but not with Cu^{2+}.

To further address this issue we investigated a bis-phenanthroline system in which two moieties are covalently linked through an amino or thioether bond. Such short linkers should favour juxtaposition in cis of the two tricyclic residues. The remarkable ΔTm observed in comparison to similar phenanthroline-based ligands strengthens the simultaneous involvement of both the phenanthrolines in G-quadruplex interaction[151,165]. For these bifunctional ligands efficient G-quadruplex stabilization occurred even in the absence of coordinating-metal ions. Nevertheless, in line with expectations, metal ion coordination to form 1:1 planar complexes

drastically further increments G-quadruplex binding likely stabilizing a co-planar Phen-Phen arrangement.

The emerging picture points to an active role of the metal ion, which may be ampler than just granting planarity of the ligands in the complex. Previous studies on phenanthroline-containing metal complexes considered Pt^{2+} as the metal centre, because of its planar coordination geometry. Planar coordination represents a common rationale considering that the most G-quadruplex effective ion-ligand combination was Cu^{2+}-terpyridine and Mn^{2+}-porphyrine (both producing planar complexes)[148,153]. In our case, Ni^{2+} turned out to be most effective for our bis-phenanthroline ligands. Indeed, in addition to complex geometry, the metal centre influences the complex formation constant, it must properly fit onto the DNA quadruplex and, possibly, it may have different efficiency for K^+ replacement when in the presence of the quadruplex-forming sequence. This point clearly is a novel point of relevance. Furthermore, bis- phenanthroline complexes are effective inducers of the folded DNA structure: among the herein tested compounds this property is peculiar of the metal complexes, which suggests that a positive charge of the binder is required to actively promote the G-quadruplex folding. Likewise bis-phenanthroline complexes do not require monovalent ions to induce this DNA arrangement. These findings suggest that the coordinating ion surrogates the physiologically relevant K^+ (or Na^+) by interacting with the electron-rich cavity produced by the guanine oxygens pointing toward the centre of the G-quartet. To confirm this, the structural features of the DNA bound to tested metal complexes are not affected by the presence/absence of K^+ in solution as indicated by CD experiments. This further allows to infer that the

monovalent ion bound to G-quadruplex at physiological conditions might be displaced by the bis-phenanthroline complexes.

Since phenanthroline-containing Cu^{2+} complexes are reported as efficient DNA damaging agents[166,167], their redox properties could be possibly exploited for targeted irreversible modification of G-quadruplex. This is not the case for bis- phenanthroline complexes. Indeed, upon reduction of freely diffusing $(Phen)_2Cu^{2+}$ to $(Phen)_2Cu^{2+}$, the two aromatic functionalities need to be located perpendicularly to generate the DNA-reactive species[168]; this geometry is prevented for our ligands due to the nature of the short linker connecting the two phenanthroline units which forces them into a coplanar arrangement. For group one, this structural rearrangement is obviously not prevented. However, when it occurs it suppress efficient stacking over a G-tetrads or a base pair of double strand DNA, resulting in DNA damage randomly distributed along any sequence. If this point prevents the possible application of our metal complexes as diagnostic tools, it opens up opportunity for a potential drug application as antiproliferative agents in particular for the bis-phenanthroline-Ni^{2+} complexes. Indeed, it is worth recalling that they i) selectively discriminate between G-4 and ds-DNA, ii) are remarkably effective G-4 inducers iii) efficiently interfere with telomerase function and iv) do not promote DNA modification. Hence, at the cellular level, they could affect the telomeric regions without producing unselective toxic events. In this connection, the low short-term ctotoxicity exhibited by the bis-phenanthroline Ni^{2+} complexes is encouraging to consider them as valuable leads for antiproliferative drug discovery.

In conclusion, our study showed that assembly of otherwise inactive planar structures through metal coordination may represent an effective strategy to

achieve selective G-quadruplex binding and recognition. Metal ions, on the other hand, can play an important role in modulating affinity and stoichiometry of complex formation. Therefore, it is possible to play with the nature of the ion species as well as of the ligands to produce a variety of complexes rationally designed for specifically targeting/damaging DNA. This represents a promising approach to work out novel biochemical probes and diagnostic tools in addition to new chemical entities for drug design and development.

Chapter 4

INTERACTION OF *trans*-PLATINUM PLANAR AMINES (TPA) WITH DNA SUBSTRATES

4. 1 AIM OF THE CHAPTER

Cisplatin successfully represents the effectiveness of metal-based drugs in cancer chemotherapy. Although it has been widely used since many years in the treatment of a variety of tumors, the onset of toxic side effects and resistance phenomena focused the interest in the development of new analogues. The clinically relevant compounds belong to the cispaltinum family. Indeed, structure activity relationships studies pointed out the clinical inactivity of the *trans* isomer. However some transplatin derivatives seem to exhibit a different spectrum of cytostatic activity even in cisplatin resistant cancer cell lines.

The pharmacologically relevant target of platinum drug is the double strand DNA through the formation of adducts[169,170]. The nature of these adducts can change according to structural features of the platinum complex. This explains also the different biological activity between cis and transplatin. Different ligands and isomers (Figures 4.2 and 4.3) can lead to altered binding modes on the DNA and ultimately in different profiles of antitumor activity. Cisplatin, for example, can form different types of adduct. The most common is intrastrand crosslinks between two adjacent guanines (1,2-GG) but also between an adenine and the adjacent guanine (1,2-GA). Less common, but still observed are intrastrand crosslinks between two guanines separated by the presence of another base (1,3-GNG) and interstrand adducts involving a guanine and the closest guanine residue on the complementary strand[171]. On the other hand, transplatin can form interstrand crosslinks between guanine and cytosine residues involved in the same base pair (Figure 4.1).

The reactive sites on the bases available for adduct formation are known to be the nitrogen in 7 position of the guanine and the nitrogen in 3 position of the adenine[172].

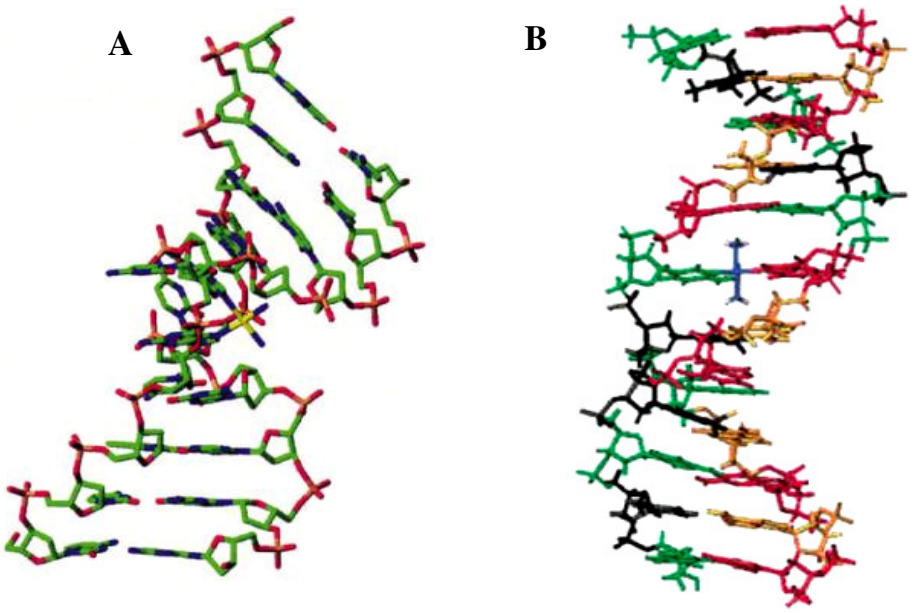

Figure 4.1 Interstrand cross-link for cisplatin[173] (A) and transplatin[174] (B). Interaction of the two compounds leads to different DNA bending.

With the goal of develop new cisplatin active derivatives and to avoid the toxicity problem, lots of empirical rules have been defied, for example the need for charge neutrality and the presence of two leaving groups which seemed to be fundamental for DNA interaction and modification[175]. Different modifications recently performed on the *trans* isomer led to interesting biological properties. In particular, they are obtained when the canonical aminic group is replaced with a heterocyclic planar system giving rise to a new group of derivatives called trans-platinum planar amines (TPA). In general TPAs show equivalent cytotoxicity than *cis* isomers and cisplatin while at the same time, they look more effective than transplatin[176,177,178]. Furthermore, they demonstrate an incremented

activity in different cancers when compared to cisplatin and negligible cross-resistance (Table 4.1). It has been shown that the replacement of NH_3 with planar amines affects both the structural nature of adducts as well as the kinetics of formation[179,180]. Both cis and tranplatin needs to be converted to monoaquo- or diaquo-species in order to be activated and to react with the DNA. The synthetic scheme shows the hydrolytic activation of transplatin. Once the chloride groups are converted into the corresponding aquo-substituents, there is an equilibrium (at physiological pH) involving monoaquo and hydroxo species (Figure 4.2). When this equilibrium occurs, the reactivity of the hydroxilic groups with N-donor groups of the DNA bases is allowed[181].

Scheme 4.1 Proposed scheme for hydrolytic activation of transplatin

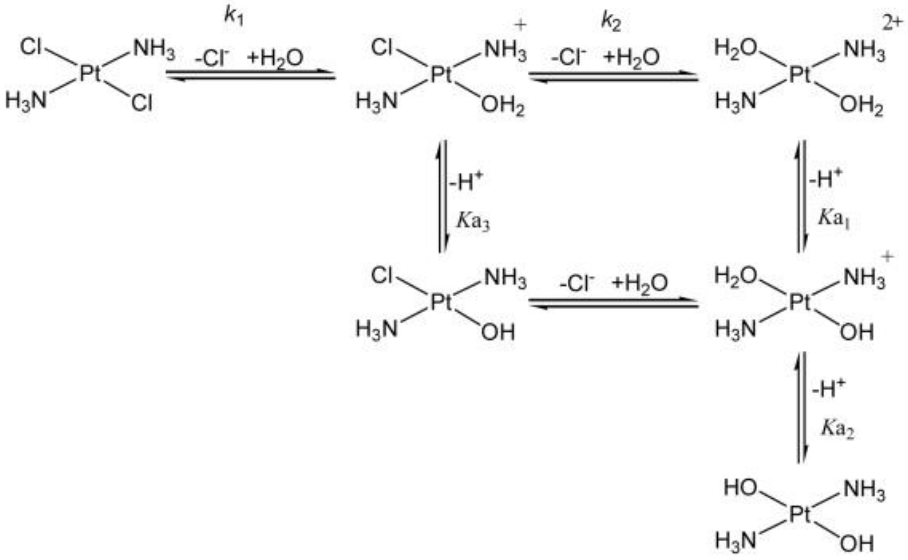

In this Chapter four TPAs (Figure 4.3) were analyzed and compared with cisplatin and transplatin. In compound SA1, *trans*-amminedichloro(thiazole)platinum(II), one aminic group was substitute with a thiazole. In compounds SA2 and SA3, both the aminic groups were replaced by pyridines and in SA4 a quinoline was inserted in place of NH_3 to investigate if a bulky substituent can play a role in the formation or in the type of the adduct. Moreover, the substitutions of

chlorides with carboxylate (SA3 and SA4) and acetate groups (SA2) were performed with the goal of enhancing the solubility. At the same time this might provide a reduced conversion toward aquo-forms and so a more "controllable". Based on the chemical modifications performed, we know expect these new derivatives to show chemical reactivity toward the DNA in comparison to their related leading compounds cis and trans.

The aim of this work is to characterize by biophysical techniques the effects of these modifications on DNA binding and reactivity. Two of these compounds (SA1) and SA2 have been already tested for cytotoxicity in human ovarian cell lines. SA1 results more efficient than cis and transplatin in tumor cells growth inhibition while SA2 appears to be less cytotoxic than SA1 and cisplatin (Table 4.1). Based on this features we focused our attention on defining the compounds capability to form adducts, the nature/type of adducts and the kinetics of adduct formation by applying a number of different experimental methods such as gel electrophoresis, fluorescence melting and mass spectrometry. Moreover, we compared biophysical data obtained with biological results (when they are available) to search for any correlation or consistency.

Table 4.1 In vitro cytotoxicity (IC_{50}, μM) of TPA platinum compounds in a human ovarian cell line panel[182]

Compound	HX/62	SKOV-3	PXN94	41M	41McisR	CH1	CH1cisR
Cisplatin	12.6	4.4	3.0	0.23	1.4	0.1	0.67
Transplatin	245	255	222	57	69	30	68.5
***trans*-[$PtCl_2(tz)_2$] (SA1)**	4.1	6.2	9.6	2.2	1.6	1.3	1.4
***trans*-[$Pt(O_2CCH3)_2(py)_2$] (SA2)**	-	31.0	-	14.0	4.5	19.0	4.1

Additionally, DNA adducts formation by the tested transplatin derivatives have been evaluated not only with double strand DNA but also using single strand as well as

high ordered DNA structures (G-quadruplex) as targets. This idea was suggested by recent studies in which platinum complexes have been used to target G-quadruplex through stable, covalent adduct[183,184] or as luminescent probes[185]. Indeed, platinum-complexes were shown to exhibit G-quadruplex stabilization properties which are not intrinsic of the ligand but are governed by the balance between the geometry of the metal center and the nature of the aromatic ligand[186,187,188].

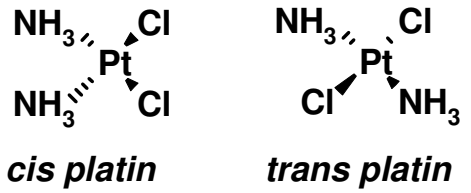

Fig 4.2 Chemical structures of cisplatin and transplatin

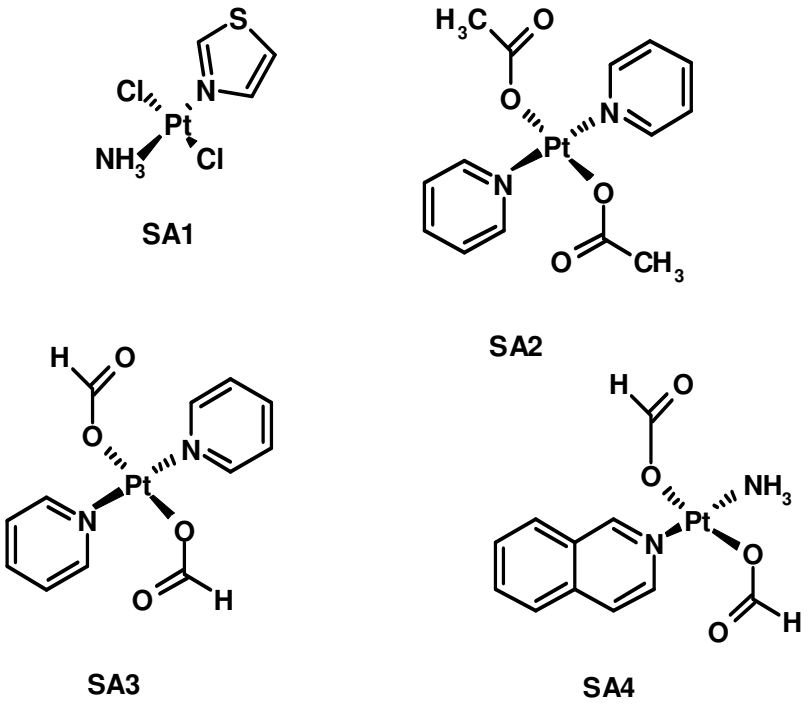

Figure 4.3 Chemical structures of the tested novel TPA derivatives

4. 2 MATERIALS AND METHODS

4. 2. 1. Instrumentation

Table 4.2 Instrumentation used

Autoclave	International PBI
Developing sheets Hyperfilm MP	Amersham Pharmacia Biotech
Lambda 20 Spectrophotometer	Perkin Elmer
ESI-TOF Mass Spectrometer	Mariner
LightCycler	Roche S.p.A
Phosphor Imager STORM 840	Amersham Pharmacia Biotech
Scintillation Counter TRICARB 2800 TR	Perkin Elmer
Speed Vac	UniEquip, Milano
pHmeter 713 Metrohm	Metrohm Italiana s.r.l
Geliance 600 Imagyng System	Perkin Elmer
Multilabel Counter VICTOR^3	Perkin Elmer
Horizontal Electrophoresis Apparatus	Biorad
Vertical Electrophoresis Apparatus	CBS Scientific

4. 2. 2.Natural nucleic acids and synthetic oligonucleotides

Plasmid pBR322 was provided by Fermentas International INC (Burlington, Ontario, Canada). It is double-stranded circle, 4361 base pairs in length.

The lyophilized synthetic oligonucleotides were purchased from Eurogentec S.A. (Seraing, Belgium) and Metabion International AG (Martinsried, Germany) with HPLC purification and mass spectrometry characterization. The concentrations of oligonucleotides were determined by absorbance at 260 nm using molar extinction coefficient obtained from nearest-neighbour model[189].

The G-quadruplex DNA sequences were dissolved in the required buffer to the desired concentration, heated at 90 °C for 5 minutes and cooled slowly to insure the

proper folding of the sequence prior to each experiment. Double strand DNA was obtained by heating equimolar solutions of complementary stands. The solution was cooled slowly to insure the annealing of the two strands.

Table 2.2 Oligonucleotide sequences used

Tel22 (22mer):	5'-AGG-GTT-AGG-GTT-AGG-GTT-AGG-G-3'
Scramble (22mer):	5'-GGA-TGT-GAG-TGT-GAG-TGT-GAG-G-3'
Coscramble (22mer):	5'-CCT-CAC-ACT-CAC-ACT-CAC-ATC-C-3'

Table 2.3 Oligonucleotide sequences used for Fluorescence Melting experiments

HTS (23mer):	Dabcyl-5'-AGG-GTT-AGG-GTT-AGG-GTT-AGG-GT-3'-FAM
3'-FAM-Scramble (22mer):	5'-GGA-TGT-GAG-TGT-GAG-TGT-GAG-G-3'-FAM
5'-Dab-Coscramble (22mer):	Dabcyl-5'-CCT-CAC-ACT-CAC-ACT-CAC-ATC-C-3'

4. 2. 3.Compounds

Cisplatin and Transplatin were obtained from Sigma-Aldrich. The syntheses and purifications of transplatinum derivatives were performed by Dr. Nicholas Farrell's group at Virginia Commonwealth University, Richmond, VA (USA) and will be reported elsewhere. Appropriate stock solution of each compound was prepared in water and diluted to required concentrations with appropriate buffer.

4. 2. 4.Buffers

The buffers have been prepared using MilliQ water and then filtered:

TK 10/50: 10 mM Tris, 50 mM potassium chloride, pH 7.5

TBE 1X: 89 mM Tris, 89 mM Boric Acid, 2 mM EDTA, pH 8.0.

TAE 1X: 4 mM Tris, 4 mM Acetic Acid, 0.1 mM EDTA

GEL LOADING BUFFER (10X): 50% glycerol, 50% water, 0.05% bromophenol blue, 0.05% xylene cyanol.

LiP: 40 mM lithium hydroxide; potassium chloride or sodium chloride at the reported concentrations, at pH 7.4 with phosphoric acid.

4. 2. 5. Adduct formation on pBR322

pBR322 (0.15 μg) was added of increasing complexes concentrations in 10 mM Tris, 50 mM potassium chloride, pH 7.5. Immediately or after 24 hours incubation at the required temperature, the reactions were cooled down on ice, added with 4 μL of Gel Loading Buffer and loaded on 1% agarose gel.

For kinetic studies 0.15 μg of pBR322 was incubated with 100 μM of compound in 10 mM Tris and 50 mM potassium chloride at pH 7.5. Withdraws of the reaction mixture incubated at 37 °C, 50 °C and 70 °C were made at defined times.

Gels were run at room temperature on a Biorad apparatus at 70 V cm^{-1} in 1X TAE buffer and the reaction products were visualized by ethidium bromide staining at 590 nm. When required, the gel as well as the gel loading buffer was added of SDS to a final concentration of 1%.

4. 2. 6.Mass spectrometry

All mass spectra were obtained using a Mariner™ mass spectrometer, Applied Biosystems (Foster City, CA). Sample solutions were prepared in acetonitrile:water (1:1) and 1% of formic acid and contained 1 nM complex solution. They were infused using a Harvard model 11 syringe pump (Holliston, MA) set at flow rate of 20 μl/ min. The ESI source was set in positive ion mode with an electrospray voltage of 4.5 kV. Spectra were acquired over the *m/z* range 100-4000 by summing 100 scans.

4. 2. 7. Adduct formation on distinct DNA folding

Single stranded oligonucleotide (Tel22 or scramble) were 5'-labeled with ^{32}P and T4 polynucleotide Kinase, by incubating the reaction mixture at 37 °C for 30 min. The kinase activity was inactivated by heating the reaction mixture at 85°C for 5 min, followed by two phenol extractions.

A mixture containing 20.000 cmp/ lane of labelled oligonucleotide, 1 μM of not labelled oligonucleotide and increasing concentrations of compound in 10 mM Tris and 50 mM KCl at pH 7.5 was incubated at 37 °C for 24 hours. For evaluation of multistrand adduct formation, 20.000 cmp/ lane of labelled oligonucleotide and 100 μM of compound were added of increasing concentrations of not labelled oligonucleotides and incubated at 37 °C for 24 hours. The buffer was evaporated and the samples resuspended in 5 μL of 80% Formamide Gel Loading Buffer containing 0,1% xylene cyanole and bromophenol blue. Denaturating gel electrophoresis was performed with 20% polyacrylamide gels (19:1 acrylamide:bisacrylamide) in 1X TBE. Resolved bands on dried gels were visualized and quantified on a PhosphorImager (Amersham).

4. 2. 8.Fluorescence melting experiments

Melting experiments were performed in a Roche LightCycler fluorimeter, using an excitation source at 488 nm and recording the fluorescence emission at 520 nm. Target DNAs were HTS) and ds-random (Fluorescin 3' labelled 5'-GGA-TGT-GAG-TGT-GAG-TGT-GAG-G-3') annealed with its complementary strand labeled with Dabcyl at 5' end). Mixtures (20 □L) contained 0.25 □M of target DNA and variable concentrations of tested derivatives in 10 mM lithium hydroxide, 50 mM potassium chloride at pH 7.4 with phosphoric acid. The temperature was slowly increased (1 °C/min) up to 90 °C and again lowered at the same rate to 30°C. Recordings were taken during both these

melting and annealing reactions to check for hysteresis. Each curve was repeated at least three times and errors were ± 0.4°C.

4. 2. 9. 96 wells fluorescence quenching assay

The measures were performed with a Perkin Elmer VICTOR plate reader using an excitation source at 488 nm. Wells were filled with a 200 µL solution of ds-random in which one strand was labelled with a fluorophore (FAM) in 3' and the complementary one with a quencher (Dabcyl) in 5' position. DNA and increasing concentrations of compounds were incubated at 70 °C for 2 hours. Each sample was loaded and the changes in fluorescence emission recorded at 520 nm and plotted as a function of compound concentration using SigmaPlot 11.0 software.

4. 3 RESULTS

4. 3. 1. Evaluation of adduct formation on plasmid pBR322

A first evaluation of the interaction properties of the compounds with nucleic acids was performed by employing plasmidic DNA as substrate and by solving the reaction products by agarose electrophoresis. This technique was used to evaluate if the interaction of the compounds with the DNA can provide changes in its electrophoretic mobility.

First results indicate that the absence of compound incubation seems not to have any effect on the electrophoretic mobility suggesting that this treatment could be required to induce the adduct complex formation. Indeed, after 24 hours incubation at 37 °C, the tested compounds point different behaviours. Gels performed with SA2 and SA3 do not show any changes in the electrophoretic mobility of the plasmid (Figures 4.4 and 4.5) suggesting their inability to stably interact with this substrate, even after incubation.

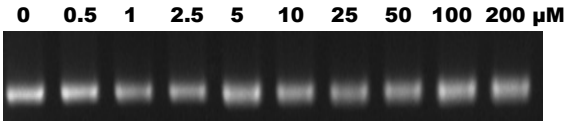

Figure 4.4 1% agarose gel of plasmid pBR322 and increasing concentrations of SA2 (0-200 µM) after 24 hours incubation at 37 °C in 10 mM Tris, 50 mM KCl buffer at pH 7.5

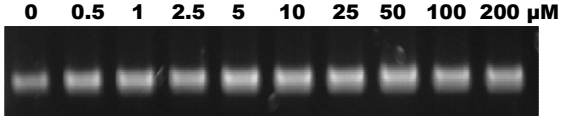

Figure 4.5 1% agarose gel of plasmid pBR322 and increasing concentrations of SA3 (0-200 µM) after 24 hours incubation at 37 °C in 10 mM Tris, 50 mM KCl buffer at pH 7.5

On the other hand, gels relative to compounds SA1 and SA4 show a delay in the electrophoretic mobility suggesting the formation of a complex compound-DNA that unwinds the plasmid (Figures 4.6 and 4.7). Since preliminary studies[190] indicate that formation of covalent adduct can unwind the plasmidic DNA, we verified if the observed DNA modifications are the result of a covalent interaction with the metal complex by adding 1% of Sodium Dodecyl Sulphate (SDS) in the gel matrix as well as in the reaction

mixture after incubation. In fact, considering that SDS has the intrinsic property to interfere with reversible ionic interactions, the presence of this surfactant as part of the gel can provide indications about the nature of the complex. Even in these environmental conditions, compounds SA1 and SA4 showed to efficiently reduce plasmidic DNA electrophoretic mobility starting from 25 μM concentrations. Addition of SDS to the gel matrix as well as to the incubated reagents does not alter the DNA mobility profiles, thus confirming that the observed unwinding is the result of adduct formation and is not linked to reversible intercalation of the aromatic portion of the compounds into the double helix. SA1 reactivity occurs at lower concentrations than SA4. If we compare the shift provided by the two active derivatives we observe that this can be the result of different factors: the adduct geometry, the DNA affinity or the reaction kinetic.

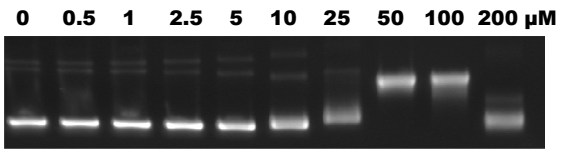

Figure 4.6 1% agarose gel of plasmid pBR322 and increasing concentrations of SA1 (0-200 μM) after 24 hours incubation at 37 °C in 10 mM Tris, 50 mM KCl buffer at pH 7.5

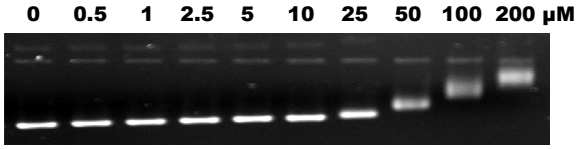

Figure 4.7 1% agarose gel of plasmid pBR322 and increasing concentrations of SA4 (0-200 μM) after 24 hours incubation at 37 °C in 10 mM Tris, 50 mM KCl buffer at pH 7.5

4. 3. 2. Kinetic of adduct formation

Based on the results obtained by the previous experiments, we decided to investigate how the reaction kinetics can be influenced by compounds reactivity and by temperature. The reaction products of pBR322 by the active compounds SA1 and SA4 at 100 μM were monitored at different incubation time. At this concentration both compounds previously demonstrated to efficiently react with the plasmidic DNA.

At 37 °C, faster reactivity of SA1 compared to SA4 was confirmed. Indeed SA1 starts to unwind the plasmidic DNA after 3 hours of incubation, while SA4 starts after 5 hours. After 24 hours of incubation, incrementing of the reaction temperature (37 °C, 50 °C and 70 °C) results in faster reactivity for both the compounds, as shown in Figures 4.9-4.14.

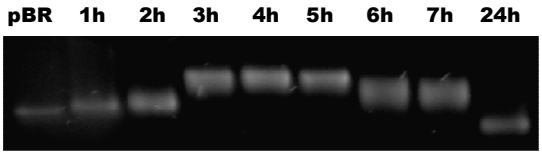

Fig.ure 4.9 Kinetic of SA1 at 37 °C, in 10 mM Tris, 50 mM KCl buffer at pH 7.5

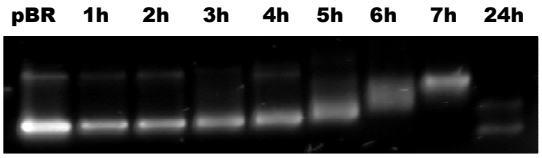

Figure 4.10 Kinetic of SA4 at 37 °C, in 10 mM Tris, 50 mM KCl buffer at pH 7.5

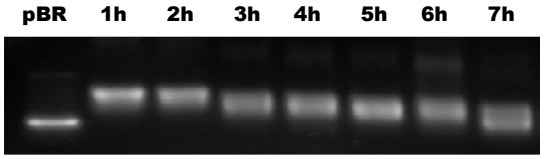

Fiure 4.11 Kinetic of SA1 at 50 °C, in 10 mM Tris, 50 mM KCl buffer at pH 7.5

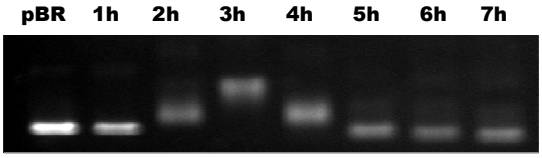

Figure 4.12 kinetic of SA4 at 50 °C, in 10 mM Tris, 50 mM KCl buffer at pH 7.5

At 70 °C faster reactivity is observed for compound SA4. This is probably due by different temperature effects on the exchange of the leaving groups.

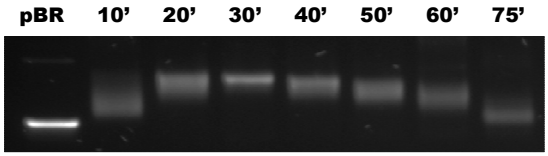

Figure 4.13 Kinetic of SA1 at 70 °C, in 10 mM Tris, 50 mM KCl buffer at pH 7.5

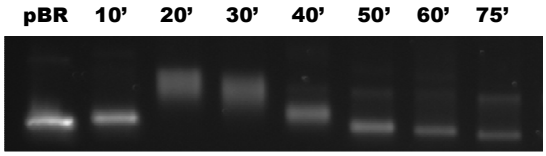

Figure 4.14 Kinetic of SA4 at 70 °C, in 10 mM Tris, 50 mM KCl buffer at pH 7.5

These results indicate that adduct formation is a process differently regulated by the temperature for the two derivatives.

4. 3. 3. Effect of DNA template folding on adduct formation

To investigate if the different reactivity observed with SA1 and SA4 on pBR322 is affected by the DNA template and folding, a single strand sequence, a double strand

sequence and the human telomeric sequence Tel22 were employed. These sequences were accurately chosen with the same number of guanine residues but in different positions on the strand so that the Tel22 sequence is be able to fold in the G-quadruplex conformations while the scramble DNA remains unfolded. The idea was to evaluate preferential sites of interactions since the nitrogens in 7 positions of the guanines are involved in the formation of the Hoogsten bonds of the G-quartets. This feature could drive the reactivity toward another base residue or protect the DNA by compound interaction.

Increasing concentrations of the compounds were incubated with the three DNA templates for 24 hours at 37 °C. Gels were then run in denaturating conditions. In these conditions the original folding of the nucleic acid is prevented. This feature can provide indications about the complex-DNA interaction stability and reversibility.

The gels show a decreased intensity of the band relative to the free DNA and the presence of smeared bands (A1 and A2) with slower electrophoretic mobility. These bands suggest the formation of different types of adduct species. SA1 and SA4 show comparable efficiency in adduct formation on G-quadruplex. The reactivity of the two compounds on this DNA folding results increased if compared to the reference compounds cisplatin and transplatin. On single strand DNA no relevant differences in the platination degree were observed by SA1, SA4 and cispaltin while transplatin generates lower adduct amount at comparable concentrations. The compounds reactivity results mainly different on the duplex template. Cisplatin was the most efficient in promoting adduct formation on double strand DNA followed by SA1 and tranplatin. In agreement with results obtained on pBR322, SA4 showed lower reactivity on this DNA template.

4. 3. 4. Multistrand DNA adduct formation

From the PAGE analysis, formation of multiple species of adducts, which can result in smeared bands (Figures 4.14-4.17), is also observed at the higher tested ligands concentrations. This is likely the result of the presence of many potential platination sites on each DNA strand. This allow us to attribute adduct species identified with A1 as generated by platination of one DNA strand. However, the adduct species identified as A2 present a remarkably reduced electrophoretic mobility that can be reasonably due to cross-linking between DNA two strands. This is expected to occur on double strand DNA but in the presence of SA1 and SA4 we observed it also on G-quadruplex and single strand DNA substrates.

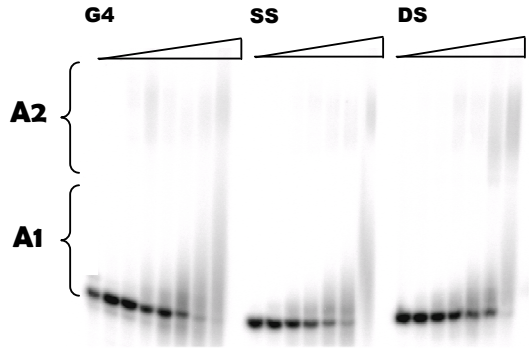

Figure 4.14 PAGE analysis of SA1 after 24 hours incubation at 37 °C, in 10 mM Tris, 50 mM KCl buffer at pH 7.5

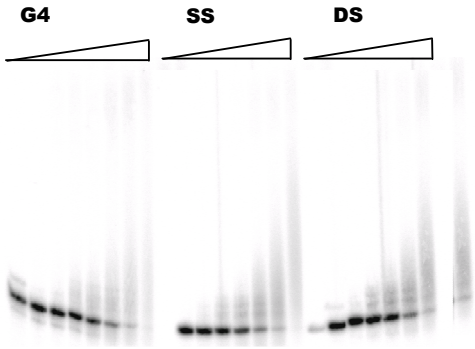

Figure 4.15 PAGE analysis of SA4 after 24 hours incubation at 37 °C, in 10 mM Tris, 50 mM KCl buffer at pH 7.5

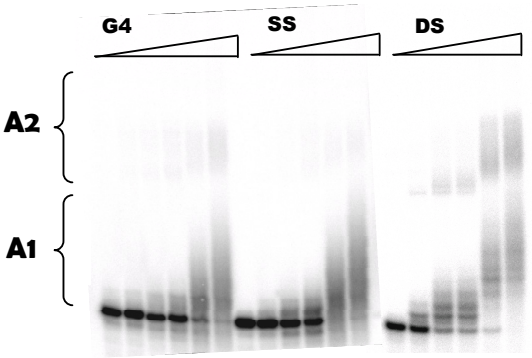

Fig.ure 4.17 PAGE analysis of cisplatin after 24 hours incubation at 37 °C, in 10mM Tris, 50 mM KCl buffer at pH 7.5

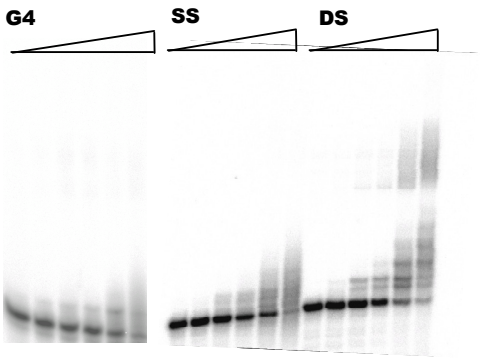

Fig.ure 4.18 PAGE analysis of tranplatin after 24 hours incubation at 37 °C, in 10mM Tris, 50 mM KCl buffer at pH 7.5

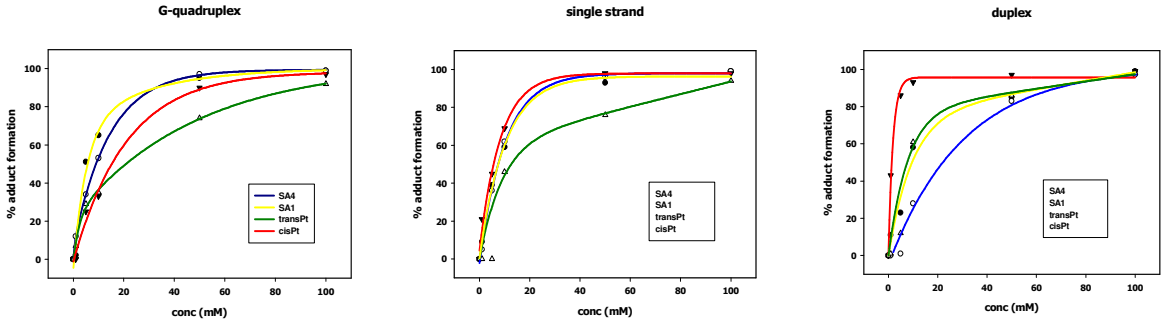

Figure 4.19. Plots of the the percentage of adduct formation as a function of compound concentrations on the three different DNA templates evaluated

In order to verify the hypothesis of the formation of interstrand adducts due to cross-linking between two non-paired DNA strands, alkilation experiments were performed at fixed concentration of compound (50 μM) but in the presence of increasing concentrations of DNA by including cold oligonuclotides into the reaction mixture. When we increased the dsDNA concentration, a suppression of both A1 and A2 occurred as a result of the redistribution of the reactive species between the labelled (visualized) and unlabelled (not visualized) DNA. In presence of increasing concentrations of single strand and quadruplex DNA this behaviour is conserved but it is limited to the A1 adducts. Indeed the presence of multimeric adducts (A2) is preserved. These data further sustained the presence of interstrand adducts involving two not paired DNA strands. A comparison with cis- and transplatin indicates that this behaviour is mainly relevant for SA1 and SA4 on G-quadruplex DNA

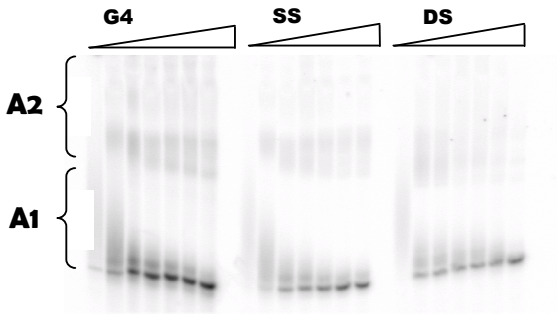

Figure 4.20 PAGE analysis of SA1 after 24 hours incubation for at 37 °C with addition of unlabelled DNA in 10mM Tris, 50mM KCl buffer at pH 7.5

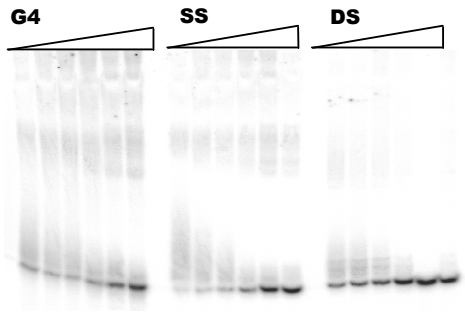

Figure 4.21 PAGE analysis of SA4 after 24 hours incubation for at 37 °C with addition of unlabelled DNA in 10mM Tris, 50mM KCl buffer at pH 7.5

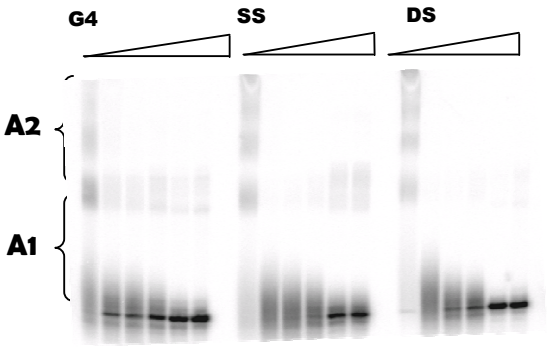

Figure 4.22 PAGE analysis of cisplatin after 24 hours incubation for at 37 °C with addition of unlabelled DNA in 10mM Tris, 50mM KCl buffer at pH 7.5

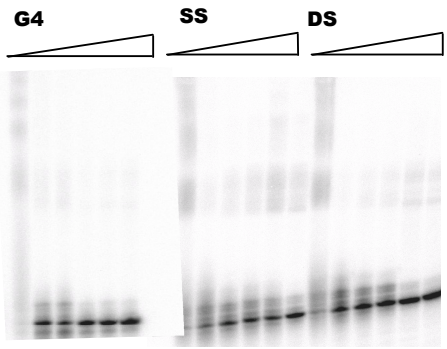

Figure 4.23 PAGE analysis of transplatin after 24 hours incubation for at 37 °C with addition of unlabelled DNA in 10mM Tris, 50mM KCl buffer at pH 7.5

4. 3. 5. Effect of adduct formation on DNA thermal stability and annealing efficiency

In order to evaluate if the alkylation process can interfere with the double strand annealing, the active compounds were incubated with a duplex sequence composed by a strand labelled with a fluorophore (FAM) and the complementary one with a quencher (Dabcyl). The fluorescence intensity was then measured at increasing concentrations of the compounds with a Roche LightCycler fluorimeter.

In absence of incubation the compounds do not alter the fluorescence melting profiles relative to the oligonucleotide confirming no interference of the metal complex on the DNA stability. The same result was observed when compounds were incubated with DNA at 37 °C for 24 hours. In these condition previous data indicated that DNA folding is preserved and adduct formation can occur. Although the melting curves do not provide any indication of the stabilizations of the DNA induced by the compounds, the comparison between melting and annealing profiles clearly indicate inability of the DNA to correctly refold (Figures 4.24 and 4.25). Indeed, the plot relative to the annealing curves shows high fluorescence intensity values at low temperatures indicating that the fluorophore and the quencher are held separated by the presence of

the adduct. Interestingly, no modification both of the melting and annealing curve were recorded in the presence of SA2 and SA3. Due to the promotion of adduct formation by the temperature DNA was incubated with SA1 and SA4 for 2 hours at 70 °C, a temperature that grants denaturation of the two strands and high alkylation reactivity. The experiment was also performed with a single strand sequence and the complementary one was added at the end of the incubation. Fluorescence intensity of the samples was then measured with a plate reader fluorimeter. To avoid inaccuracy due to interference of the metal complexes with the oligonucleotides fluorescence signal the results of a fast cooling or a slow annealing of the reaction mixture, which prevent or favour DNA strand pairing respectively, was detected.

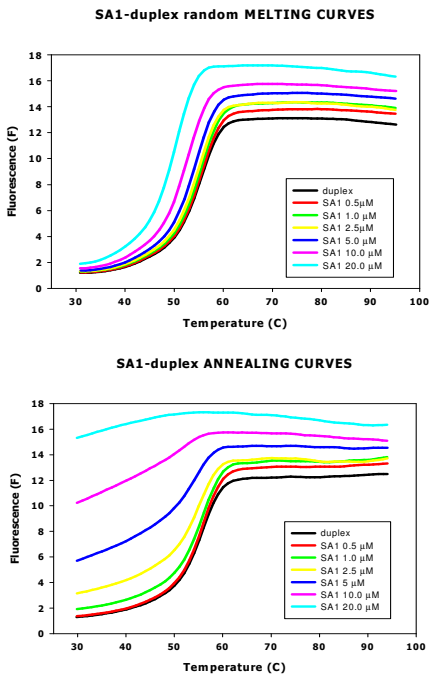

Figure 4.24 Melting (top) and annealing (bottom) profiles of the duplex sequences under evaluation and compound SA1

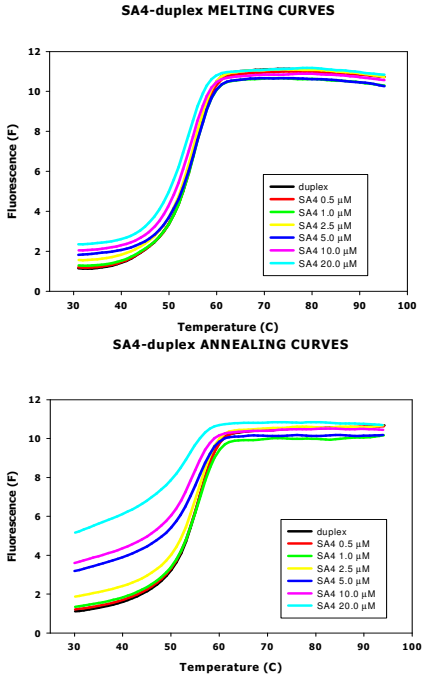

Figure 4.25 Melting (top) and annealing (bottom) profiles of the duplex sequences under evaluation and compound SA1

In consistency with previously reported results, the absence of incubation does not affect the compounds reactivity while after incubation the compounds are able to prevent the effective approach of fluorophore and quencher resulting in higher fluorescence values. . Data indicate a better contribution of SA1 in interfering with the DNA annealing process. These results allow not only a comparison between the compounds highlighting the better effectiveness of SA1 (in agreement with other results) but confirm how the alkylation process can alter the DNA annealing process of the oligonucleotide employed.

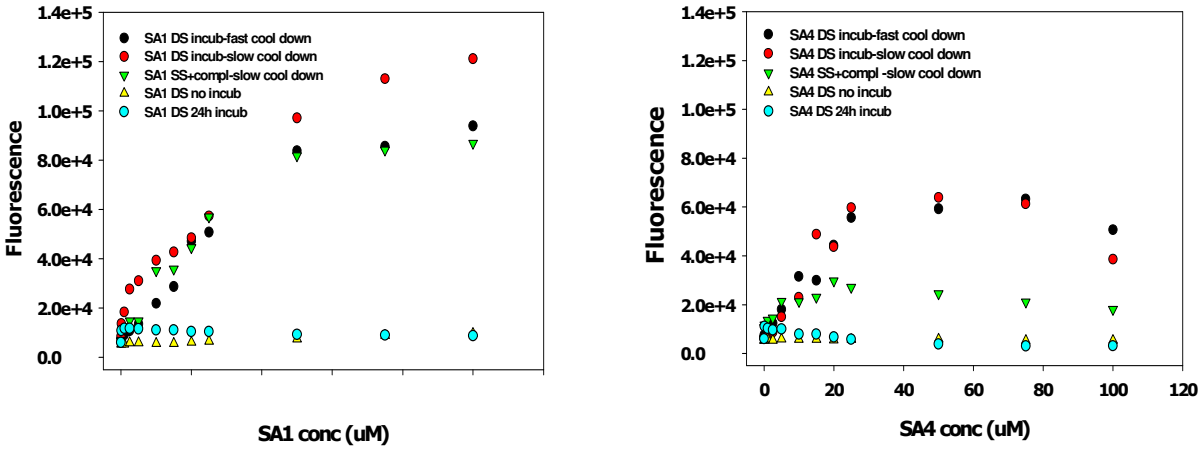

Figure 4.26 Plot representing the fluorescence intensity of the duplex oligonucleotide at increasing concentrations of SA1 (left) and SA4 (right) and at different annealing conditions

4. 3. 6. Identification of reactive species in solution

As previously mentioned, the reactivity of the compounds is due to their conversion into reactive mono and diaquo species. Thus the four TPA were tested by electrospray mass spectrometry immediately after dilution and after 24 hours incubation at 37 °C in water.

SA1 pre- and post-incubation spectra showed one conserved peak at 373 m/z. This value corresponds to the loss of one chloride group and its replacement with one

acetonitrile deriving from the buffer used for the analysis. The rapid exchange rate of the original leaving group with one solvent molecule is evident even without incubation, in line with the fast reactivity of SA1 in solution above reported.

SA1 pre-incubation

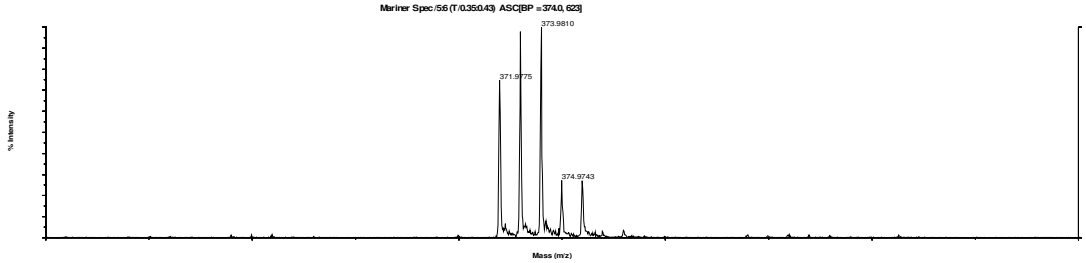

SA1 post-incubation at 37 °C for 24 hours

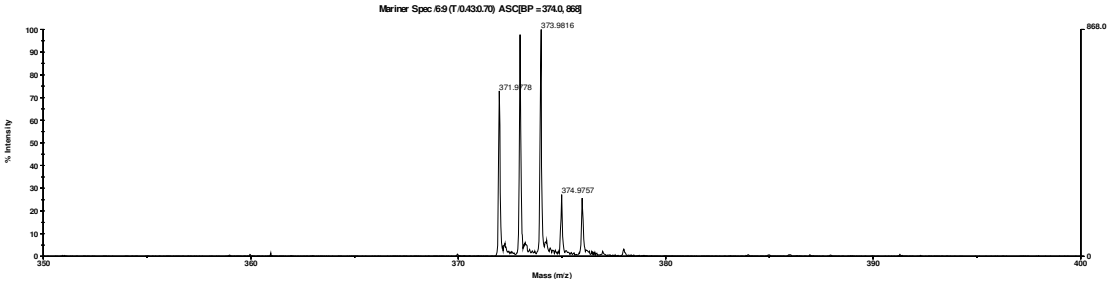

On the other end, the mass spectrum of not incubated SA4 presents a peak at 431 m/z relative to the free compound and a smaller peak at 386 m/z corresponding to the loss of a carboxylic group. The spectrum recorded on the solution of the ligand after 24 hours at 37 °C evidences the peaks at 386 and another peak at 404 m/z which correspond to the monoaquo species.

SA4 pre-incubation

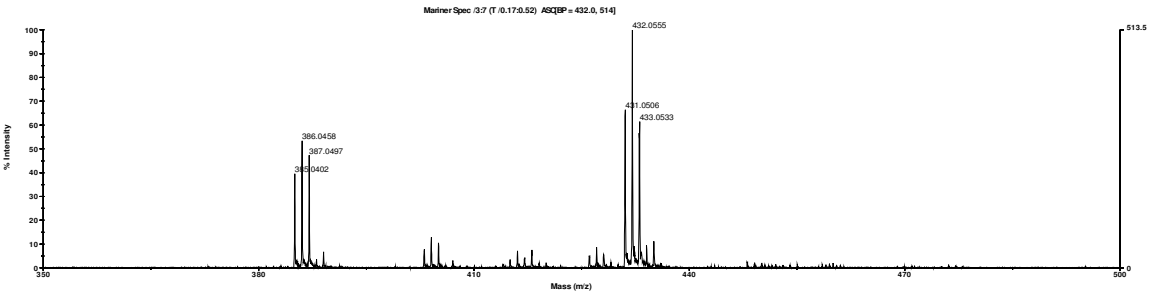

SA4 post-incubation at 37 °C for 24 hours

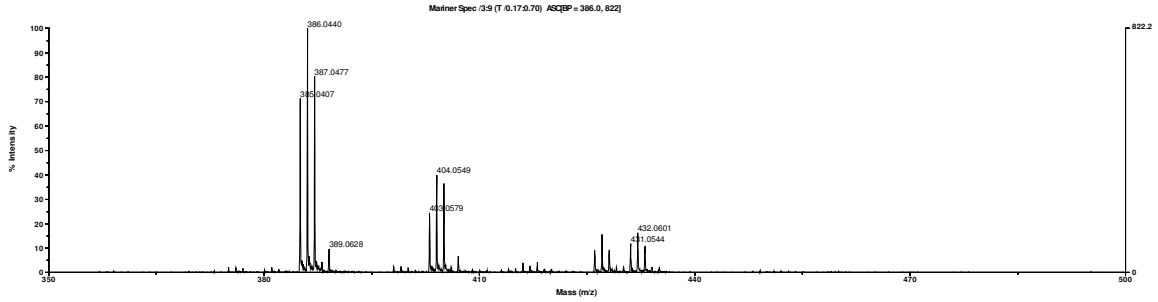

We focused on compounds SA2 and SA3 with the goal of understanding if this lack of reactivity was due to the inability of the compounds to convert into aquo species.

SA2 pre-incubation spectrum shows a peak at 472 m/z that is relative to the free compound. The same peak but of smaller intensity is still observed after incubation. In the same conditions, a peak at 412 indicates the loss of the acetate group. Unfortunately we have not been to characterize the other two peaks so far.

SA2 pre-incubation

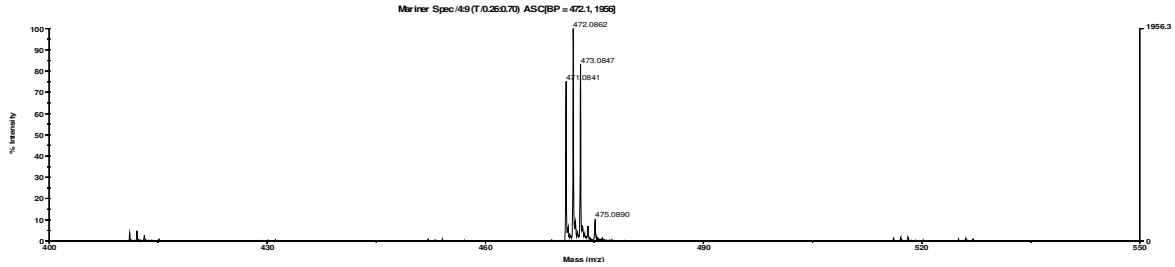

SA2 post-incubation at 37 °C for 24 hours

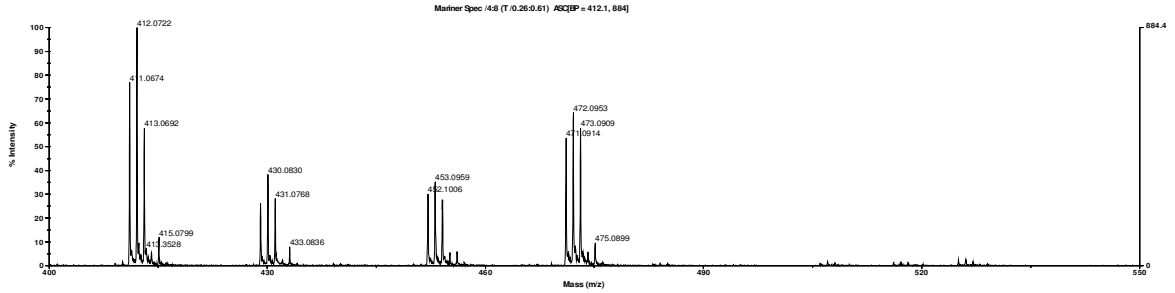

SA3 spectra present both the same peak at m/z 444. This is the peak of the free compound and so indicates that it is unable to react since it is not convert into any reactive species.

SA3 pre- incubation

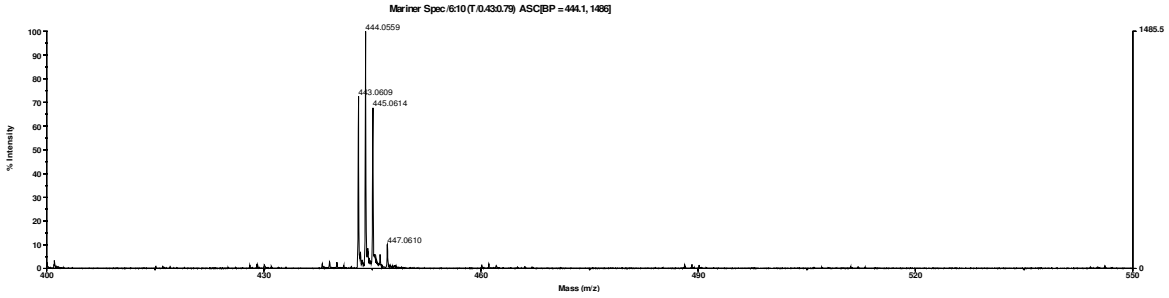

SA3 post-incubation at 37 °C for 24 hours

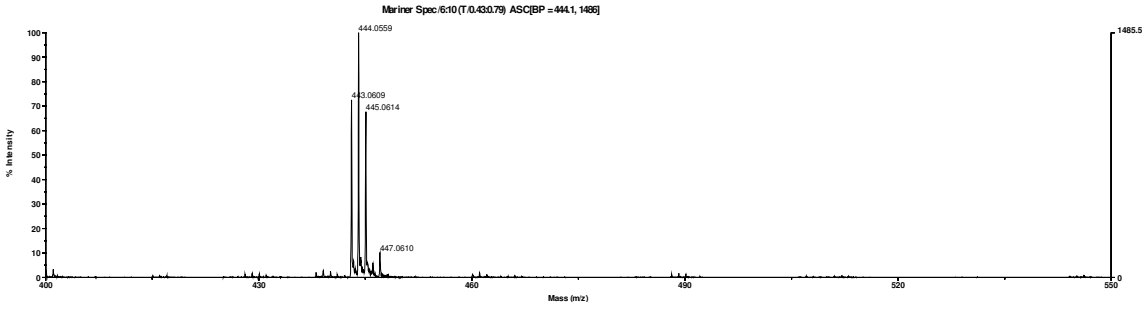

4. 4. DISCUSSION

The data herein presented showed how distinct structural modifications can cooperate to greatly affect the interaction of TPAs with nucleic acids. Among tested Pt complexes, we identified two active and two inactive compounds. SA1, the *trans*-amminedichloro(thiazole)platinum(II), [$PtCl_2(NH_3)$(thiazole)], showed the best DNA adduct formation in physiological conditions. Interestingly, this compound is the only one presenting two chlorides as leaving groups in analogy to the reference compounds cis- and transplatin. Activation through hydrolysis is faster when compared to the other herein tested derivatives when the chlorides were replaced by carboxylates. The nature

of the carboxylate affects the rate of reaction with DNA, as also observed for hydrolysis reactions and reactions with model oligonuucleotides.. SA4 is the second active compound. Examination of structures shows that the presence of two pyridines produces very sterically hindered compounds resulting in slow or negligible DNA-adduct formation. These results are in agreement with studies on *trans*-[$PtCl_2(pyr)_2$] DNA binding. These features suggest that the substitution of only one amino group on the transplatin nucleus is optimal for modulation of DNA platination properties. *In vitro*, this effect is not linked to a reduced recognition of the target DNA but on the formation of the reactive aquo species. Interestingly, in cells, there is DNA platination, even of the unreactive compounds such as SA-2, reminiscent of the drug carboplatin which is substitution-inert but yet produces Pt-DNA adducts in cells. .

For the DNA-active compounds in this study, mass spectra evidenced the exchange of only one leaving group that might suggest the formation of monofunctional species and thus of monofunctional adducts. However, interstrand crosslinks, and thus bifunctional adducts, have been confirmed to occur with SA1 and SA4, confirming previous results. The most interesting point, however, is that the nature of the DNA template affects preference for binding; a hither to unnoticed observation is that TPAs have no specific preference for double stranded DNA in comparison to single stranded or G-quadruplex DNA than on double stranded DNA. This is possibly due to steric effects of the planar amine groups when the molecule interacts with the DNA substrate. If we extend these results at cellular level this may reflect a distinct distribution of platination sites along the genome in comparison to cisplatin and even transplatin. Further, the DNA-binding profile of SA4 does resemble that of SA1 and these observations may help explain the unique cytotoxic profile of TPAs. These results increment the available

knowledge of DNA-Pt complex interaction at the molecular level and provide a rationale for SAR analysis and subsequent drug structure optimization.

CONCLUSIONS

The studies conducted in this thesis work are aimed to the evaluation of the ability of different classes of compounds to recognize nucleic acids substrates with a particular interest for the G-quadruplex DNA. A first approach was oriented toward the investigation of the affinity and the stabilization properties of the quadruplex arrangement by means of a number of biophysical methods. Subsequently enzymatic and cellular assay have been used to check for a correlation between biological and biophysical data.

The whole set of collected data represents a complex matrix of information that we had to rationalize according to the properties of the G-quadruplex system and to the biological results obtained. In general, the data provided useful indications about the structural requirements fundamental for efficient G-quadruplex targeting. We demonstrated that assembly of otherwise inactive planar structures through metal coordination represents an effective strategy for increasing G-quadruplex binding and promoting its selective recognition by reducing the undesired double strand DNA binding. Therefore, by combining proper ligands with selected metal ions it is possible to produce a variety of complexes rationally designed for specifically targeting or damaging the DNA. In line, a general correlation between G-quadruplex affinity and telomerase inhibition *in vitro* emerged. This is not peculiar among each family of compounds but it can be extended to cross-correlate data. However, in some cases we observed relevant outliers when comparing biophysical, enzymatic (Telomerase inhibition) and cellular (cell citotoxity) results. These features turned

our attention to a close examination of the ligand binding mode that we believe to be possibly involved in driving distinctive cellular effects. As an example, we showed that even modest bioisosteric substitutions on a common scaffold can affect more parameters than the simple DNA binding affinity. In particular we showed how they can alter drug DNA binding shapes. As a consequence a shift towards different binding modes on the same substrate occurs. At cellular level this can be translated in the potential of the drug to drive different cytotoxic effects due to the involvement of different cell pathways. A rational explanation can be found in the intrinsic complexity of the G-quadruplex target emphasized by 1) the polymorphic nature of the system 2) different conformations all along the genome and 3) its involvement at different levels of the cell regulatory machineries.

To conclude, the data herein obtained are useful to better understand the molecular processes involving the nucleic acids and to design new drug candidates characterized by safer and more efficient anticancer profile.

REFERENCES

[1] Ghosh, A.; Bansal, M.; *Acta Crystallogr. D. Biol. Crystallogr.,* **2003,** *59*, 620–626

[2] Blackburn, G. M.; Gait, M. J.; "Nucleic Acids in Chemistry and Biology". Oxford University Press, **1996**

[3] Watson, J. D.; Crick, F. H. C.; *Nature,* **1953**, *171*, 737-738

[4] http://www.genome.gov/25520880. The National Human Genome Research Institute website

[5] Smith, J. A.; Martin, L.; *Proc. Natl. Acad. Sci. U.S.A,* **1973***, 70*, 1263–1267

[6] Murray, A.W., Hunt, T.; "The Cell Cycle: An Introduction", Oxford University Press., **1993**, 251

[7] Norbury, C.; Nurse, P.; *Annu. Rev. Biochem.,* **1992**, *61*, 441-470

[8] Okazaki, R.; Okazaki, T.; Sakabe, K.; Sugimoto, K.; *Jpn. J. Med. Sci. Biol.*, **1967**, *20*, 255-260

[9] Ogawa, T.; Okazaki, T.; *Annu. Rev. Biochem.,* **1980**, *49*, 421-457

[10] Secko, D.; "The cell cycle: a universal cellular division program". *The Science Creative Quarterly*, **2009**, Issue 4

[11] Neidle, S.; Parkinson, G.; *Nat. Rev. Drug Discov.*, **2002**, *1*, 383- 393

[12] Levy, M. Z.; Allsopp, R. C.; Futcher, A. B.; Greider C. W.; Harley, B. C.; *J. Mo.l Biol.,* **1992**, *225*, 951-960

[13] Blackburn, E. H., Szostak, J. W.; *Annu. Rev. Biochem.,* **1984**, *53*, 163-194

[14] Blackburn, E. H.; *Cell*, **1984**, *37*, 7-8

[15] Muller, H. J.; "The remaking of chromosomes". *The collecting net-Woods Hole*, **1938**, *13*, 181–198

[16] Bailey, S. M.; Murnane, J. P.; *Nucleic Acids Res.,* **2006**, *34*, 2408-2417

[17] Meyne, J.; Ratliff, R. L.; Moyzis, R. K.; *Proc. Natl. Acad. Sci. USA*, **1989**, *86*, 7049–7053

[18] Moyzis, R. K.; Buckingham, J. M.; Cram, L. S.; Dani, M.; Deaven, L. L.; Jones, M. D.; Meyne, J.; Ratliff, R. L.; Wu, J. R.; *Proc. Natl. Acad. Sci. USA*, **1988**, *85*, 6622–6626

[19] Blackburn,E.H.; *Nature,* **1991**, *350*, 569–573

[20] Griffith, J.D.; Comeau, L.; Rosenfield, S.; Stansel; R. M.; Bianchi, A.; Moss,H.; de Lange, T.; *Cell*, **1999**, *97*, 503–514

[21] Li, G. Z.; Eller, M. S.; Firoozabadi, R., Gilchrest, B. A.; *Proc. Natl. Acad. Sci. USA*, **2003**, *100*, 527- 531

[22] Cesare, J. A.; Reddel, R. R.; "Alternative lengthening of telomeres in mammalian cells", http://www.ncbi.nlm.nih.gov/bookshelf/br.fcgi?book=eurekah&part=A74264

[23] Chong, L.; van Steensel, B.; Broccoli, D.; Erdjument-Bromage, H.; Hanish, J.; Tempst, P.; de Lange, T.; *Science*, **1995**, *270*, 1663–1667

[24] Zhong, Z.; Shiue, L.; Kaplan, S.; de Lange, T.; *Mol. Cell. Biol.,* **1992**, *12*, 4834–4843

[25] Bilaud, T.; Brun, C.; Ancelin, K.; Koering, C. E.; Laroche, T.; Gilson, E.; *Nature Genet.,* **1997**, *17*, 236–239

[26] Broccoli, D.; Smogorzewska, A.; Chong, L.; de Lange, T.; *Nature Genet*., **1997**, *17*, 231–235

[27] Hayflick, L.; Moorhead, P. S.; *Exp. Cell. Res.,***1961,** *25*, 585-621

[28] Hayflick, L.; *Exp. Cell Res.,* **1965**, *37*, 614–636

[29] Greider, C .W.; Blackburn, E. H.; *Cell,* **1985**, *43*, 405–413

[30] http://nobelprize.org/nobel_prizes/medicine/laureates/2009/press.html

[31] Artandi, S. E.; DePinho, R. A.; *Carcinogenesis,* **2010**, *31*, 9–18

[32] Greider, C. W.; Blackburn, E. H.; *Nature*, **1989**, *337*, 331–337

[33] Kirkpatrick, K. L.; Mokbel, K.; *Eur. J. Surg. Oncol.,* **2001,** *27*, 754–660

[34] Mergny, J. L.; Riau, J. F.; Mailliet, P.; Teulade-Fichou, M. P.; Gilson, E.; *Nucleic Acids Res.*, **2002**, *30*, 839-865

[35] Meyerson, M.; Counter, C. M.; Eaton, E. N.; Ellisen, S. W.; Steiner, P.; Caddle, S. D.; Ziaugra, L.; Beijersbergen, R. L.; Davidoff, M. J.; Liu, Q.; Bacchetti, S.; Haber, D. A.; Weinberg, R. A.; *Cell*, **1997**, *90*, 785-795

[36] Chen, J. L.; Blasco, M. A.; Greider, C. W.; *Cell*, **2000**, *100*, 503-514

[37] Neidle, S.; Parkinson, G.; *Nat. Rev. Drug Discov.*, **2002**, *1*, 383- 393

[38] Morin, G.B.; *Cell,* **1989,** *59*, 521–29

[39] Bosoy, D.; Lue, N. F.; *Nucleic Acids Res*, **2004**, *32*, 93–101

[40] Wright, W. E.; Pyatiszec, M. A.; Rainey, W. E.; Byrd, W.; Shay, J. V.; *Dev. Genet.,* **1996**, *18*, 173-179

[41] Kim, N. W.; Piatyszek, M. A.; Prowse, K. R.; Harley, C. B.; West, M. D.; Ho, P. L.; Coviello, G. M.; Wright, W. E.; Weinrich, S. L; Shay, J. W.; *Science*, **1994**, *266*, 2011–2015

[42] Shay, J. W.; Bacchetti, S.; *Eur. J. Cancer*, **1997**, *33*, 787–791

[43] Bottius, E.; Bakhsis, N.; Scherf, A.; *Mol. Cell Biol*., **1998**. *18*, 919-925

[44] Cano, M. I.; Dungan, J. M.; Agabian, N.; Blackburn, E. H.; *Proc. Natl. Acad. Sci. U S A*, **1999**, *96*, 3616-3621

[45] Han, H; Cliff, C. L.; Hurley, L. H.; *Biochemistry,* **1999**, *38*, 6981- 6986

[46] Han, H.; Hurley, L. H.; Salazar, M.; *Nucleic Acids Res*., **1999**, *27*, 537- 542

[47] Damm, K.; Hemmann, U.; Garin-Chesa, P.; Hauel, N.; Kauffmann, I.; Priepke, H.; Niestroj, C.; Daiber, C.; Enenkel, B.; Guilliard, B.; Lauritsch, I.; Muller, E.; Pascolo, E.; Sauter, G.; Pantic, M.; Martens, U. M.; Wenz, C.; Lingner, J.; Kraut, N.; Rettig, W. J.; Schnapp, A.; *EMBO J.,* **2001**, *20*, 6958- 6968

[48] Zahler, A. M.; Williamson, J. R.; Cech, T. R.; Prescott, D. M.; "Inhibition of telomerase by G-quartet DNA structures". *Nature*, **1991**. *350*, 718-20

[49] Phan, A.T.; Kuryavyi, V.; Patel, D. J.; *Curr. Opin. Struct. Biol.*, **2006**, *16*, 288- 298

[50] Catasti, P.; Chen, X.; Moyzis, R. K.; Bradbury, E. M.; Gupta, G.; *J. Mol. Biol*., **1996**, *264*, 534-545

[51] Lemarteleur, T. ; Gomez, D. ; Paterski, R. ; Mandine, E. ; Mailliet, P. ; Riou, J.F. ; *Bioch. Bioph. Res. Comm.*, **2004**, *323*, 802- 808

[52] Huppert, J.L.; Balasubramanian, S.; *Nucleic Acids Res.*, **2006**, *35*, 406- 413

[53] Hurley, L.H.; *Bioch. Soc. Trans.*, **2001**, *29*, 692- 696

[54] Hershman, S. G.; Chen, Q.; Lee, J. Y.; *Nucleic Acids Res.*, **2008**, *36*, 144-156

[55] Srivastava, M.; Pollard, H. B.; *FEBS J.*, **1999**, *13*, 1911-1922

[56] Hanakahi, L. A.; Sun, H.; Maizels, N.; *J. Biol. Chem.,* **1999**, *274*, 15908-15912

[57] Drygin, D.; Siddiqui-Jain, A.; O'Brien, S.; Schwaebe, M.; Lin, A.; Bliesath, J.; Ho, C. B.; Proffitt, C.; Trent, K.; Whitten, J. P.; Lim, J. K. C.; Von Hoff, D.; Anderes, K.; Rice, W.; *Cancer Res.,* **2009**, *69*, 7653-7661

[58] Lingner, J.; Cech,T. R.; *Curr. Opin. Genet. Dev*., **1998**, *8*, 226–232

[59] da Silva, M. W.; *Methods*, **2007**, *43*, 264–277

[60] Lane, A. N.; Chaires, J. B.; Gray, R. D.; Trent. J. O.; *Nucleic Acids Res.,* **2008**, *36*, 5482-5515

[61] Burge, S.; Parkinson, G. N.; Hazel, P.; Todd, A. K.; Neidle, S.; *Nucleic Acids Res.*, **2006**, *34*, 5402- 5415

[62] Dai, J.; Carver, M.; Yang, D.; *Biochimie,* **2008**, *90*, 1172-1183

[63] Wang, Y.; Patel, D, J.; *Structure*, **1993**, *1*, 263–282

[64] Parkinson, G. N.; Lee, M. P. H; Neidle, S.; *Nature*, **2002**, *417*, 876–880

[65] Dai, J. X.; Carver, M.; Punchihewa, C.; Jones, R. A.; Yang, D. Z.; *Nucleic Acids Res.,* **2007**, *35*, 4927–4940

[66] Ambrus, A.; Chen, D.; Dai, J.; Bialis, T.; Jones, R. A.; Yang, D. Z.; *Nucleic Acids Res.*, **2006**, *34*, 2723- 2735

[67] Xu, Y. ; Noguki, Y. ; Sugiyama, H.; *Bioorg. & med. Chem.,* **2006**, *14*, 5584- 5591

[68] Burge, S.; Parkinson, G. N.; Hazel, P.; Todd, A. K.; Neidle, S.; *Nucleic Acids Res.*, **2006**, *34*, 5402-5415

[69] Siddiqui-Jain, A.; Grand, C. L.; Bearss, D. J.; Hurley, L. H.; *Proc. Natl. Acad. Sci.*, **2002**, *99*, 11593-11598

[70] Facchini, L. M.; Penn, L. Z.; *FASEB J*, **1998**, *12*, 633-51

[71] Marcu, K. B., Bossone, S. A.; Patel, D. J.; *Annu Rev Biochem*, **1992**, *61*, 809-60

[72] Hurley, L. H.; *Nature Rev. Cancer*, **2002**, *2*, 188- 200

[73] Simonsson, T.; Sjoback, R.; *J. Biol. Chem*, **1999**, *274*, 17379–17383

[74] Seenisamy, J.; Rezler, E. M.; Powell, T. J.; Tye, D.; Gokhale, V.; Joshi, C. S.; Siddiqui-Jain, A.; Hurley, L. H.; *J. Am. Chem. Soc.*, **2004**, *126*, 8702-8709

[75] Sun, D.; Thompson, B.; Cathers, B. E.; Salazar, M.; Kerwin, S. M.; Trent, J. O.; Jenkins, J. C.; Neidle, S.; Hurley, L. H.; *J. Med. Chem.,* **1997***, 40*, 2113- 2116

[76] Perry, P. J.; Reszka, A. P.; Wood, A. A.; Read, M. A.; Gowan, S. M.; Dosanjh, H. S.; Trent, J. O.; Jenkins, T. C.; Kelland, L. R.; Neidle, S.; *J. Med. Chem*, **1998**, *41*, 4873- 4884

[77] Neidle, S.; *Curr. Opin. Struct. Biol.*, **2009**, *19*, 239-250

[78] De Cian, A.; Lacroix, L.; Douarre, C.; Temime-Smaali, N.; Trentesaux, C.; Riou, J. F.; Mergny, J. L.; *Biochimie*, **2008**, *90*, 131-155

[79] Monchaud, D.; Teulade-Fichou, M. P.; *Org. Biomol. Chem.*, **2008**, *6*, 627-636

[80] Zhao, J.; Bacolla, A.; Wang, G.; Vasquez, K. M.; *Cell Mol Life Sci.*, **2010**, 67, 43-62

[81] Phan, A. T.; Kuryavyi, V.; Patel, D. J.; *Curr. Opin. Struct. Biol.*, **2006**, *16*, 288- 298

[82] Hurley, L. H.; *Bioch. Soc. Trans.*, **2001**, *29*, 692- 696

[83] Zahler, A. M.; Williamson, J. R.; Cech, T. R.; Prescott, D. M.; *Nature*, **1991**, *350*, 718-20

[84] Huppert, J. L.; Balasubramanian, S.; *Nucleic Acids Res.*, **2006**, *35*, 406- 413

Capitolo 2 [85] Kankia, B. I.; Marky, L. A.; *J. Am. Chem. Soc.***, 2001, *44*,** 10799–10804

[86] Ellington, A. D.; Szostak, J. W. *Nature*, **1990**, *346*, 818–822

[87] Drygin, D.; Siddiqui-Jain, A.; O'Brien, S.; Schwaebe, M.; Lin, A.; Bliesath, J.; Ho, C. B.; Proffitt, C.; Trent, K.; Whitten, J. P.; Lim, J. K. C.; Von Hoff, D.; Anderes, K.; Rice, W.; *Cancer Res.,* **2009**, *69*, 7653-7661

[88] Dai, J.; Carver, M.; Yang, D.; *Biochimie,* **2008**, *90*, 1172-1183

[89] Burge, S.; Parkinson, G. N.; Hazel, P.; Todd, A. K.; Neidle, S.; *Nucleic Acids Res.*, **2006**, *34*, 5402- 5415

[90] Mazur, S.; Tanious, F. A.; Ding, D.; Kumar, A.; Boykin,, D. W.; Simpson, I. J.; Neidle, S.; Wilson, W. D.; *J. Mol. Biol.* **2000**, *300,* 321-327

[91] Tanious, F. A.; Nguyen, B.; Wilson, W. D.; *Methods in Cell Biology*, **2008**, *84*, 53-77

[92] Mergny, J. L.; Phan, A. T.; Lacroix, L.; *FEBS Lett*. **1998**, *435*, 74–78

[93] Mergny, J. L.; Lacroix L.; *Curr. Protoc. Nucleic Acid Chem.,* **2009**, Chapter 17

[94] Ambrus, A.; Chen, D.; Dai, J. X.; Bialis, T.; Jones, R. A.; Yang, D. Z. *Nucleic Acids Res.* **2006**, *34*, 2723–2735

[95] Nguyen, B.; Wilson, W. D.; *J. Phis. Chem. B.* **2009**, *113*, 14329-14335

[96] Monchaud, D.; Allain, C.; Bertrand, H.; Smargiasso, N.; Rosu, F.; Gabelica, V.; De Cian, A.; Mergny, J. L.; Teulade-Fichou, M. P.; *Biochimie.* **2008**, *90*, 1207-1223

[97] Nygren, J.; Svanik, N.; Kubista, M.; *Byopolymers,* **1998**, *46*, 39-51

[98] Rodger, A.; Nordén, B.; "Circular Dichroism & Linear Dichroism". Oxford University Press, **1997**, Chapter 2

[99] Burge, S.; Parkinson, G. N.; Hazel, P.; Todd, A. K.; Neidle, S.; *Nucleic Acids Res.*, **2006**, *34*, 5402-5415

[100] Williamson, J. R.; *Annu. Rev. Biophys. Biomol. Struct.,* **1994**, *23*, 703–730

[101] Bugaut, A.; Balasubramanian, S. A.; *Biochemistry,* **2008**, *47*, 689–697

[102] Kypr, J.; Keinovska', I.; Renciuk, D; Vorlikova', M.; *Nucleic Acids Res.* **2009**, *37*, 1713-1725

[103] Nguyen, B.; Tanious, F. A.; Wilson, W. D.; *Methods*, **2007**, *42*, 150-161

[104] Tanious, F. A.; Nguyen, B.; Wilson, W. D.; *Methods in Cell Biology* **2008**, *84*, 53-77

[105] Dass, C.; "Fundamentals of Contemporary Mass Spectrometry", John Wile&Sons Ina, New Jersey, **2007**, Chapter 6

[106] Bailly, C.; Tardy, C.; Wang, L.; Armitage, B.; Hopkins, K.; Kumar, A.; Schuster, G B.; Boykin, D. W.; Wilson, W. D.; *Biochemistry*, **2001**, *40*, 9770-9779

[107] Athri, P.; Wilson, W. D.; *J Am Chem Soc.*, **2009**, *131*, 7618-7625

[108] Miao, Y.; Lee, M.P.; Parkinson, G. N.; Batista-Parra, A.; Ismail, M. A.; Neidle, S.; Boykin, D. W.; Wilson, W. D. *Biochemistr,y* **2005**, *44*, 14701-14708

[109] Munde, M.; Ismail, M. A.; Arafa, R.; Peixoto, P.; Collar, C. J.; Liu, Y.; Hu, L. David-Cordonnier, M. H.; Lansiaux, A.; Bailly, C.; Boykin, D. W.; Wilson, W. D.; *J. Am. Chem. Soc.* **2007**, *44*, 13732-13743

[110] Nguyen, B.; Tardy, C.; Bailly, C.; Colson, P.; Houssier, C.; Kumar, A.; Boykin, D. W.; Wilson, W. D.; *Biopolymers*, **2002**, *63*, 281-297

[111] Huang, J.; Li, Guorui; Wu, Z.; Song, Z.; Zhou, Y.; Shuai, L.; Weng, X.; Zhou, X.; Yand, G.; *ChemComm.*, **2009**, 902-904

[112] Shin-Ya, K.; *Biosci. Biotechnol. Biochem.;* **2005**, *69*, 867-872

[113] Cetinkol, O. P.; Engelhart, A. E.; Nanjunda, R. K.; Wilson, W. D.; Hud, N. V.; *Chembiochem.,* **2008**, *9*, 889-892

[114] Chen, Q.; Kuntz, I. D.; Shafer, R. H.; *Proc. Natl. Acad. Sci. U S A.*, **1996**, *93*, 2635-2639

[115] White, E. W.; Tanious, F.; Ismail, M. A.; Reszka, A. P.; Neidle, S.; Boykin, D. W.; Wilson, W. D., *Biophys. Chem.,* **2007**, *126*, 140-153

Capitolo 3 [116] Allain, C.; Monchaud, D.; Teulade-Fichou, M. P., *J. Am. Chem. Soc.* **2006**, *128*, 11890-11893

[117] Guo, Q.; Lu, M.; Marky, L. A.; Kallenbach, N. R.; *Biochem.*, **1992**, *31*, 2451-2455

[118] Freyer, M. W.; Buscaglia, R.; Kaplan, K.; Cashman, D.; Hurley, L. H.; Lewis, E. A.; *Biophys J.*, **2007**, *92*, 2007-2015

[119] Hazel, P.; Huppert, J.; Balasubramanian, S; Niedle, S.; *J. Am. Chem. Soc.,* **2004**, *126*, 16405-16415

[120] Neidle, S; Parrkinson, G. N.; *Curr. Opin. Struct. Biol.,* **2003**, *13*, 275-283

[121] Miyoshi, D; Nakao, A.; Sugimoto, N.; *Nucleic Acids Res.,* **2003**, *31*, 1156-1163

[122] Martino, L.; Virno, A.; Pagano, B.; Virgilio, A.; Di Micco, S.; Galeone, A.; Giancola, C.; Bifulco, G.; Mayol, L.; Randazzo, A.; *J. Am. Chem. Soc.*, **2007**, *129*, 16048-16056

[123] Cosconati, S.; Marinelli, L.; Trotta, R.; Virno, A.; Mayol, L.; Novellino, E.; Olson, A. J.; Randazzo, A; *J. Am. Chem. Soc*., **2009**, *131*, 16336-16337

[124] Rodger, A.; Norden, B. "Circular Dichroism and Linear Dichroism". Oxford Chemistry Masters, ed. R.G. Compton, S.G. Davies, and J. Evans. **1997**, New York: Oxford University Press

[125] Munde, M.; Ismail, M. A.; Arafa, R.; Peixoto, P.; Collar, C. J.; Liu, H.; Hu, L.; David-Cordonnier, M. H.; Lansiaux, A.; Bailly, C.; Boykin, D. W.; Wilson, W. D.; *J. Am. Chem. Soc.,* **2007**, *129*, 13732-13743

[126] Burge, S.; Parkinson, G. N.; Hazel, P.; Todd, A. K.; Neidle, S.; *Nucleic Acids Res.*, **2006**, *19*, 5402-5415

[127] Xu, Y.; Noguchi, H.; Sugiyama, H.; *Bioorg. Med. Chem.*, **2007**, *14*, 5584-5591

[128] Okamoto, K.; Sannoe, Y.; Mashimo, T.; Sugiyama, H.; Terazima, M.; *Bioorg. Med. Chem.,* **2008**, *16*, 6873-6878

[129] Pasternack, R. F.; Bustamante, C.; Collings, P. J.; Giannetto, A.; Gibbs, E.; *J. Am. Chem. Soc.,* **1993**, *115*, 5393-5399

[130] Greider, C. W.; Blackburn, E. H.; *Cell*, **1985**, *43*, 405-413

[131] Ambrus, A.; Chen, D.; Dai, J. X.; Bialis, T.; Jones, R. A.; Yang, D. Z. ; *Nucleic Acids Res.,* **2006**, *34*, 2723–2735

[132] Phan, A.T.; Kuryavyi, V.; Luu, K. N.; Patel, D. J.; *Nucleic Acids Res*., **2007**, *35*, 6517–6525

[133] Dai, J. X.; Carver, M; Punchihewa, C.; Jones, R. A.; Yang, D. Z.; *Nucleic Acids Res.,* **2007**, *35*, 4927–4940

[134] Zhang, Z.; Dai1, J.; Veliath, E.; Jones, R. A., Yang, D.; *Nucleic Acids Res.* **2010**, *38*, 1009-1021

[135] Mergny, J. L.; Phan, A. T.; Lacroix, L.; *FEBS Lett*. **1998**, *435*, 74–78

[136] Kerwin, S. M.; *Curr. Pharm. Des*., **2000**, *6*, 441-78

[137] Neidle, S.; Read, M. A.; *Biopolymers*, **2001**, *56*, 195-208

[138] Cao, R.; Venezia, C. F.; Armitage, B. A.; *J. Biomol. Strut. Dyn.,* **2001**, *18*, 844–856

[139] Nygren, J.; Svanik, N.; Kubista, M.; *Byopolymers,* **1998,** *46*, 39-51

[140] Garner, T. P.; Williams, H. E. L.; Gluszyk, K. I.; Roe, S.; Oldham, N. J.; Stevens, M. F. G.; Moses, J. E, Searle, M. S.; *Org. Biomol. Chem.*, **2009**, *7*, 4194-4200

[141] Martino, L**.;** Virno, A**.;** Pagano, B**.;** Virgilio, A**.;** Di Micco, S**.;** Galeone, A**.** Giancola, C**.;** Bifulco, G**.;** Mayol, L**.;** Randazzo, A.; *J. Am. Chem. Soc.,* **2007**, *129*, 16048-16056

[142] Chen, Q.; Kuntz, I. D.; Shafer, R. W.; *Proc. Natl. Acad. Sci. USA*, **1996**, *93*, 2635-2639

[143] Han, H; Langley, D. L.; Rangan, A.; Hurley, L. H; *J. Am. Chem. Soc.,* **2001**, *123*, 8902-8913

[144] Matsugami, A.; Xu, Y.; Noguchi, Y.; Sugiyama, H.; Katahira, M.; *FEBS J,* **2007**, *274*, 3545-3556

[145] Zeglis, B. M.; Pierre, V. C.; Barton, J. K..; *ChemComm*, **2007**, 4565-4579

[146] Reed, J. E.; White,A. J.; Neidle, S.; Vilar, R.; *Dalton Trans.*, **2009**, *14*, 2258-2268

[147] Georgiades, S. N.; Karim, N. H.; Suntharalingam, K.; Vilar, R.; *Angew. Chem. Int. Ed.,* **2010**, *49*, 4020-4034

[148] Dixon, I. M.; Lopez, F.; Tejera, A. M.; Esteve, J. P.; Blasco, M. A.; Pratviel, G.; Meunier, B.; *J. Am. Chem. Soc.*, **2007**, *129*, 1502-1503

[149] IDixon, I. M.; Lopez, F.; Esteve, J. P.; Tejera, A. M.; Blasco, M. A.; Pratviel G.; Meunier, B.; *Chembiochem*, **2005**, 6, 123-132

[150] Reed, J. E.; Arnal, A. A.; Neidle, S; Vilar, R.; *J. Am. Chem. Soc.*, **2006**, 128, 5992-5993.

[151]. Reed, J. E.; Neidle, S.; Vilar, R.; *ChemComm*, **2007**, 4366-4368.

[152] Reed, J. E.; White, A. J.; Neidle, S.; Vilar, *Dalton Trans*, **2009**, 2558-2568

[153] Bertrand, H.; Monchaud, D.; De Cian, A.; Guillot, R.; Mergny, J. L.; Teulade-Fichou, M. P.; *Org. Biomol. Chem.*, **2007**, *5*, 2555-2559

[154] Monchaud, D.; Yang, P.; Lacroix, L.; Teulade-Fichou, M. P.; Mergny, J. L.; *Angew. Chem. Int. Ed. Engl.*, **2008**, *47*, 4858-4861

[155] Harris, D. C.; *"Quantitative Chemical Analysis"*, 4th edition, W. H. Freeman, NY

[156] Hirohama, T.; Kuranuki, Y.; Ebina, E.; Sugizaki, T.; Arii, H.; Chikira, M.; Tamil Selvi, P. Palaniandavar, M. *J. Inorg. Biochem.*, **2005**, *99*, 1205-1219

[157] Rachwal, P. A.; Fox, K. R.; *Methods*, **2007**, *43*, 291-301

[158] Talib, J.; Green, C.; Davies, K. J.; Urathamakul, T.; Beck, J. L.; Aldrich-Wright, J. R.; Ralph, S. F.; *Dalton Trans.*, **2008**, 1018-1026

[159] Paramasivan, S.; Rujan, I.; Bolton, P. H.; *Methods*, **2007**, *43,* 324-331

[160] Qin, Y.; Hurley, L. H.; *Biochimie*, **2008**, *90,* 1149-1171

[161] Sun, D.; Hurley, L. H.; *J. Med. Chem.*, **2009**, *52*, 2863-2874

[162] Sigman, D. S.; Graham, D. R.; D'Aurora, V.; Stern, A. M., *J. Biol. Chem.*, **1979**, *254*, 12269-12272

[163] Muller, J. G.; Chen, X.; Rokita, Dadiz, A. C.; Rokita, S. E.; Burrows, C. J; *J. Am. Chem. Soc.*, **1992**, *114*, 6407-6411

[164] Kha, H.; Zhou, W.; Chen, K.; Karan-Tamir, B.; San Miguel, T.; Zeni, L.; Kearns, K.; Mladenovic, A.; Rasnow, B.; Robinson, M.; Wahl, R. C.; *Anal. Biochem.*, **2004**, *331*, 230-234.

[165] Nielsen, M. C.; Borch, J.; Ulven, T.; *Bioorg. Med. Chem.*, **2009**, *17*, 8241-8246

[166] Sigman, D. S.; Graham, D. R.; D'Aurora, V.; and A. M. Stern, *J Biol Chem*, **1979**, 254, 12269-12272.

[167] Robertazzi, A.; Vargiu, A. V.; Magistrato, A.; Ruggerone, P.; Carloni, P.; de Hoog, P.; Reedijk, J.; *J. Phys. Chem. B.*, **2009**, *113*, 10881-10890

[168] Veal J. M.; Rill, R. L.; *Biochemistry*, **1991**, *30*, 1132-1140

[169]Wang, D.; Lippard, S. J.; *Nat. Rev. Drug Discov*., **2005**, *4*, 307-320

[170] Kelland, L.; *Nat. Rev. Cancer.,* **2007**, *8*, 573-584

[171] Bernal Mendez, E.; Boudvillain. M.; Gonzales Vilchez, F.; Leng, M.; *Biochemistry*, **1997**, *36*, 7281-7287

[172] Ford, G. P.; Scribner, J. D.; *Chem. Res. Toxicol.*, **1990**, *3*, 219–230

[173] a) Takahara, P. M.; Rosenzweig, A C.; Frederick, C. A.; Lippard, S.J.; *Nature*, **1995**, *377*, 649–652 b) Coste. F.; Malinge, J.M.; Serre, L.; Shepard, W.; Roth, M.; Leng, M.; Zelwer, C.; *Nucleic Acids Res.* **1999**, *27*, 1837–1846

[174] Leng, M.; Schwartz, A.; Giraud-Panis, M. J.; in: Platinum-Based Drugs in Cancer Therapy, by Kelland, L. R., Farrell, N.P.; editors. Humana Press; Totowa, New Jersey: 2000. pp. 63–85

[175] Natile, G.; Coluccia, M.; Metal ions in biological systems, Basel, **2004**, 42, 251-296

[176] Farrell, N.; Ha, T. T.B.; Souchard, J. P.; Wimmer, N. P.; Johnson, N.P.; *J. Med. Chem*., **1989**, *32*, 2240-2241

[177] Farrell, N.; Kelland, L.R.; Roberts, J.D.; Van Beusichem, M.; *Cancer Res.*, **1992**, *52*, 5065-5072

[178] Van Beusichem, M.; Farrell, N.; *Inorg. Chem.*, **1992**, *31*, 634-639

[179] Kasparkova, J.; Novakova, O.; Farrel, N.; Brabec, V.; *Biochemistry*, **2003**, *42*, 792-800

[180] Novakova, O.; Kasparkova, J.; Malina, J.; Natile, G.; Brabec, V. Nucleic Acids Res., **2003**, *31*, 6450-6460

[181] Aris, S. M.; Farrell, N. P.; *Eur. J. Inorg. Chem.*, 2009, 10, 1293, 1302

[182] Ma, E. S. F.; Bates, W. D.; Edmunds. A.; Kelland, L. R.; Fojo, T.; Farrell, N.; *J. Med. Chem.*, **2005**, *48*, 5651–5654

[183] Pierce, S. E.; Kieltyka, R.; Sleiman, H. F.; Brodbelt, J. S.; *Biopolymers*, **2009**, *91*, 233-243

[184] Bertrand, H.; Bombard, S.; Monchaud, D.; Talbot, E.; Guedin, A.; Mergny, J. L.; Grunert, R.; Bednarski P. J.; Teulade-Fichou, M. P.; *Org. Biomol. Chem.*, **2009**, *7*, 2864-2871

[185] Ma, D. L.; Che, C. M.; Yan, S. C.; *J Am. Chem. Soc.*, **2009**, *131*, 1835-1846

[186] Bertrand, H.; Monchaud, D.; De Cian, A.; Guillot, R.; Mergny, J. L. and M. P. Teulade-Fichou, *Org Biomol Chem*, 2007, 5, 2555

[187] Reed, J. E.; Arnal, A. A.; Neidle, S.; Vilar, R.; *J. Am. Chem. Soc*., **2006**, *128*, 5992

[188] Reed, J. E.; Neidle S.; Vilar, R.; *Chem. Commun. (Camb)*, **2007**, 4366-4368

[189] Von Ahsen, N.; Oellerich, M.; Armstrong, V. W.; Schütz, E.; *Clin Chem.*, 1999, *45*, 2094-2101

[190] Baruah, H.; Rector, C. L.; Monnier, S. M.; Bierbach, U.; *Biochem. Pharmacol.,* **2002**, *64*, 2191-200